FABRICATION OF HYDROGEL MASK USING A MICROFLUIDIC TECHNIQUE

by

Hilal Kılıç

Submitted to Graduate School of Natural and Applied Sciences

in Partial Fulfillment of the Requirements

for the Degree of Master of Science in

Biotechnology

Yeditepe University

2020

FABRICATION OF HYDROGEL MASK USING A MICROFLUIDIC TECHNIQUE

APPROVED BY:

Assist. Prof. Dr. Gülengül Duman ……
(Thesis Supervisor)
(Yeditepe University)

Assoc. Prof. Dr. İsrafil Küçük ……
(Thesis Co-supervisor)
(Gebze Technical University)

Prof. Dr. Ece Genç ……
(Yeditepe University)

Prof. Dr. Işıl Kurnaz ……
(Gebze Technical University)

Assist. Prof. Dr. Feride Sermin Utku ……
(Yeditepe University)

DATE OF APPROVAL: …./…./2020

ACKNOWLEDGEMENTS

I would like to thank my MSc principal investigator Assistant Professor Gülengül DUMAN for her continuous support and motivation during my MSc thesis work. I would like to specially thank my MSc research work second supervisor Assistant Professor İsrafil KÜÇÜK, who has contributed a lot to the formation and planning of my thesis work and enabled me to gain experimental skills. I would also like to thank Assistant Professor Erdem Yeşilada who helped me in supplying the *Hypericum perforatum* oil used in the experiments and I would like to thank Konya Selcuk University Technocity laboratories producing this oil. I would like to thank Gebze Technical University NANO-delight Research Laboratory members, Ph.D. student Işıl Ünal and research assistant Hasan Topaç and MEng student Dila Zorşahin and Experts Ahmet Nazım (SEM) and Adem Şen (XRD, TGA) who have technical assistance during the experimental works. For a use of the facilities, I would like to thank Gebze Technical University Nanotechnology Institute, which provided me with assistance for the use of materials and laboratory and all the necessary equipments for the characterizations. The other institutions that I would like to express my gratitude for are Sabancı University Faculty of Engineering and Natural Sciences, Materials Science and Engineering Program, Laboratory Officer, Burçin Yıldız for Differential Scanning Calorimeter (DSC) analysis and Sakarya University Faculty of Engineering, Department of Materials and Metallurgy; Research Assistant Erhan Mutlu for Raman spectroscopy analysis. Finally, I would like to thank my family for their lifetime support.

ABSTRACT

FABRICATION OF HYDROGEL MASK USING A MICROFLUIDIC TECHNIQUE

Skin masks are used in a wide range in the cosmetics industry. It is often used to restore the skin's lost moisture, acne, wound and blemish treatments, anti-aging care and daily care. Among the mask types, the most innovative solution designs are hydrogel skin masks with highest moisture level, which have abilities such as cell renewal and cellular functional increase. In this study, we produced alginate-based hydrogel masks using a microfluidic technique. Microbubbles were firstly produced with a T-junction microfluidic device and by converting microbubbles to hydrogel; a porous polymer skin masks were successfully achieved. The resultant maks contains *Hypericum perforatum* oil and honey in its own polymeric structure. It is desired to benefit from the moisturizing, antibacterial and wound-healing properties in honey, and antibacterial and wound-healing properties of *Hypericum perforatum*. A porous structural alginate-based hydrogel mask was produced and the dispersions used during this production were examined by physical property measurements and dispersion characterizations, such as surface tension, viscosity, density and contact angle. The microbubbles produced for the fabrication of hydrogel by a T-junction microfluidic technique were taken with an optical microscope, the hydrogel structure produced was dried and structural, thermal and chemical characterizations were performed using SEM, FT-IR, FT-Raman, XRD, DSC and TGA methods. The masks obtained contain the active ingredients of honey and *Hypericum perforatum* oil produced and they were tested on six volunteered patients. Skin moisture measurements before and after hydrogel applied were examined with a digital moisture meter and a comparison was made by visually examining the changes in acne and wound formation on the patient's skin.

ÖZET

MİKROAKIŞKAN TEKNİK KULLANILARAK HİDROJEL MASKE ÜRETİMİ

Cilt maskeleri kozmetik sektöründe çok geniş bir alanda kullanılmaktadır. Sıklıkla cildin kaybolmuş nemini geri kazandırmak, akne, yara ve leke tedavileri, yaşlanma karşıtı tedavi ve günlük bakım için kullanımı tercih edilmektedir. Maske türleri arasında, en fazla nemi tutan, hücre yenileme özelliğine sahip ve hücresel işlevini artıran en yenilikçi maske tipi hidrojel cilt maskeleridir. Bu çalışmada T-şekilli geometriye sahip bir mikroakışkan teknik kullanılarak aljinat esaslı hidrojel maske üretimi amaçlandı. Bu çalışmada öncelikle, mikron boyutlu baloncuklar, bir T-geometrili mikro-akışkan cihaz ile üretildi ve mikron boyutlu baloncuklar hidrojele dönüştürülerek, gözenekli bir polimer cilt maskesi elde edildi. Aljinat bazlı hidrojel maskesi belirlenen oranlarda Sarı Kantaron yağı ve bal içerdi. Baldaki nemlendirici, antibakteriyel ve yara iyileştirici özelliklerden ve *Hypericum perforatum*'un antibakteriyel ve yara iyileştirici özelliklerinden faydalanmak hedeflenildi. Gözenekli yapıda aljinat bazlı bir hidrojel maske üretildi ve bu üretim sırasında kullanılan emülsiyon çözeltilerinin fiziksel özellikleri olan yüzey gerilimi, viskozite, yoğunluk ve temas açısı gibi fiziksel özellik ölçümleri ve kullanılan malzemeler ve elde edilen ürüne yapısal, ısısal ve kimyasal yapı karakterizasyon çalışmaları yapıldı. Mikroakışkan tekniği ile hidrojel üretimi için üretilen mikrobaloncuklar bir optik mikroskop ile incelendi ve kurutulmuş hidrojellerin yapısı ve karakterizasyonu SEM, FT-IR, Raman, XRD, DSC ve TGA yöntemleri ile gerçekleştirildi. Maske, üretilen bal ve sarı kantaron yağının aktif bileşenlerini içermekle birlikte, bu maske altı gönüllü hasta üzerinde test edildi ve maskenin hastalara tatbik edilmesinden önce ve sonra her bir hastanın cildinin nem seviyesi, akne ve yara oluşumu değişimleri görsel olarak incelenerek, bir karşılaştırma yapıldı.

TABLE OF CONTENTS

LIST OF FIGURES

LIST OF TABLES

LIST OF SYMBOLS/ABBREVIATIONS

2D	Two dimensional
°C	Degree centigrade
cm^{-1}	Reciprocal centimeters
g	Gram
mL	Milliliter
mPas	Millipascal
rpm	Revolutions per minute
%	Percentage sign
α	Alpha
β	Beta
θ	Theta
µm	Micrometer
µM	Micromolar
µl / min	Microliter per min
µg	Microgram
$\mu g / cm^2$	Microgram per square centimetre
$A_{crystal}$	The sum of the areas under the crystalline diffraction peaks
AHPA	American Herbal Products Association
AQP3	Aquaporin-3
A_{Total}	The total area under the diffraction curve
BC	Before Christ
C	Carbon
Ca	Capillary number
Ca2 +	Carbonic anhydrase 2
$CaCl_2$	Calcium chloride
CAS no	Chemical abstracts service registry number
CH	Hydrocarbon
CH_2	Methylene
$C_{12}H_{22}O_{11}$	Maltose and sucrose
$C_6H_{12}O_6$	Fructose and glucose

CI	Crystallinity index
Cl	Chloride
DNA	Deoxyiribo nucleic acid
DPPH	2,2-diphenyl-1-picrylhydrazyl radical scavenger
DSC	Differential scanning calorimetry
DTG	Differential thermal gravimetry
EC	Epidermal cells
F	Fluoride
FDA	Food and Drug Administration
FEP	Fluoro ethylene polypropylene
FMG	Alternative blocks
FMM	Mannuronic acid blocks
FRAP	Ferric reducing antioxidant power
FT-IR	Fourier-transform infrared spectroscopy
FT-Raman	Fourier transform raman
G	Guluronic acid monomers
GC / MS methods	Gas chromatography / Mass spectrometry
GF	Growth factor
H	Hydrogen
H_20	Water
H_20_2	Hydrogen peroxide
HCl	Hydrogen chloride
HIV virus	Human immunodeficiency virus
HMF	Hydroxymethylfurfural
HMPC	Herbal Medicinal Products Committee
INCI	International cosmetic ingredients
IPN	Interpenetrating network
LCD	Liquid-crystal display
M	Mannuronic acid
MAO inhibitors	Monoamine oxidase inhibitors
MCMV	Murine Cytomegalovirus
MECLR	Mixed EC lymphocyte reaction
MED	Minimal erythema dose

M-G block	Mannuronic acid / Guluronic acid
MRSA	Methicillin-resistastant *Staphylococcus aureus*
Na +	Sodium
NaCl	Sodium chloride
NH_2	Aminyl radical
NH_3	Ammonia
NMF	Natural moisturizing factor
NO	Nitric oxide
NO_2	Nitrogen dioxide
O	Oxygen
OH	Hydroxyl molecule
ORAC	Oxygen radical absorbance capacity
P. acnes	Propionibacterium acnes
PDMS	Polydimethylsiloxane
PEG	Polyethylene glycol
PEGDA	Poly (ethylene glycol) diacrylate
PGE	Prostaglandins E2
pH	Power of hydrogen
PLA	Polylactic Acid
PMMA	Polymethylmethacrylate
PRSA	Penicillin-resistant
PVA	Polyvinyl alcohol
PVAc	Polyvinyl acetatecontent
PVP	Polyvinyl pyrollidone
R functional group	Alkyl group
ROS	Reactive oxygen species
RSA	Radical scavenging activity
S-S bond	Disulfide bond
SAP	Superabsorbent polymers
SEM	Scanning electron microscopy
semi-IPN	Semi-interpenetrating network
SO_3H	Sulfonic acid
SPA	Surface perimeter area

SPH	Superporous hydrogels
SSR	Solar simulated radiation
T region	Forehead, nose, chin regions
TEAC	Trolox equivalent antioxidant capacity
TECA	Titrated centella asiatica
TGA	Thermogravimetric analysis
U region	Cheeks, temples region
UV	Ultraviolet
VIS	Visible light
VRE	Vancomycinresistant *Enterococcus* spp
XRD	X-Ray diffraction spectroscopy

1. INTRODUCTION

1.1. AIM OF THE STUDY

The aim of the work described in this thesis is to investigate a porous hydrogel mask produced by a T-junction microfluidic method and their moisture performance on volunteered patients and other properties.

Microbubbles were produced with a T-junction microfluidic system, which was established using alginate-based dispersion containing honey and *Hypericum perforatum* as an active ingredients and nitrogen gas, and gelling was formed by crosslinking them with calcium chloride ($CaCI_2$) solution. The use of microfluidic technique is an advantageous technique for the production of porous hydrogels that will be created in a controlled manner. It has been observed that monodispers microbubbles with a regular distribution can be produced in this system. Thanks to the moisture and antibacterial properties provided by the active ingredients of honey and *Hypericum perforatum*, the wound healing process was evaluated by visual observation and moisture increase in the skin was evaluated with a moisture meter.

1.2. HYDROGEL STRUCTURE

Hydrogel is a candidate biomaterial for soft tissues, which has a content with high water and porous structure, which is highly compatible with human tissue and body. Hydrogel with its three-dimensional polymeric networks can be applied inside and outside of the body. It is a biopolymer that can be used locally and transdermally from the outside by embedding medication or cosmetic products or used for tissue regeneration and drug release into the body. The cross-linked structure of hydrogels and the fact that they have a single polymer molecule explain the structure that clings to each other without dissolution. Due to its hydrophilic polymers, it has water-absorbing structures, swelling in water but do not dissolving. It is a hydrophilic polymer because there have groups such as $-NH_2$, -COOH, -OH, $-CONH_2$, -CONH- and $-SO_3H$ [1].

1.2.1. Key Properties of Hydrogel

The most important feature of hydrogels is it is swelling capability in water environment. The water character in the hydrogel determines the permeability and can be used for free diffusion of some substances. Hydrogels are swollen by absorbing water and reach saturated level while the osmotic driving force causes additional swelling and there is a pulling force and cross-linking structure to prevent this. The porous structure in the hydrogel is a structure that can be formed by changing later. Important parameters in hydrogels are size, distribution and inter-connections of pores. The pore size distributions of the hydrogel is influenced by properties such as crosslinked concentrations of polymer strands, the mixed structure of polymer strands and the charge of the polyelectrolyte hydrogel. The porous structure of the hydrogel can be used for various applications such as controlled release of drugs and molecules and cell migration in hydrogel scaffolds. The crosslinking feature is a feature of the natural structure of hydrogels, but its degree can be modifying by changing later with various application. [1] There are two types of cross-linking: chemical bonds with permanent junction and temporary junction. Another key feature of hydrogels is mechanical strength. Increasing the crosslinking excess increases the mechanical strength. If the stretch percentage of the gel decreases, the gel turns into a brittle structure. Biocompatibility is also another significant property of hydrogels. It is desired that the polymers used in or in contact with the body are non-toxic, do not cause irritation and have a structure that does not produce an immunological response [2].

There are two types of hydrogel: synthetic and natural. Natural hydrogels are collagen, fibrin, hyaluronic acid, matrigel and chitosan, alginate and derivatives of these materials and their natural structures are all different. Synthetic hydrogels are, for instance, polyethylene glycol (PEG), polymethacrylate (PMMA), polyvinyl pyrollidone (PVP), polylactic acid (PLA), etc. Synthetic hydrogels can be reproduced and skeletal structures can be modified. Its flexibility, degradability or hydrolyzability can be changed by external interventions, but such intervention is not possible in natural polymers [3].

Polymers are divided into groups in synthesis methods: homopolymer, copolymer, semi-interpenetrating network (semi-IPN) and interpenetrating network (IPN). Homopolymers consist of one monomer and crosslink structure; copolymer consists of at least two monomers. A semi-IPN occurs when a linear polymer enters another crosslinked network.

IPN is formed by combining two existing polymers with the help of a solution, one is self-synthesized by cross-linking and the other is present. Thanks to their porous structure, especially IPN and semi-IPN, they are used for controlled release of drugs and can encapsulate drugs or cells safely [4].

As a new category, superabsorbent polymers (SAP) and superporous hydrogels (SPH) are being produced. SAPs have fewer water absorbing properties than SPHs but much more than the overall hydrogel structure. SPHs have been renewed and more properties that are mechanical which have been improved, now they have more absorbency and elasticity. Production methods of SPH are varied such as freeze-drying, microemulsion formation and phase separation. In addition to homogeneous, cross-linking and water-absorbing enhancing properties, different substances can be added in the production methods of SPH hydrogels. In addition to the general process, one of the production methods for SPH hydrogels is added foam stabilizer, and for SPH composite, matrix swelling, additive, composite agent are added during the construction phase. When producing the third generation SPH, hybrids are added after they are created. Examples of hybrid agents are synthetic and natural polymers such as sodium alginate, pectin, chitosan or polyvinyl alcohol. The hybrids involved in the production phase are an improvement to create a second network as a crosslink, to increase the elasticity of the gels and their mechanical strength and resistance to external stresses [5].

1.2.2. Methods of Hydrogel Production

If hydrogel production methods in terms of gelation process type are defined, they can be divided into 4 groups: physical crosslinking [6], chemical cross-linking [7], grafting polymerisation [8], and radiation cross-linking [9,10].

Physical crosslinking is produced without the use of cross-linking agents and they are divided into groups in terms of method. Heating/cooling a polymer solution process that gelatin or carrageenan solutions first change from hot to cold, and then crosslinks are formed. A double helix structure is formed, which helps to create a stable structure. Ionic interaction method is a process that forms hydrogels by creating a cross-link with the help of ionic structures. Counter-loads interact and form gelling by binding. For example, Na^{+} alginate- and Ca^{2+}, Cl- counter-loads can be shown. In complex coacervation method, the

connection of opposite charges with each other and creates soluble or insoluble complexes and they depend on the pH of the solution. H-bonded hydrogel-made can be achieved by lowering the pH of the carboxyl groups, and in the presence of acids, a crosslinking pathway can be observed. Maturation with the clustering of protein compounds of molecules with different molecular weights and protein content with heat and increasing molecular weight and their mechanical properties and challenge the production of hydrogels with water binding ability. Microcrystals are formed in its structure by freezing and thawing of the polymer, which causes physical cross-linking and gelling is the method of freeze thawing. In the chemical cross-linking method, a new bond formation is created using new molecules, and gelling occurs. Grafting method, which is a different class in chemical crosslinking, is grafting a pre-formed polymer with chemical reagents or radiation of a different monomer. Grafting method can be chemical and radiation. Chemical grafting is grafted with a different chemical reagent effect. In radiation grafting, in addition to chemical reagents, gelling is created by using radiation such as gamma and electron beam [8]. There is a different method of radiation cross-linking without using chemicals. Using high-energy radiation sources such as gamma ray, x-ray or electron beam; gelling is formed due to the reproduction of free radicals by the effect of rays in the polymer. Since chemicals are not used, polymer biocompatibility is not damaged and gelation can be achieved in one step [11]. Hydrocolloids can be irradiated in aqueous and solid form. The concentration of the polymer in the aqueous form is high and both irradiation results in free radicals and radicals can occur in the presence of OH. In this way, cross-linking can be bidirectional with radical-radical and polymer-polymer radical reactions. By radicalization of water, H atoms separate from the polymer chain and produce free radicals. Being an aqueous polymer causes cross-linked hydrogel formation, while irradiation of solid hydrocolloids causes direct free radical formation of radiation. During the radiation of solid hydrocolloids, energy is transferred directly to the macromolecules and the molecular weight decreases and fragmentation occurs. Hydrolysis occurs due to the presence of naturally occurring moisture, and primary radicals are produced and new products are formed and gelation occurs. For solid or aqueous solutions of synthetic polymers are gelled with radiation, but natural polymers are degraded after this type of treatment. A new method has been developed for polysaccharides and natural polymers. In the method, conductive wire or stones are used. The polymer is wrapped in this way and crosslinked by radiation. In the presence of alkyne gas, modification is

created by radiation. Natural polymers are crosslinked by this method and converted into macromolecules [12,13][3].

Microfabrication techniques are also used to create tissue blocks containing intracellular hydrogel building blocks and to produce hydrogel materials. For these, different microfluidic based polymerization techniques are used such as chemical, photographic and thermal polymerization techniques [14].

1.2.3. Microfluidic Fabrication of Hydrogels

Hydrogel microfibres previously made by conventional spinning methods can now be made via using microfluidics. Using microfluidic methods, microfibres with natural cross-links similar to collagen fibers can be made. For instance, calcium alginate microfibres have been produced with coaxial flow based microfluidic devices [15]. Here, the alginate produced by using a microfluidic device can be modified as desired. Porous structure is desired in hydrogels that will be used for tissue skeleton or drug release. For this, the use of porogen and the process of changing the solvent can be used [16]. Photocroslinkable hydrogels can be produced by microfluidic technique. Meanwhile, microparticles can be produced with photopolymerization technique, which allows microparticles to be produced in various sizes and shapes. By interfering with the micro flow rate, monodispers and shape-controlled hydrogel particles can be produced [16]. In addition to photocrosslinkable connectable microparticles, alginate microbeads can be produced in monodispers structure in the microfluidic device [17]. Calcium ions and sodium alginate are bonded in T-shaped microchannels, and geled in perforated polydimethylsiloxane (PDMS) microfluidic device. Flow lithography technique is used to high efficiency particle production, different models and multifunctional particles can be produced [18]. Stop-flow lithography technique is important for producing cell-laden microparticles. When used together with PEGDA or photoinitiator concentrations and UV radiation, higher cell-laden hydrogel formation was observed [19]. Hydrogel particles containing magnetic nanoparticles can be produced with t-junction microfluidic device. Hydrogel particles produced in a microfluidic device containing an aluminum reflector have high magnetism and are an advantageous system since they provide continuous production with high monodispersity of particles [20]. The microfluidic hydrodynamic flow focusing system played an important role in the

production of emulsion-based particles of liquid monomers or micro-droplets derived from thermal solidification. Micro-molding techniques are also a method used to produce shaped hydrogel particles. Micro molding techniques are a method used to produce shapely hydrogel particles. Cross-linked hydrogel microparticles can be formed by micro-molding gelling calcium ions onto the hydrogel alginate. With the micro transfer molding technique, it enables the creation of both cell-laden hydrogels and processed hydrogels for controlled release of drugs and proteins [21].

1.2.4. Microfluidic Systems

Many different methods have been used for microfluidic devices such as cross-flowing shearing, perpendicular flowing shearing, hydrodynamic flow focusing, coflowing rupturing, and geometry-dominated breakup [22]. In T-shaped microfluidic devices, two different flow directions intersect with each other and continue together, creating a new mixed product. There may be liquid flow from two different directions or gas and liquid flow may be combined as different substances [23]. Microfluidic devices using T-shaped junctions model combine a mixture of gas and liquid or two different liquid mixtures with a volume less than millimeters to produce monodisperse micro bubbles. T-shaped junctions have two different models: Unconfined T-shaped junction is a model where the bubbles or droplets formed are not trapped inside the channels and flow freely. The second model is confined T-shaped junction in which the formed bubbles or droplets are limited by channels. Thorsen et al. [24], according to his study, when the droplet and bubble size were interpreted according to confined T-shaped intersections, it was found to be found in proportion between flow rates [24]. It is found by the ratio of the flow rate of the dispersed phase to that of the continuous phase. In gas and liquid combinations, the inlet pressure to channel of the gas is considered instead of the flow rate for the gas [24].

The use of microfluidics is an extremely useful system for synthesizing the particles to be formed in the shape and concentration controlled microsize range. Pore sizes are very important for hydrogel structures. Smaller pores are both high mechanical strength and stresses that are more resistant to compressive. Also, if a hydrogel is produced that will be in or in contact with the tissue, small pores increase the compatibility with the tissues [25]. Among the microfluidic devices used in the production of alginate micro-droplets and

microbubbles containing shape and size controlled, there are microchannel cross junction, Y-shaped and T-shaped microfluidic devices, a microfluidic device consisting of two separate flow focusing channels, micronosse array, membrane emulsification technique for Ca-algae particles. Production is more controlled in T-shaped microfluidic devices. Compared to other systems, production is made by controlling one continuous phase, not two continuous phases, and a second scan is not required [26].

1.2.5. Microbubbles and Production in T- Junction Microfluidic Device

Microbubbles have many applications such as drug release, tumor destructive effect, ultrasound contrast agent, gen delivery and can be used in different areas: energy, food, chemistry, cosmetics and medical fields. Different methods have been produced for microbubble production; sonication, ink-jet printing, coaxial electrohydrodynamic atomization and gyration. For these applications, it is necessary to produce monodisperse microbubbles that can remain stable for a long time [27]. The most effective method of microbubble production is the use of microfluidic devices [28]. Microfluidic systems are processed at a smaller level than the millimeter studied. Bubbles with a diameter of 1–1000 μm can be called microbubbles. The difference of microfluidics from the macrofluidic system is both low-volume liquid and gas interaction, as well as behaviors such as surface tension, viscosity, energy distribution and flow resistance. In the microfluidic system, it can provide differences in physical and chemical properties such as concentration, pH, temperature, shear force as well as properties such as movement, resistance and flow of liquids [29].

Microfluidics is a system in which liquid - gas or liquid - liquid flows in given through different channels and inter-mixed at T-connection and flow through a single channel. In the T-junction microfluidic device, the dispersed phase through which gas passes and the continuous phase through which liquid passes are formed. The dispersed phase blocks the outlet channel and the upstream pressure in the liquid phase forms the dispersed phase. (Fig.1.1.) Thanks to the balance between these phases, progress is made and this balance and flow are related to the capillary number. Normal stress, not tangential stress, is effective in this flow break up. The hydrostatic pressure balance is the main factor in breaking up liquid or gas streams in the continuous fluid. In this system, the dispersed

phase is through gas pumps that regulate the gas flow, and the continuous phase is through syringe pumps that can be controlled with certain values. In the T-junction microfluidic device, the bubble takes place in three stages: the growth stage, the necking stage, and finally the pinch off stage. After gas and liquid meet at the intersection, the balloon filled with gas on a micro scale expands into the liquid and moves through the channel until it leaves the outlet channel. The gas bubble first expands as it flows and spreads downward as its diameter decreases and eventually breaks. Bubble formation is influenced by a wide variety of parameters such as viscosity ratio, flow rates, gas pressure, and channel geometry and channel wettability. Once the system is installed, two main factors are the router in the system as micro bubble production method: the bubbling pressure and the flow rate [25, 30, 32].

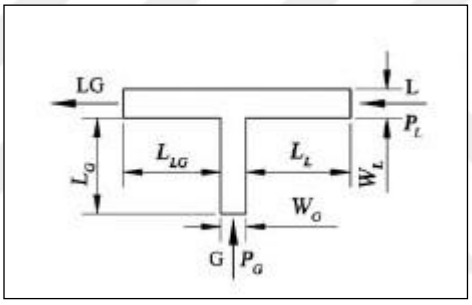

Figure 1.1. Schematic flow diagram of a microfluidic T-junction [31].

1.2.6. Factors Affecting the Microfluidic System

Many factors affect and change the microbubble or microdroplet to be produced in the microfluidic system. These are variables such as parameters of the setup of the system, instruments of the system and continuous or dispersed phase.

The number of reynold evaluates the fluid flow in microfluidic systems. In the calculations for the Reynold number, the density, viscosity and flow rate of the liquid are also included in the calculation. This is based on the small Reynold number, which indicates that the viscous force of the fluid exceeds the inertia force, providing a linear flow [33]. In this system, in order to increase the flow rate, long diameter and narrow diameter of capillaries are more effective [34]. The flow rates of the gases and liquids used as inputs in the system

affect the bubble size. While increasing the flow rate by keeping the gas pressure constant leads to a decrease in microbubble size, increasing the gas pressure by keeping the liquid arrival constant has been observed to increase the bubble size [32]. It has been found that the bubble size decreases with increasing fluid flow rate and viscosity and increases with increasing gas pressure, there are studies in which it is observed that the bubble size depends on both the capillary number and the flow rate ratio [32].

The angles of the contact lines are important in T-shaped junction devices and must remain stationary. The contact angles below 90° degrees indicate that they have stable structures. In addition, it has been seen that the angles of the junctions of microchannels in the system affect the formation of bubbles [23, 32].

The contact angle and surface tension also affect bubble size and formation. It is effective in combining and mixing of phases [35]. Contact angle and slip lengths, injection angles close to perpendicular and parallel conditions have an increasing effect on the droplet diameter. Other contact angles and density of the liquid have a decreasing effect on microbubbles. The slip ratio of the channel and interface properties of the channel walls causes a change in bubble size, a decrease in slipping causes a cylindrical structure to be observed in bubble shapes. As the slip length increases, the droplet diameter increases. Another effect that converts the droplet shape from the circle to the cylinder is the change in the angle of injection. Injection angle must have $\theta = 9\theta / 10$ to create the smallest droplet size [36].

The main channel is the channel with a continuous flow, the extraneous channel is the channel in which the liquid flow is included in the system and is called a discontinuous or dispersed flow. In this structure, the width and length of the channels are important parameters [33]. The properties affecting bubble volume in bubble formation are the width and length of channels through which liquids and gases pass, viscosity and flow rate of liquids, surface tensions, gas inlet pressure [28]. The bubble volume increases as the gas inlet pressure and surface tension increases, and the liquid viscosity and flow rate decrease [28].

The channel size in the microfluidic device is an important factor affecting the shape and size of the microbubbles. It was observed that the bubble size increased by increasing the capillary diameter. The ratio of viscose to surface tension forces is called capillary number

and this value affects the size and structure of the bubble formed in this system [23]. Studies have investigated the effect of capillary number and volume of microbubbles. A capillary number represents the effect of viscosity on bubble formation. Capillary number is found with an equation and is used by knowing the viscosity of the continuous phase, the mean velocity of the continuous phase, the channel width joint, the channel height and the interface tension. It was observed that the bubble volume decreased exponentially as Ca decreased and in general, it causes the microbubble size to decrease with increasing viscosity of the liquid [28, 37].

In the dispersion processes between gas-liquid, the dispersion size decreases with increasing Ca value. The effect of dispersed phase flow rate is lenaer in the gas-liquid dispersion process than in the liquid-liquid dispersion process. The reason for this is thought to be due to different growth mechanics in the mixture of gases and liquids. If the viscosity ratio of the dispersed phase is lower than that of the continuous phase, it was found that the dispersed phase caused the dispersion size to be larger due to the elastic deformation. The shear force direction in the system is especially important for the dispersion process [22].

The use of surfactants is important in these studies and plays a very important role in reducing balance interface tension. The use of surfactants reduces the diameter of the microbubble and the type of surfactant used and the concentration that affect the formation of bubbles [38].

1.2.7. Alginate Biopolymers Properties Used as Base in Microfluidic System

Sodium alginate obtained by extracting brown algae. It is a naturally occurring compound in cell walls of brown algae, and alginates are the most abundant polysaccharides in algae, which can be up to 40 percent of dry weight. Filtering is done by extracting different types and structures of brown algae. Sodium or calcium chloride is added to the filtered product to precipitate the alginate. This alginate salt is treated with dilute HCl to form alginic acid. Sodium alginate is formed after the subsequent purification processes. Sodium alginate is used for superabsorbent nanocomposite copolymerization synthesis [39]. Besides algae, it is also found as capsular polysaccharide in the structure of some soil bacteria [40]. The molecular and chemical structure of alginates are binary copolymers, which are linear

sequences of (1-4) -bound bD-mannuronic acid (M) and aL-guluronic acid (G) monomers. This M / G ratio and sequence in its chemical composition has been shown to be effective in the physical structure of alginates. It has been observed that the M / G ratio depends on the location of algae, the temperature and time it was collected. The gels formed when the M / G ratio is higher are softer and more elastic and the gels formed when the M / G ratio is lower are more fragile. Just as the gelling characteristic depends on the M / G ratio, it is also effective in the physical structure of gelling in the homopolymeric block structures called mannuronic acid blocks (FMM), guluronic acid blocks (FGG) and alternative blocks (FMG) [41]. However, gelling of alginates depends on anion cation binding in its chemical structure. There is a chain-like junction between cations and G residues. Ion binding is selective and M and MG blocks are more passive to Ca2 + binding and more binding is seen with G blocks. The greater the chain bond made with the G block in the alginate, the more gelling is harder and a more intense alginate is observed in the association with Na^+ [40].

Various bonding methods such as ionic crosslinking, covalent crosslinking, Thermal gelling, cell crosslinking, and different gel formations formed by them are seen. Ionic cross-linking is the most common method for alginate hydrogel creation. It causes the formation of gel by binding of the cations to guluronate blocks called G blocks and by crosslinking them. Alginate is the most common method for hydrogel creation. It causes the formation of gel by binding of the cations to guluronate blocks called G blocks and by crosslinking them. The more bond it makes and the gel will have a strong, hard and durable structure, so much as G blocks are in the chemical structure of the alginate. Because of the high dissolution rate in the water, a weak gelling occurs. Slow gelling causes hydrogel to have a stronger bond and structure. In tissue engineering applications, gels formed by covalent crosslinking are used generally. This is because of its more durable structure. When ionic crosslinking occurs, in stress-related strains, the bond structure is weakened by losing water from the gel and plastic deformation occurs. Alginate has been tried to bind with different molecules to improve and strengthen the bond structure. The swelling and hydrophilic structure of hydrogel was ensured by crosslinking with poly (ethylene glycol) -diamines and using different molecular weights. Alginate has been tried to bind with different molecules to improve and strengthen the bond structure. The swelling and

hydrophilic structure of hydrogel was ensured by crosslinking with poly (ethylene glycol) - diamines and using different molecular weights [42].

These natural polysaccharides are generally used in many fields such as biomedical, cosmetic, food, medicine and textile due to the gelling of the materials with homogeneous solubility and their viscous and stable structure [41]. Among the medical applications of alginate, the most popular is its use for drug release. Tissue regeneration and skeletal processes and local drug release are other usage area. Due to the very small nano-sized por surfaces of alginate gels, small molecules can enter the gel by rapid diffusion. Another usage of alginates is wound dressings. Wound dressings, which are generally used, provide a dry environment and it works to provide a protective effect by closing the wound from any external substance and microorganism entry. On the other hand, alginate gels provide a protective and moist environment for the wound, increasing the healing rate more. Substances such as silver and zinc added to the alginate gels have reinforced the treatment thanks to their wound-healing properties, antibacterial, antmicrobial, encouraging keratinocyte migration, and epithelization properties. Ionic cross-linked alginate gels are used. Ionic cross-linking with molecules injected into the alginate gel created it. For use on wound, calcium ions in the alginate are replaced with sodium ions in the skin and form a dissolved sodium alginate gel on the wound. Absorption of fluid in the wound causes the hydrogel to swell. Then, alginate gel is renewed and treatment is continued. Concurrently, it absorbs the bacteria into the gel and with this replacement; the bacteria are removed from the wound. At the same time, the anti-bleeding effect of the alginate gel is observed. If the rate of guluronic acid in the alginate content is more than the ratio of mannuronic acid, a gel formation with higher absorbency is observed [43].

1.3. SKIN

Skin is the most important organ that protects us from external factors. In addition to providing protection against chemical biological and physical external factors, our skin has duties such as balancing body temperature, blood pressure, removing toxins from the body through sweat, fluid and body waste and providing air intake from the outside environment with its breathable surface [44]. Skin is an area where beneficial flora and bacteria can survive while protecting the skin from external microbial agents, infections and external

factors [45]. In addition, the structure of the skin can be interpreted about diseases and disorders in the internal organs and body by observing the color sensitivity and quality by medical staff. While at the same time, externally applied substances such as perfume cosmetics and materials used for skin care are absorbed by the skin in a controlled manner [45].

1.3.1. Skin Morphology

Human skin structure is multilayered. The outermost epidermis, dermis in the middle and the innermost layer is called subcutaneous tissue. The epidermis, which is the outermost surface, has layers in itself. To explain the structure of the epidermis simply, it can be summarized as three basic cell types and four separate layers. The cell types in the epidermis are divided into 3 categories: keratinocytes, langerhans cells, melanocytes [44]. The epidermis with four layers has an important role in the absorption of cosmetic products applied from the outside. These can be classified as the basal cell layer (stratum germinativum), the squamous cell layer (stratum spinosum), the granular cell layer (stratum granulosum), and horny cell layer (stratum corneum) (see Figure 1.2.a) [46, 47]. There are stratified squamous epithelial cells in the epidermis. Cells that separate the balance between the internal and external atmosphere of the body in a way that will not harm the body is epithelial cells. There is a tight epithelial tissue structure on the skin surface, but this does not prevent the entry and exit of substances. The main component of the epidermis is keratinocytes. These cells produce protein fibers and their assignment is synthesised keratin. Keratinocytes bind to the basal layer as well stratum germinativum perpendicular to the dermis [44]. Keratinocytes are a very strong protection shield with a tight protein structure for the skin, as well as protecting the skin against UV radiation by holding melanin pigment after its maturation. melanin cells are not produced in keratinocytes. Apart from the UV radiation protection of melanin pigment in keratinocytes, there are other effects to protect against injuries, to provide free radical cleaning and antimicrobial effects and help epidermal cells maintain their balance [48]. The basal cells also contain the pigment melanin produced by melanocyte. It is the second mitotically active region that turns into outer epidermal cells in the basal layer. Epidermal stem cells with a very slow cell cycle are located in the basal layer but can increase speed by changing the division of stem cells in cases of injury and wounding. Changes in cell cycle

and growth rates may also occur in cases caused by DNA damage. Cell migration between the epidermis layers occurs over a long period. They traverse 14 days from the basal layer to the cornified layer and from there to the outer epidermis, which takes 14 days. Squamous cell layer above and adjacent to the basal layer. The spaces between desmosomes that support the link between epidermis cells and resistant to physical impact and stress and spinous cells are bridged and connected. These intersections allow physiological communication, and thanks to this communication, necessary actions can be taken for cell metabolism growth and differentiation. In the granular layer, keratinization takes place. When the hard granules produced by the cells move upwards and become in motion, they can experience differentiation by turning into keratin and epidermal lipids. The cells that protect the epidermis and prevent water loss and incursion are horny cells. Corneocytes surrounded by an extracellular lipid matrix have a high protein content and low lipid content [44]. Melanocytes are cells that color our skin, but they do not exist only in the epidermis, hair, and iris [49]. Melanocytes can be found in both layers of our skin; dermis and epidermis [48]. There are melonocyte cells in different parts of human body such as inner ear, nervous system and heart. This shows that the only task of melanocytes is not to produce melanin. However, encolouring will be examined and with its presence and reaction of the epidermis against sunlight. The life cycle of melanocytes can be explained in several stages. melanocytes migrate and growth after embryonic neural crest cells lineage specification. In the next stage, melanoblasts are divided into melanocytes and melanin forming [49]. Melanin in the epidermis is available in two different forms. These are pigment eumelanin, which is abundant in dark-skinned individuals and causes the dark color of the skin, and pheomelanin, a light-color sulfated pigment [48]. Melanosomes move to keratinocytes before they reach the final stage that cell deaths. Embryonic melanocyte cells in the epidermis and hair and eyes are the same, but their development is different. The emergence, development, functioning and life cycle of melanocyte cells helps to understand some skin diseases. These diseases are related to the color or colorlessness of the skin [49]. Another epidermal cell, langerhans cells are the more common cell types in the squamous and granular layers of the epidermis [50]. When these cells that recognize soluble antigens encounter a membrane-bound antigen, they form cell granules [51].

Merkel cells are found in the stratum basale but they are very few. It is in cells related to sensation and is associated with cutaneous nerves. It is found more in palms, soles and fingertips [44].

There are auxiliary structures in the epidermis cells (see Fig 1.2. (b)). These are hair follicles, sweat glands, sebaceous glands and nails. There are three (3) types of sweat glands; eccrine, apocrine, apoecrine and these are epithelial cell groups. Eccrine sweat glands are effective in regulation of heat; apocrine glands are related to odor release. Apocrine glands are not on the surface of the skin, they are found in the subcutaneous fat. Apoeccrine sweat glands are dressings that open directly to the skin surface, their precursors are the eccrin sweat gland, but it has been shown that they secrete much more than eccrine [52]. Sebaceous glands are located on the underside of the hair follicle. The arrector pili (AP) is a muscle bundle attached to the bottom of the hair follicle and is an important factor in the hair growth cycle. Hair follicles vary in size and thickness depending on their area in the body, but they all have the same basic structure. There is a third bud at the level of the sebaceous gland and under the hair follicle, which is attached to the apocrine gland. Hair color is determined by melanosomes in hair and hair shafts extend under the dermis [46]. The sebaceous glands attached to the hair follicles are mostly found in the face and head area. Lipid droplets known as sebum are found in the sebaceous glands. Sebum production is related to the functioning of hormones, especially androgen hormones are also stimulated by thyroid and growth hormones [44]. Another cause of acne is skin pores. The pores naturally found on the skin are pilosebaceous or ostia of the sweat ducts. They are too small to be seen with the naked eye, 40-80 μm size and about 5-10 μm in diameter, and are evenly distributed on the skin surface. However, the skin pores, which called laymen, are visible to the naked eye and their sizes range from 250 to 500 μm. They are generally seen on the nose, chin, forehead and cheeks, and are considered as a problematic structure, not a normal structure. It has been observed that the distribution and size of this porous structure changes in factors such as race and age [53].

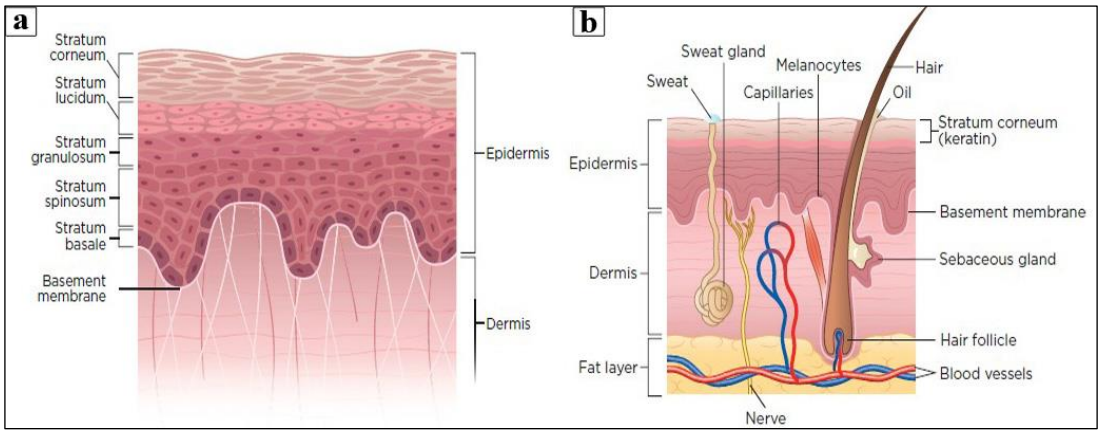

Figure 1.2. Anatomical structure of the skin (a) Epidermal layers of the skin, (b) Cross-section view through the skin [54].

The dermal epidermal junction consists of two layers. Lamina lucida, which is a thin layer and located under the stratum basal, and lamina densa, is a thicker layer in connection with the dermis [54]. The dermis and epidermis are connected by a porous structure. This interface is an active structure where cell and fluid interchanges are observed [46]. This layer contains more basal keratinocytes, in addition, a small amount of dermal fibroblasts [55]. This structure acts as a support for the epidermis and determines the skeletal structure of the cells. Basal lamina is a layer synthesized by type IV collagen and dermal microfibrils [44].

The dermis is the skin layer that supports the epidermis and interacts. It is effective in injuries, skin repair, epidermal and dermal cell renewal and development. The dermis is effective to protect both its own tissue and epidermis tissue. Since there are no cells that provide blood-circulation in the epidermis, blood and oxygen-circulation is provided by the dermis. Dermis is a connective tissue that contains nerve and vascular networks, epidermis-related appendages, and contains fibroblasts, macrophages and mast cells. It has groups of cells that contain lymphocytes, plasma cells, and leukocytes. With its structure supporting the epidermis, it protects the elasticity and strength of the skin, provides thermal regulation and fluid balance [50]. Collagen and collagen fibers main component type I collagen that provide the strength of the skin, elastic fibers that provide the elasticity of the skin are found in the dermis [46]. The weakening of elastin and collagen due to external factors and loss of structure appear as wrinkles on the skin. The hypodermis

contains a subcutaneous fat cell layer. It is a skin and body connection and contains blood vessels and nerves that nourish the skin [50].

Hypodermis is located under the dermis. It generally consists of fat but is found in blood vessels and nerves. It supports the skin and provides its posture while at the same time isolating it from the cold [54].

1.3.2. Skin Barrier

It is the stratum corneum layer of the skin, which helps and acts as a barrier, which protects our body from the external factors. This structure, which is in the outermost layer of the epidermis, is a structure rich in protein and lipid. At the same time, this structure, which is in the outermost layer of the epidermis, which protects the internal homeostasis by preventing water loss and providing thermal insulation and balance, is a structure rich in protein and lipid. It consists of stratum basale division, consisting of tightly combined keratinocyte layers. With the differentiation and upward movement of keratinocytes, keratins, microfilaments and microtubules are formed. These structures begin to act as a protective layer on the outermost layer of the skin. Stratum momentum consists of dead cells without nucleus. This outer protective structure includes comeocytes and lamellar lipids. Comeocytes is a structure that has water retention and natural moisturizing factor (NMF) effect, which the skin's moisture storage can be called. High water content is important for the smooth and tidy establishment of this structure. The elasticity and pliability of the skin is related to the water content. Skin defects may occur in the loss of water and in the loss of function and association in the barrier lipids. The amount of lipid in the stratum corneum is much more important than the cell number and thickness in terms of barrier function [56]. The effectiveness of nonpolar lipids in the epidermal barrier is greater. It has been found that the barrier structure has two forms: a layer formed by nonpolar lipids and a layer with second level sphingolipids [57].

1.3.3. Skin Types

Skin type’s classification is an important guide for skin treatments and skin care. In general, four skin types are defined in the classification: normal, dry, oily, combination.

However, the skin types classification is accepted in this way, but there are different approaches, for example, it can be classified as dry or oily, sensitive or resistant, with or without pigment, and without wrinkles or wrinkles [58]. While making the skin type classification, the amount of sebum secreted by the skin is considered. Sebum secretion in the T (forehead, nose, and chin) region of the face is much more than the U (cheeks, temples) region. Sebum secretion can be changed by external factors such as seasonal changes. The average sebum secretion for the whole face is 118.7-180.9 μg / cm^2. The average sebum secretion for dry, oily and mixed skin types is different for each skin type. 97.3 - 147.6 can be evaluated as dry skin, 204.6 - 235.4 for oily and 109.8-145.5 μg / cm^2 for mixed skin. It is known that individuals with normal and healthy skin have a slightly acidic value between 4 and 6. Secretions such as sebum secretion, sweat, acid, butyric acid, protocatechuic acid, amino acids and free fatty acids affect ph. Acidity level of secreted sebum is 5.6-6. Therefore, sebum thrown from the skin is related to the ph of the skin. In the characterization of the skin types, the features that can be distinguished visually are determined. In normal skin type, it has an ideal size pore a normal skin tone and structure, and a skin type with generally less pimple and generally balanced distribution. The oily skin type has large pores, a glossy but dull appearance, a thick skin, mostly a spotty appearance. In dry skin, sebum secretion is low compared to normal skin, it is a type of skin that often has a feeling of tension, wrinkled and broken appearance and less porosity. If T zone is oily and U zone is dry skin types, that is called combination skin type can be said determine according to mixed skin areas [59, 60].

1.3.4. Skin Problems

1.3.4.1. Wounds

The wound is the deterioration of tissue integrity and skin structure because of trauma. In deep injuries, blood vessels, muscles and nerves can be affected.

Wounds are generally categorized in two classes: acute wounds and chronic wounds. Acute wounds heal as expected and during the period required to heal. Hovewer, chronic wounds do not heal for a long time, the healing process does not end for more than about 6 weeks and the process is blocked [64]. Apart from the difference between acute and

chronic wounds healing time, bacterial environment, growth factor and protease profiles and inflammatory responses were found to be important [65]. If the wound types should be divided into small subheadings, these are; puncture wounds, bite wounds, abrasions, burns, chronic wounds, diabetic foot ulcers, pressure ulcers, venous insufficiency ulcer and ıschemic wounds [64].

There is already a bacterial balance on the skin; this bacterial natural flora also helps to provide a natural protection against external factors. Stratum corneum and eccrine, apocrine and sweat gland secretions are important for the function of normal flora. Thanks to these secretions, pH takes a value between 3 and 5 and creates an unfavorable surface for organism development. Skin natural flora consists of many types of bacteria species and eukaryotic fungi. On dry surfaces of the skin, organisms such as *Staphylococcus Epidermidis, Micrococcus* organism, propionobacteria, hair follicule mite and *Pityrosporon* yeast, generally moist surfaces, corynebacteria, mycobacteria, *Staphylococcus aureus,* and gram-negative bacteria are found. The growth of pathogenic bacteria is limited as a result of the competition of beneficial bacteria in the normal flora for nutrients and the balance of pH [45].

However, many bacteria accumulate and reproduce in chronic wounds. Inflammation and bacterial growth around the wound are a factor that delays wound healing. When the bacterial balance in flora is measured quantitatively in general, is below 10^5 bacteria per gram of tissue. B-hemolytic Streptococcus is at a dangerous level of pathogenicity. Conditions that exceed the value of 10^5 and disrupt balance are considered dangerous for wound healing. Open wounds and granulation tissue is an opportunity for bacteria to enter and reproduce. *Staphylococci, Streptococci, Enterococci,* the gram-negative bacilli *Pseudomonas sp, Enterobacter cloacae, and Escherichia coli,* and the anerobe *Peptococcus magnus* [66, 67]. *P. aeruginosa, Providencia,* peptococci, *Bacteroides* sp, and *Clostridium* sp. are found in chronic wound tissues and and block the healing process [68, 69].

Wound healing is simply a restoration of damaged tissue. Wound healing is a complex process in which different cell types, various cytokines and growth factors are effective. Cytokines are molecules with protein structure that provide the interaction and communication between cells and growth factors are a subset of cytokines. Platelet-derived growth factor, fibroblast growth factor, transforming growth factor, epidermal growth

factor, insulin-like growth factor, granulocyte nacrophage colony stimulating factor, tumor necrosis factor are examples of growth factors [61]. The role of cytokines in wound healing is the transfer of inflammatory cells and fibroblasts to the wound site, they provide cell proliferation, activate angiogenesis and extracellular matrix formation [62].

To summarize the healing process after injuries includes hemostasis, inflammatory and proliferative cellular responses and extracellular matrix remodeling phases. All wounds heal with the same basic steps. With the guidance of cytokines, hemostasis is achieved by contacting the collagen in the vascular wall, which opens the platelets, by contacting the collagen and forming a temporary clot. During the inflammation process, coagulation factors are activated after coagulation in the hemostasis process, the clot is further reinforced by forming fibrin. Vascular permeability increases, neutrophils, monocytes and macrophages are activated. Neutrophil leukocytes destroy bacteria. Monocytes turn into macrophages, and various growth factors and cytokines are secreted. Macrophages destroy bacteria as well as dead tissue and cells. New vessel formations begin with angiogenic growth factor release and granulation tissue develops. Thanks to the veins, oxygenated blood reaches the wound and the healing process is accelerated. Fibroblasts make collagen around new vessels. With the proteoglycans and fibronectin, they produce, collagen and other cells are connected. At this stage, granulation tissue is formed. Fibroblasts produce collagen fibers then epithelizationand contraction improves occurs. Regeneration if tissue damage is too large starts from the edges of the wound and continues with the epithelial granulation tissue. Migration continues until the epithelial tissues unite. Then, thanks to myofibroblasts, the size of the wound is reduced by contraction. When epithelialization is completed, the proliferation phase ends and the transition to the remodeling phase is made. The remodeling phase is the remodeling and exchange of collagen fibers. Type III collagen, which is hypotonic, turns into type I collagen, which is tighter over time. In summary, the wound healing process is completed by providing coagulation, phagocytosis, reconstruction and repair of skin functions and finally damaged tissue tension force [63].

1.3.4.2. Acne

It is known that the formation of acne is caused by excess sebum in the skin, and this is due to excessive secretion of the sebaceous glands. The sebaceous glands and their anatomical

location are associated with the differentiation of the hair follicle and the epidermis. While the number of sebaceous glands remains the same throughout life, their size increases with age. If the sebum needs to be identified, a nonpolar lipid mixture is synthesized by the sebaceous gland and synthesized to help evolutionally heat insulation. Androgens and prolactin hormones that affect the sebaceous glands, thereby causing sebum secretion. Estrogens and glucocorticoids and show an inhibitory effect on sebum release, which affects the sebaceous glands. The human sebaceous glands secrete a lipid mixture that contains some free cholesterol. This lipid composition was found to be affected by excess sebum secreted by age and sebaceous gland activities. These sebaceous lipids ensure the integrity of the skin barrier. It has been determined that sebum carries antioxidants to the surface of the skin and sebaceous lipids show anti-inflammatory effects. In summary, acne vulgaris can be define as an immunological response to products different from extracellular products on the skin surface [70].

Combining keratinocytes and increased sebum secretion causes the formation of a lesion called microcomedo. Comedones are formed by enlarging the follicle and accumulating sebum residues and keratinous in the microcomedo [71]. The transformation of Propionibacterium acnes, which is normally found on the skin surface, into an inflammatory papule or nodule with its accumulation in the sebaceous follicle causes acne pathogenesis. After these stages, the accumulation of polymorphonuclear leukocytes, distention and pustule formation were observed, and an inflammatory response was observed in the acne lesions at an early stage. Accordingly, some studies have shown that the perifollicular and papillary dermis contain CD^{3+} and CD^{4+}, T cells and a much higher number of macrophages than normal [72]. Studies have shown that there is no link between proinflammatory cytokine levels and the number of microorganisms. It has been observed that cytokines, which play a role in the regulation of inflammatory and immune responses, are effective in acne pathogenesis. Although the onset and spread of inflammation in acne is not fully understood, the presence of P. acnes has been proven, but in the absence of P. acnes, other inflammatory routes have been observed. It can be said that inflammation is versatile for acne lesions [73]. Acne vulgaris trigger P. acnes produces propionic acid, acetic acid and free fatty acids, so the skin ph changes accordingly. However, acne presence has not been observed as a factor affecting skin ph in studies [59].

1.3.4.3. Wrinkles

Wrinkles are thought to be related to facial movements, as skin wrinkles are particularly active in areas of the skin that are very mimic and have repeated movements. It was thought to be related to the degree of facial movements and the number of repetitions. Wrinkles that occur regardless of muscle movements are called dynamic wrinkles, while wrinkles in immobile areas are called static wrinkles. In a study conducted with volunteers, the degree of wrinkles formed after performing very mimic muscle movements, facial movements were measured, and they compared with the control group. In this way, wrinkles in static and dynamic states are compared and analyzed and and it has been found that facial movements are associated with static and dynamic wrinkles. It is known that static wrinkles increase with age depending on the area around the eyes, forehead and lips, and other movement muscles of the face, while it is also known to increase in dynamic wrinkles [74]. Wrinkles occur mostly due to cutaneous aging and can occur both through years with time transition and through external factors. Intrinsic and natural aging of the skin is associated with tissue loss and change. It has been observed that older skin is drier and less flexible compared to younger skin. Deeper and coarse wrinkles occur in wrinkles of external factors; spotted hyperpigmentation and a marked loss of elasticity are observed. The factors that cause exogenous aging are chronic exposure to ultraviolet (UV) rays of the sun and smoking. Reducing the production of extracellular matrix proteins and increasing the level of remodeling is the biological process of skin aging. The loss and degradation of the elastic fiber network, especially in the dermal-epidermal junction, and loss of microfibrils are among the causes of aging. Cosmetic products applied externally can be used to recover this network [75]. Sunlight causes changes and wrinkles in the skin structure known as photoaging on the skin. Some grading systems are used in wrinkle formation assessment. Grading scales, visual analog scales and photographic grading scales are some of them [76]. Using sunscreens, anti-aging products, reconstructive masks and creams has been shown to be a potential benefit. It has been observed that topical applications related to hormones and biological based, vitamin, mineral and herbal cosmetic products are effective in reducing the natural wrinkles due to external factors or aging [77].

1.3.4.4. Skin Damages Due to UV Radiation

When the skin is exposed to sunlight, differentiations occur in the epidermis cells it contacts. This reaction occurs in melanin cells. When our skin is exposed to sunlight, differentiations occur in the epidermis cells it contacts. This reaction occurs in melanin cells. It plays a protective role in the skin's exposure to UV radiation. Melanomas and basal / squamous cell carcinomas are more common in fair-skinned people than congenital skin color. Differences in melanin levels were observed inversely proportional to DNA damage caused by UV radiation compared to different ethnic groups. DNA damage in the upper and lower epidermal layers was investigated in different skin types. Photocarcinogenesis increased in light-skinned individuals. It was seen that there are two main reasons for this. The first of these is said to be easier to prevent DNA damage in the lower epidermis of individuals with darker skin, namely the pigmented epidermis. Secondly, apoptosis caused by UV radiation, in other words, cell death caused by self-destruct mechanism is more common in dark skinned individuals. This indicates that individuals with dark skin have the potential to self-escape from UV-damaged cells. Therefore, the reason for this decreased photocarcinogenesis in dark-skinned individuals has turned out to be the ability to remove the damaged cells, naturally [49].

UV radiation is classified as a complete carcinogen because it is a tumor initiator agent. In addition to being carcinogenic, it has many negative effects on the skin such as atrophy, pigmentary changes, wrinkling and malignancy, inflammation and degenerative aging [78].

One of the permanent effects of uv radiation is that it causes decreased synthesis of collagen and elastin structures in the dermis [79]. Photoaging in the skin depends on the degree of UV radiation and the amount of melanin in the skin. It activates the cell surface receptors of keratinocytes and fibroblasts in the skin and causes disruption of the extracellular matrix structure and dermal collagen breakdown. Dermal collagen destruction causes damage and wrinkles to the skin [80].

Freckles are hyperpigmented molecules. In skin type with freckles, melanized long granules are observed, while in those without freckles, round and short melanized granules are observed. There are two different types of melanocytes production in individuals with freckles. Apart from its natural freckle structure, it has a type called sunburn freckles

caused by exposure to sunlight. These freckle types have clinically distinctive features. Erythema and edema followed by tanning and peeling occur after a normal person's UV exposure. People who have freckles, signifying a genetic component on their body may develop new freckles and the type and color of freckles may differ from each other [81].

1.3.4.5. Dryness

Presence of water is of great importance for the skin to continue its normal function. The outer layer of the skin that is stratum corneum has important role in water retention by preventing the loss of transepidermal water in natural corneocytes with natural hygroscopic agents and through intercellular lipids in the stratum corneum preventing transepidermal water loss. In cases where transepidermal water loss occurs, the skin's enzymatic functions are disrupted, and its desquamation function changes, causing the skin to dry and flaky. The dermis contains hyaluronic acid with hydrophilic properties that help the skin hydrate and maintain its plastic structure. Hyaluronan is an ingredient that helps maintain the epidermis barrier structure and is present in the structure of the stratum corneum. Another water dispersing and protective component is the water-carrying protein aquaporin-3 (AQP3). The bonds in between the layers of the epidermis stratum granulosum and stratum corneum have water-retaining properties [82]. In general, the biggest problem with dry skin is the excessive shedding of the horny layer caused by dehydration and weakening of the protective epidermal barrier [83]. Climatic factors such as temperature, humidity and wind effects can cause water to move away from the skin through evaporation [84]. Skin problems such as atopic skin, psoriasis, ichthyosis and contact dermatitis also cause damage in the functioning of the epidermal barrier caused by dryness. The epidermal barrier can be hydrated with topical moisturizers; the moisturizers can remain on the surface, absorbed into the skin, metabolized or disappear from the surface by evaporation or contact with other materials [85]. The absorption ability of the skin is affected by the degree of dryness and dermatitis. The loss of water in the skin due to dryness in the stratum corneum layer disrupts the barrier function and the size of the corneocytes may decrease, which reduces the intercellular penetration. While the absorption rate in the epidermis may be affected by dryness, it is likely that there is a stronger barrier formation in the underlying surface layer of skin [86]. The water binding properties of the applied moisturizing products activate the moistening feature by forming an occlusive layer in the

upper layer of the epidermis, which prevents water evaporation and increases the water content. In addition, breaks on the skin are filled with water taken from the applied product and the skin becomes more elastic and smoother [87]. Moisturizing application smoothes the skin, fills the gaps between desquamated skin scales and restores the ability of lipid layers between cells to absorb, retain and redistribute water. Increased hydration prevents corneocyte build-up. Moisturizing products are also absorbed from the skin surface and have effects on the skin mechanism.

Moisturizing agents do not only save the skin from cosmetic dryness or wrinkled appearance, they have also other benefits such as by blocking various inflammatory mechanisms. They provide anti-inflammatory effect, cooling effect due to water evaporation, reduce itching symptoms and provide antipruritic effect and show antimitotic activity by providing therapeutic benefit for dermatoses with increased epidermal mitotic activity such as psoriasis protects and strengthens the skin barrier and provides wound healing effect with different ingredients [88].

1.3.5. Mask Types Treating the Skin Problems

Facial skin is much more sensitive from body because of internal factors effects and biologically and structurally open to external factors than other parts of the body. Generally, the skin on the face has more problems and requires care, protection and treatment. One of the most used products for skin care are cosmetic masks. It is a product that the benefit of active ingredient content can be seen more than topical applying product by both having a practical use and staying on the skin for a long time. Skin care with mask can be done to purify the skin from makeup and air pollution effects to the skin, dehydration, ultraviolet (UV) exposure, aging, stress, oiliness, rapid sebum production, enlarged pores. If the skin is oily, excess sebum, oil and contaminants should be removed, and if the humidity is low, it should be supplemented with moisture. They should also have non-acnegenic, non-comedogenic and hypoallergenic effects. In terms of content, masks can have many different types and types of content such as moisturizers, exfoliants, brightening and herbal compounds, vitamins, proteins, minerals, growth factor (GF), biopharmaceutical and coenzyme. There are four types of masks on the market: sheet mask, peel-out mask, rinse-off mask and hydrogel mask. Sheet masks are types of masks

that are soaked in solutions with an active ingredient called serum and can take the shape of the face. The sheet mask prevents the water phase from evaporating, allowing the components to penetrate the skin thoroughly. Sheet masks are generally not recommended for oily and acne skin because it is thought to increase the number of bacteria on the face. The material of this mask type can be papers, fibers or gel types. There are varieties such as fiber (nonwoven), pulp, hydrogel, bio cellulose and it is disposable. Rinsable masks are the type of masks that have a creamy texture generally but can be waxy and muddy and are removed with water after waiting for a certain period. Waxy masks usually regulate the level of hydration in the epidermis and limit transepidermal water loss. Their intended use can be moisturizing, cleaning, toning, peeling. Peeling masks are peeled off in one layer afterwards sticking to the skin after waiting for a certain time. Peel-off masks often contain polyvinyl alcohol (PVA) or polyvinyl acetate (PVAc) content, which causes occlusion and tensor action. Alcohol has a lower vapor pressure than water and is used as a drying agent that can control the application time because it evaporates more quickly. Matrix concentration determines the viscosity, thickness and film formation of the applied mask. It is used for a smoother and deeper cleaning. Since it is used by peeling, it removes the dead skin, helps to regulate dullness and color inequality, to fade fine lines and to clear and remove skin pores. Although hydrogel masks are accepted as sheet masks, they are slightly different from them. Hydrogel material is much more advantageous than other mask types in terms of its properties. They are masks made from a gel polymer that holds 99 percent liquid due to their capacity to hold 500 times more the size of the molecule. Therefore, it gives much more moisture than others do. Hydrogel is cover with serum containing therapeutic or restorative active substance or it is produced embedded in the material for release to the skin during penetration. At the same time, it helps to increase cellular function thanks to its structure that is compatible with the skin structure and easily penetrated. Sensitive skin is also a type of skin that can react quickly and have a range of conditions, from genetic ailments to serious allergies, and skin diseases such as rosacea, eczema, dermatitis. Hydrogel mask is the most used type in the treatment and care of this sensitive skin. Hydrogel masks are used to take advantage of cooling and soothing effects with both high water content and polymer soft texture. The hydrogel mask is also suitable for long-term use and is more preferred because it exposes such disorders to long-term treatment. It is used in clinical practice in cases such as injury, burns and irritation with its cooling and soothing effects [89-96].

1.4. *HYPERICUM PERFORATUM*

Hypericum perforatum, an herbaceous plant species belonging to Europe and Asia. It is referred to as commonly St. John's Wort, and its Latin name *Hypericum perforatum*. It belongs to the Clusiaceae family and hypericum class [97]. Some taxonomists call the hypericum family a different name; the Hypericaceae [98]. *Hypericum perforatum* L, which has been trial studies in the clinical and laboratory areas for 30 years, is the most used medical type among Hypericum species [99]. The parts of the plant used are those that are above the ground. This plant, which was used even in ancient times, is used topically in complaints such as burns, wounds and snakebites that cause complications such as inflammation, redness and inflammation on the skin surface. In present, it has antidepressant, antibacterial, anti-inflammatory, anticancer, antimicrobial and antioxidant effects. This plant, which can be used topically and systemically, is an herbal medicine used by people [97]. These plants have the same effects both in their raw extracts and in the form of oil [100]. It is seen that the *Hypericum perforatum* is in the class 2D record in evaluating the effect and effectiveness of the medicinal use of the plant on human health. In this assessment by the American Herbal Products Association (AHPA) has made this classification on the reliability of this product based on Commission E monographs and in vitro studies, and stated that it can strengthen pharmaceutical MAO inhibitors in the standards, but there is insufficient evidence to prove this [101]. The official 2009 HMPC monograph of the European Medicines Agency is allowed to be used topically to treat minor wounds and inflammation as a traditional medicine product [102].

1.4.1. Composition of *Hypericum perforatum*

When the plants collected from different regions or oils extracted from different parts of plants in the same regions were analyzed, different compounds were detected. In a study in which the components of *Hypericum perforatum* oil were analyzed, 134 components were identified in the analysis made with GC and GC / MS methods. The main components in the analysis of this oil, we can classify it as two chemotypes, the first one is essential oils containing germacrene D (18.6 percent), (E) -cariophylene (11.2 percent) or cariophyllene oxide, and 2-methylostane (9.5 percent), a-pinene (6.5 percent) in the second group and

other compounds are bicyclogermakrene (5.0 percent) and (E) -p-okimin (4.6 percent) [100]. Hydroalkalic extracts of the *Hypericum perforatum* plant contain 60 percent ethanol and 80 percent methanol [103].

The chemical structure of the plant is remarkably diverse. It can be listed flavonoids (0.5-1.0 percent, including hyperoside, quercetin, and rutin), naphthodianthrones (0.1-0.3 percent of which 80-90 percent are hypericin and pseudohypericin), phloroglucins (up to 3 percent hyperforin), xanthones, biflavones, phenylpropanes, proanthocyanidins, sterols, essential oils, tannins, carbolic acids, aminoacids, anthraquinones, carotenoids, cumarine, and vitamins [97,104]. Naftodiantron compounds in the plant are generally substances that cause intense red color in oil and extract production and are said to have phototoxic properties. The most effective component of the naftodiantron group is hypericin. (Figure 1.3.a). There are stable types such as hypericin and pseudohipherin, unstable types such as protohiperis and pseudoprotohiperis. Compounds of unstable structure turn into compounds of stable structure. Pseudohypericin is the main compound as a naftodiantron and is found 2 - 4 times more than hypericin. Hypericin and pseudohypericin show antiretroviral properties, activate this by inhibiting protein kinase C, and have a lethal and growth-inhibiting effect on cells. Although phototoxicity is observed in the application of high amounts of hypericin, it can be converted into a benefit and used as a photosensitizing agent for photodynamic cancer therapy. In addition, no phototoxic effects were reported in pseudohypericin. There are two close compositions contained in the content of phloroglucin, these are; hyperforin and adhyperforin containing methyl groups. Hyperforin compound has antibacterial properties and shows antidepressive effects in oral use, in this case, inhibition of neurotransmitter systems. (Figure 1.3.b) In addition, hyperforin has been found to have anti-malarial activity and have a destructive effect against Plasmodium falciparum [103]. Flavonol Clycosides contain quercetin as aglycon. Their content varies from 2-4 percent, and hyperoside (hyperin) and routine are predominantly dominated by H. perforatum glycosides followed by quercitrin and isocersitrine [98, 105] There are studies showing that quercetin is an anticancer agent [106]. Two compounds of biflavones, in amounts of 0.1 to 0.5 percent 3,8p-biapigenin and in amounts of 0.01 to 0.05 percent amentoflavone, were detected in H. perforatum [98]. Anti-inflammatory and analgesic activities of amentoflavone have also been observed [107]. Tannins and Proanthocyanidins are found in the form of the tannin fraction, which is present in an amount of 6.2 to 12.1

percent. Proanthocyanidins have many antioxidant, antiviral, antimicrobial and vasoactive biological effects [98]. Phenylpropanes class of compounds are esters of hydroxycinnamic acids such as p-coumaric acid and caffeic acid. It has been shown to have local anesthetic effects. There is also chlorogenic acid in a concentration below 1 percent and it has central stimulating activity [104]. Proanthocyanidins have many antioxidant antiviral, antimicrobial and vasoactive biological effects [98]. Phenylpropanes class of compounds are esters of hydroxycinnamic acids such as p-coumaric acid and caffeic acid. It has been shown to have local anesthetic effects. There is also chlorogenic acid in a concentration below 1 percent and it has central stimulating activity [104]. Compared to other components, essential oil density is low for *Hypericum perforatum*, and extraction rating is between 0.05-0.9 percent. However, this ratio varies depending on the environmental effects of the plant, time and area it is collected. In previous studies, essential oils have been observed to be effective against bacteria such as *S. typhimurium, S. aureus, K. pneumoniae, E. coli, C. albicans,* and in some studies, it was observed that *P. aeruginosa* was ineffective in bacteria and low activity was observed in others. The accepted mechanism of action of terpenes in essential oils shows this activity is estimated as the lipophilic compounds disrupting the cell membranes [191].

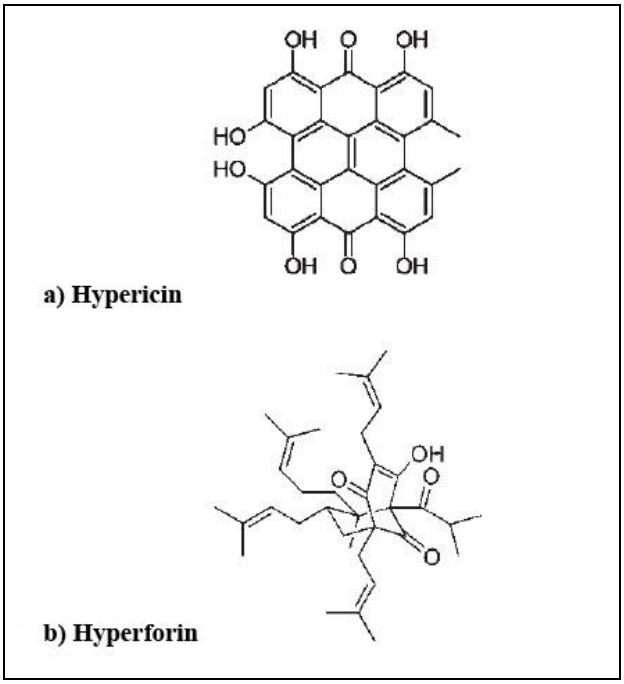

Figure 1.3. Chemical structure of important components of *Hypericum perforatum* (a) hypericin (b) hyperforin [226]

Contains eleven different secondary metabolites in hypericum species. Except for hyperforin and hypericin, there are metabolites with antibacterial, antiviral and antioxidant properties in topical use (Table 1.1).

Table 1.1. Effects of *Hypericum perforatum* metabolites in topical use [99].

Compound	**Activity**
Flavonoids (hyperoside, quercetin, and rutin)	antioxidant, antimicrobial, antiviral, anti-inflammatory, antitumor
Naphthodianthrones (hypericin and Pseudohypericin)	wound healing effects, anti-viral
Phloroglucins (hyperforin and adhyperforin)	antibacterial, anti-malarial activity and wound healing effects
Xanthones	antimicrobial and antiviral effect
Biflavones	anti-inflammatory, analgesic activity and wound healing
Phenylpropanes	anesthetic effects
Proanthocyanidins	antioxidant, antiviral, antimicrobial and vasoactive biological effects
Essential Oils	antibacterial and antifungal

1.4.2. Effects of *Hypericum perforatum* in Topical Application

1.4.2.1. Wound Healing

In a study to investigate the wound-healing effect of *Hypericum perforatum*, surgical Hypericum / Calendula mixture was applied to surgical wounds twice a day for 16 days, and a 38 percent reduction in the Surface Perimeter Area (SPA) measurements of the wound was observed [108]. When *Hypericum perforatum* was used as an ointment for burns of first degree, healing was observed after 48 hours. In the 2nd and 3rd degree burns, the healing rate increased three times compared to other treatment methods [109]. In the study in which topical *Hypericum perforatum* gel activity was performed for burns healing, 5 groups were tested comparatively, namely the control group, saline (0 percent, 9NaCl) group, silver sulphadiazine (1 percent) group, *Hypericum perforatum* and placebo group. Experimental burns on rats were divided into groups and different treatments were applied. *Hypericum perforatum* gel was obtained by methanol extraction. The methanol extract in *Hypericum perforatum* exhibited a healing effect in the burn wound by showing antioxidant effect and triggering fibroblast proliferation. *Hypericum perforatum* showed a higher healing effect in the acute period compared to other agents. It has been observed that it reduces collagen discolorization, vascular damage, damage to the hair follicle and sebaceous glands, and the epidermal thickness of the vessels is in a better state [110]. In another study, a mixture of *Hypericum perforatum* and calendula oil that the main active ingredient of which is hyperforin was applied to caesarean cuts and a comparison was made with wheat germ oil and placebo. At the end of four weeks, the hypericum mixture showed an healing improvement of 38 percent, while the recovery rate of others was 16 percent [111]. Applying *Hypericum perforatum* ointment containing 1.5 percent hyperforin to eczema wounds has been found to be much more effective for healing than placebo [112]. In a study showing *Hypericum perforatum* cellular level wound healing activity, alcoholic hypericum extract and dexpanthenol and titrated centella asiatica (TECA) were compared on embryonic chicken fibroblasts. For dexpanthenol, fibroblast proliferation is observed due to collagen production, polygonal cell count increase and mitotic activity. TECA stimulates an increase in polygonal cell count and collagen production in cells. In other words, dexpanthenol supports wound healing with mitotic activity, while TECA stimulates collagen synthesis by the proliferation of fibroblasts and thus wound healing is

supported. *Hypericum perforatum* causes wound healing in the same function as TECA. It has been observed in previous studies that it exhibits antiproliferative and apoptotic activity for hyperforin [113]. At the same time, it was observed in this study that the content of hypericin from plant extracts was not effective in wound healing [114].

1.4.2.2. Antibacterial Properties

Hyperforin, which shows antimicrobial properties in *Hypericum perforatum*, has a destructive effect against gram-positive bacteria and viruses. A photo activation process that causes cell death by disrupting some components of the cell membrane can explain this antimicrobial feature. This antimicrobial feature can be explained by a photo activation process that causes cell death by disrupting some components of the cell membrane [115]. It also has antitumor properties of hypericin, one of its active ingredients.

It showed hyperforin antibacterial activity to gram-positive bacteria such as *S. aureus, Streptococcus pyogenes* and *Corynebacterium diphtheria*. In studies, it was stated that this effect was observed at high concentrations of hyperforin [116]. Higher efficacy against gram-positive bacteria was observed compared to gram negative [112]. *Hypericum perforatum* ointment prepared in 3 different concentrations in the study on pathogenic bacteria such as *Moraxella catarrhalis, Streptococcus pyogenes (two lines), Streptococcus viridans* and *Micrococcus luteus ATCC9341* and it was observed that these bacteria stopped their development. This ointment has been prepared to be used in dermal and vaginal administration and has been shown to affect malignant bacteria, not benign bacteria in the vagina. The highest efficacy was determined in the highest concentration ointment [117]. Effectiveness has been proven against bacteria living in the large intestine, such as *Enterococcus faecium, Bifidobacterium animalis, LactobacillusIts plantarum* and *E. coli.* Two different concentrations of ointment were prepared as 10 percent water and 10/30 percent water / ethanol (v / v) solutions, and it was observed that the ointment containing ethanol was more effective against bacteria [118]. In addition to hyperforin, hypericin has antibacterial properties. In an in vitro study, the growth of *S. aureus*, not *E. coli*, was stopped when bacteria were exposed to hypericin at a concentration of 40 μM and below 30 min. The differences between bacterial membranes in gram irradiation and measurement method have been important and their effectiveness is measured by this in

contact and interaction with hypericin [119]. Comparing *Hypericum perforatum* activity, better antibacterial efficacy is seen in trials from plants harvested in August compared to July and this is considered due to hyperforin efficacy [120]. Flavonoid compounds do not appear to be antibacterially effective compared to other components of the plant [121]. Lipophilic compositions in plant components are much more effective than hydrophilic. Instead of *Hypericum perforatum* dissolved in water, its version, which dissolves in oil and cream, is much more effective as antibacterial [118,122]. In a study investigating its effectiveness on bacteria and fungi, hyperforin with a purity of 90 percent and concentrations of 0.1, 1.0, 10 and 100 μg / mL was used. Growth factor for gram-positive bacteria was observed at all hyperforin concentrations less than 0.1. No growth inhibition was observed in gram-negative bacteria and candida albicans. Penicillin-resistant (PRSA) methicillin-resistant (MRSA), *Staphylococcus aureus* reacted when using hyperforin. Cell viability comparison according to concentrations is as follows; The cell viability after treatment with 1, 0, 10 and 100 g / mL hyperforin was 100 percent, 80 percent and 75 percent [116]. There are bacteria that cause the initiation and development of dental caries and have a negative effect on caries formation even though it is normally found in the oral flora. Antibacterial activity of *Hypericum perforatum* has been observed for inflammatory bacteria in oral flora. The effectiveness of bacteria against such as *S. mutans, S. sobrinus, Lactobacillus plantarum* and *E. faecalis* was investigated using the micro-well dilution of H. perforatum ethanol extract and sub-extracts and it was found to have a destructive effect against all pathogens [123].

1.4.2.3. Antiviral Properties

Hypericum perforatum m active ingredient hypericin has been shown to inactivate viruses with a photoactivation mechanism. The effectiveness of Murine Cytomegalovirus (MCMV), Sindbis virus and herpes simplex virus 1-2 has been proven by studies. In addition, Flavonoid and catechin substances in *Hypericum perforatum* have exterminating effects against Influenza virus [124]. Hypericin and pseudohypericin are highly effective against DNA viruses with or without lipid content in cell envelopes. The preventing of propagation the spread of HIV virus intracorporeal have been observed [125]. It has been shown to be effective against hepatitis C virus in vitro [126]. The antiviral activity of hypericin and pseudohypericin can be explained by decreasing and stopping protein kinase

C and preventing its proliferation in mammalian cells [127]. The common feature of viruses affected by hyperisin is that they are enveloped viruses. Poliovirus and adenovirus are non-enveloped viruses and are not destroyed by hypericin. Another theory about the mechanism of action of hyperis is that it produces more reactive singlet oxygen induced by light and disrupts the structure of the proton in the envelope of the virus and thus has a destructive effect [128].

1.4.2.4. Antitumor Effects

In studies on hypericin with photosensitive properties, cell death occurs when hypericin of tumor cells reacts with oxygen [129,130]. In animals and in vitro studies, it has been shown that it prevents the growth and shrinkage of tumor cells in rat and human breast cancer, and other cancer cytostatic drugs show almost the same effect or lower effect. *Hypericum perforatum* and neem oil were applied together and serious therapeutic effect was observed for the treatment of acute skin toxicity in patients undergoing chemo-radiotherapy and radiotherapy for head and neck cancer treatment [131]. In addition, hypericin, a photosensitizing active substance, has been investigated in photodynamic therapy for cancer patients and has been shown to cause cytotoxic effect by causing cell death [132, 133]. The alloantigen presentation function of human epidermal cells (EC) was investigated by comparing the immunosuppressive effect of solar simulated radiation (SSR) in a mixed EC lymphocyte reaction (MECLR) to test the immunomodulator property of *Hypericum perforatum*. Hypericum ointment applied in vivo as well as hyperforin isolated and purified were compared in vivo and in vitro. Hypericum ointment and isolated hyperphorin have been shown to inhibit the proliferation of MECLR and T lymphocytes for the treatment of inflammatory skin disorders [134].

1.4.2.5. Antioxidant Effects

Hydroalcoholic *Hypericum perforatum* has antioxidant effect caused by the fact that it contains a lot of flavonoid in plants. It is evaluated in the antioxidant category especially because of its polyphenol content [135, 136].

In a study, quantification analysis of *Hypericum perforatum* methanol extract was performed and antioxidant activity was examined with DPPH radical scavenger and FRAP methods and it was determined that it has high antioxidant activity and no metal-chelation capacity. The content that causes antioxidant capacity from the plant content is flavonoids, hyperocyte more than hypericin and hyperforin [137]. Flavonoid rich extract of *Hypericum perforatum* have high antioxidant activity. In one study, the efficacy of *Hypericum perforatum* extract prepared with ethanol was measured with various tests and it was found to exhibit strong antioxidant activity. It is a hydrogen donor and an electron donor to the assay reduced to iron (II) in iron (III), preventing the peroxidation of lipid membranes in the liposome and inhibiting linoleic acid peroxidation, and also being an effective superoxide anion radical cleaner and the main antioxidant of metal ion chelation has been proven in a study that shows activity [138]. *Hypericum perforatum* component hyperforin, which has anti-inflammatory, anti-tumor and anti-bacterial properties, has also been investigated for its free radical scavenging activity with antioxidant properties. In an ex vivo study, it was seen that it significantly reduces radical formation after infrared ray exposure. In a randomized, double blind, vehicle-controlled study, it was found to be protective after UVB exposure, reduce erythema and not cause any irritation [139].

1.4.2.6. Photosensitization

It has been observed that the *Hypericum perforatum,* which is a wild plant and found in natural vegetation, has a toxic effect when pasture animals graze. When exposed to direct sunlight after eating as feed, it can cause inflammation of the skin and mucous membranes. This is called hyperism, and the causative agent thought to cause it is active ingredient hypericin. In humans, no irritation is observed in this way unless it is above the recommended dosage [128]. The component that creates sensitivity to light in *Hypericum perforatum* is hypericin. It leads to this is known to be highly reactive singlet oxygen molecules. Hypericin is a molecule with photodynamic effect and induces photohemolysis in red blood cells, increases lipid peroxidation and reduces cellular glutathione levels. The irradiation absorption spectrum of hypericin is 330nm for UV range, for the visible light (VIS) is the between 550nm and 588nm. Minimal erythema dose (MED) and skin erythema were evaluated in a study with sixteen healthy volunteers who applied hypericum oil and ointment. Phototoxic effect was tried to be observed by applying solar simulated

radiation. No phototoxic reaction was observed in any of the irradiated test areas. MED hypericum did not change after applying oil and ointment. Because of the statistical result made within the photometric measurement of skin erythema measured 24 hours after irradiation, an increase in erythrem index was observed for hypericum oil, but no change in the use of ointment was observed. In a previous study, 1000 ng / mL hypericin injection has been found to produced a phototoxic reaction, but higher hypericin concentrations (110 mg / mL, Hypericum oil; 30 mg / mL, Hypericum ointment) were observed to be non-toxic in this study. The authors indicated that this is due to the permeability of the treated skin [140]. *Hypericum perforatum* used orally to take advantage of the antidepressant effect may not show photosensitive effect [141], but photo irritation may occur on the skin in the use of hypericin topically alone. Hypericin in *Hypericum perforatum* extract has much less phototoxic effect than pure hypericin. Other components in *Hypericum perforatum* can provide cellular protection by antioxidant properties and the amount of reactive oxygen species produced by photo-induced hypericin and by reducing oxidative damage [142].

1.5. HONEY

Honey is of animal origin and is glucose, fructose, glucose oxidase, vitamins and phenolicc compounds. It has beneficial sugar and has a content that can be used safely in diabetics. Honey has a healing effect for thickening, which occurs due to the accumulation of various substances in the inner wall of the vessels. Honey can be used for skin, lips and hair in terms of cosmetics in the human body. Honey is primarily a natural moisturizer and an antibacterial, anti-inflammatory, antioxidant, deodorizing and tissue regenerating agent, and is a substance of animal origin [143]. A natural proof that honey is antimicrobial is that it can be stored at room temperature without any deterioration [144]. With these properties, honey can be used as an efficient wound-healing agent. Honey is a substance of natural origin that can be used both topically and orally. It can be used as an adjunct medicine in ulcers, wounds and other infections [145]. High fructose and glucose content provide honey to have a moisturizing effect on the skin [143].

It is known that honey has been used since ancient times, as a nutrient, in wound therapy, medical and cosmetic fields. According to the rock paintings found in Valencia, Spain in 1921, the beehive human figure and honeycomb were observed. It is believed that this

painting dates back to about 15000 years the end of the Paleolithic age. Therefore, this picture can be considered as a sign that honey has been used for human benefit and consumption since ancient times [146]. At the same time, a picture of the life cycle and honey production of the bee was found in a Neolithic temple dating back to 700 BC in Çatalhöyük, Anatolia. Apart from these, it has been frequently emphasized that the healing effect of honey as a sacred food in oral history and mythology [147]. It is mentioned in Egyptian, Islamic, Greek and Chinese sources that honey has a multifunctional feature other than being a nutrient. Firstly, moisturizing the skin thanks to its physical texture and easily recognizable moisturizing feature, then antibacterial and wound-healing properties have been used with the society's own discoveries [148].

Different types of honey depend on which flower and plant collect pollen from the bees. Although honey species showed similar activities in general, some species have different dominant effects [154]. The most common type of honey used in cosmetic products is acacia honey. Manuka honey, on the other hand, is one of the honey species with the highest antibacterial activity and this has caused it to be the most used type in wound healing [155]. The antibacterial property of this honey is not due to the hydrogen peroxide content, but from the methylglycoxal derived from dihydroxyacetone [156]. However, in studies conducted, it has been reported that manuka honey retains its antibacterial properties after neutralizing the methylglyoxal content [168]. It is seen that this different effectiveness of honey has an effect not only because of structural differences but also due to its different chemical structures when examined with a microscope [157]. Manuka honey has been used in the treatment of stomach ulcers and wounds with lethal effects on Helicobacter pylori pathogenic bacteria. Tualang honey has also been shown to exhibit activity against gram-positive and enteric bacteria [158].

1.5.1. Components of Honey

The honey made by the bees in the hive collects pollen from the flowers, swallows, and reproduces what they bring to the hive repeatedly until its quality increases [149]. Honey components have more than two hundred compounds [145]. Honey consists of various enzymes such as invertase, amylase and glucose oxidase and is produced from the hypopharyngeal glands of bees. Amylase digests starch into maltose and invertase

(saccharis, a-glucosidase) mainly provides the conversion of sucrose to glucose and fructose, but also catalyzes many other sugar conversions. The other two main enzymes regulate the production of glucose oxidase and catalase, H_20_2, one of the honey antibacterial factors [150]. Glucose is oxidized with gluconic acid and hydrogen peroxide and this prevents the honey from spoiling and provides its maturation. The components of the honey depend on which flower or plant the bee collects. Honey composition is high in carbohydrates. Honey, which mainly has glucose and fructose; It contains isomaltosis, nigerose, turanose, maltulose, cojibiosis, alpha beta-trehalose, gentiobiose, laminaribiosis, maltotriosis, 1-cystosis, panoses, isomaltosyl glucose, erlose, isomaltosyltriosis, theanderosis, centose, isoptosis, isomaltosyl, and isostostrate. honey is also a sugar mixture with these substances [151-153]. Having a sugar content of up to 76 percent causes honey to be an important sweetening nutrient when consumed as a food. Also honey, it is rich in vitamins such as thiamin, vitamin B6, pantothenic acid, folic acid, vitamin C, cyanocobalamin, riboflavin, ascorbic acid, minerals that is calcium, sodium, iron, copper, manganese, magnesium, potassium, phosphorus, and zinc and amino acids for instance phenyalanine, aspartic acid and proline [149]. Sugar and other ingredients in honey may change during storage and waiting process. The viscosity, color, smell and taste of honey varies. This is because the amino acids in the honey are degraded by exposure to heat, and sugar degradation products appear as different compounds [145]. There are many antioxidant compounds in honey. The phenolic acid found in honey has been found to contribute to the antioxidant properties of honey. Most honeys have acidic ph values below seven. The main source of acid in honey is gluconic acid, a product of glucose oxidation by glucose oxidase. Substances such as formic, acetic, citric, lactic, maleic, malic, oxalic, pyroglutamic and succinic have acidic content. The presence of protein and amino acids in honey content is at the maximum concentration of 0.7 percent. Honey contains many important amino acids; the most important one is proline. Hydroxymethylfurfuraldehyde or HMF is the decomposition product of fructose. It can be used to distinguish fresh honey because its concentration increases as the honey is stored or heated, and trace amounts are found in fresh honey. It is also found in live microorganisms in honey, but they are non-toxic to humans. Clostridium botulinum spores and Bacillus bacteria are found in some types of honey. Some high moisture content honey has contained Osmotolerant yeasts and this may cause undesired fermentation. In order to avoid fermentation in honey, ethanol, glycerol and yeasts in honey should be below a certain level [150].

1.5.2. Uses of Honey in Medical Applications

The content of honey is abundant in products in the medical and cosmetic fields. It is frequently used in formulations of wound dressings, disposable gels, antioxidants and moisturizing creams or masks. It is more effective than many chemical products and it is more preferred because it is a natural based product. It can be used with many different products such as calcium alginate wound dressing and gel-shaped products that provide a moist environment for wound and supports autolytic debridement [183-185]. Apart from being used for chronic wounds and burns, it has been seen to be used in minor abrasions and acute wounds. Most of the products available and used in the market are formulated with manuka honey, but they have been found to be used in other types of honey [159]. Other medical indications for which honey can be used externally are: Against boils and furuncles, muscle cramps, bruises and contusions, particularly suitable as a dressing included in treatments against pityriasis, tinea, seborrhea, dandruff, diaper dermatitis, psoriasis, hemorrhoids, and anal fissure [186].

1.5.2.1. Wound Healing

Thanks to the antibacterial, antimicrobial, antioxidant, anti-inflammatory and tissue regenerating properties of honey, it plays an effective and therapeutic role in wound healing thanks to changing the physiological and immunological functions of tissue. Apart from medicines and medical equipment, honey is a good dressing and a natural therapeutic agent of herbal-animal origin. Wounds that benefit from the therapeutic properties of honey used topically and orally; burns, surgical areas, infected surgical wounds, chronic ulcers, malignant wounds and newborn wounds. There are many medicinal products containing honey used in wound healing approved by the FDA [159]. Damages such as blows, cuts, scratches or peels from external factors cause injury to the skin. Wound cause injury to the skin such as blows, cuts, scratches or peels from external factors [160]. The wound is a destruction that damages tissue integrity in the adjacent areas of the place where it was formed [161]. Although this injury causes damage to the skin and deformation of the epidermis, it can easily recover, but the wound can become infected if there is any bacterial contact where the wound is located. The type and number of bacteria

determines the size and extent of the infection to occur [160]. The reason why honey is effective in wound healing is that it has an bactericidal feature on these bacteria [155]. This antiseptic feature of honey is due to the production of hydrogen peroxide, which provides glucose oxidase stimulation. The cytokine produced by hydrogen peroxide, on the other hand, helps to remove the biggest obstacle to wound healing by causing bacterial death by damaging the cell membrane of bacteria [162-164]. The effect of damaging the cell membrane largely depends on the concentration and amount of hydrogen peroxide in honey, so honey type and genus play an important role in this feature [165]. Among the wound-healing properties of honey, antioxidant properties are also indirectly effective [163]. One of the important causes of inflammation is free radicals, honey decreases these free radicals, leading to a decrease in the presence of inflamed cells, so that the pain decrease due to the wound. The ability to reduce free radicals is due to the antioxidant properties of honey [166]. It acts by protecting scar tissue from free oxygen radicals produced by H_2O_2. Low H_2O_2 levels act by stimulating angiogenesis and growth of fibroblasts. Thus, epithelial cells form and grow and healing is accelerated. The presence of oxygen required for tissue healing is provided by increased angiogenesis [163]. Therefore, low pH (3.6 to 3.7) of honey plays an active role in wound healing by accelerating acidification [167]. Honey with an acidic pH value between 3.2 and 4.5 has an unfavorable environment for bacteria [168].

Although the amount of free water is low, honey provides the necessary moist conditions for wound healing. With the dehydration of the wound and osmotic effect, it does not draw water from the tissue under the wound. Thus, the dressing does not cause tearing and pain by adhering to the wound tissue. The effect of this moist environment on wound healing is that it provides oxygenation and nutrition for the injured tissue. Honey has a healing effect on experimental wounds where bacteria are absent or scarce, because it reduces edema and improves blood circulation via capillaries. In addition, the benefit of Honey's high viscosity property is that it is a protective barrier on the wound [173].

It may have anti-inflammatory and tissue-regenerating effects in the treatment of damaged intestinal mucosa [169-170]. Inflammation is a beneficial response of blood vessels to danger. This defense mechanism of macrophages, by increasing the production of proinflammatory cytokines, nitric oxide (NO) and prostaglandins E2 (PGE 2). All these inflammatory tools have a cytotoxic effect, and excessive production of macrophages

causes tissue loss. Phenolic compounds in honey inhibit the overproduction of inflammatory media and act as cytotoxicity inhibitors as free radical scavengers. Antioxidants and anti-inflammatory agents have a similar relationship in terms of dealing with ROS [171]. The effects of honey on wound healing are the treatment actions known to develop macrophages, reduce inflammatory edema, quickly shed and regenerate dead and unhealthy tissue, and create a protective layer on the wound to be treated [172].

Honey also has a deodorizing effect in wounds or damaged and problematic tissue. The bad smell can be eliminated by producing lactic acid product instead of the foul-smelling product by replacing the bacteria on the infected wounds with the amino acids in the honey and the excess production of glucose [163].

In summary, mechanisms and causes of honey wound healing; Honey's viscosity, it's water content and sugar (primarily glucose and fructose), antioxidants, a wide variety of amino acids, vitamins and minerals, and the presence of glucose oxidase that produces hydrogen peroxide and gluconic acid, which causes honey to have an acidic pH of 3.2 to 4.5 [173].

1.5.2.2. Antibacterial Properties

Antibacterial properties can also be seen in a honey type that does not contain hydrogen peroxide. It depends on the flower types that bees get pollen. Leptospermum species is an example of this type flora [174]. Some studies have linked honey's high sugar content, low water content, low pH and high osmolarity to the reason of this antibacterial property of honey [175]. The high osmolarity of honey causes the lymph withdrawal from the wound. There are dissolved nutrients in the lymph and these remaining foods support the formation of tissues by allowing them to be fed as a source of low water and excess nutrients for tissue regeneration [163]. Also, since honey is a hygroscopic substance, it can dehydrate bacteria when applied to the wound because it has a feature that draws moisture out [168].

The lysosome contained in honey is a powerful antimicrobial agent, but honey that does not contain hydrogen peroxide has proven not to be bound by lysosome. Honey also shows bacteriostatic properties, not just bactericidal properties. In studies conducted, it has been revealed that, in addition to anaerobic and aerobic bacteria, they stop their growth in gram positive and gram-negative bacteria [163].

Honey has proven to be effective in superficial wounds without infection. Honey therapy has been shown to provide faster healing than control groups in wounds infected with *Staphylococcus aureus* [175]. The effectiveness of honey in bacterial species is in a wide range. It has been observed to have an inhibitory effect on about 60 bacterial species. In the study conducted to measure the antibacterial activity of processed and raw honey species, it was tested against grampositive bacteria (*Staphylococcus aureus, Bacillus subtilis, Bacillus cereus, Enterococcus faecalis and Micrococcus luteus*) and gramnegative bacteria (*Escherichia coli, Pseudomonon, Pseudomonas aeruginosa and Salmonella typhi*). In the study, it has been found that gram-negative bacteria are much more sensitive than gram-positive bacteria except *E. faecalis*, but when in general look, it was found that honey shows antibacterial activity (bacteriostatic and bactericidal effect) similar to antibiotics [176]. In another study where processed and honey antibacterial activity was evaluated, the most sensitive bacteria were *Salmonella* typhi, *E. coli*. and *Pseudomonas aeruginosa*. It has been observed that it is more effective against gram-negative bacteria compared to antibiotics such as tetracycline and ciprofloxacin. It is even effective against P. aeruginosa bacteria where tetracycline is ineffective. Both raw and processed honey showed antibacterial properties [177].

1.5.2.3. Burn Treatment

Complications due to sepsis or inhalation damage are the causes of burn wounds causing death. There are pathogens with antimicrobial resistance tendencies in the burn wound bacterial. It has a lethal effect against multiple resistant antibiotic-resistant organisms such as MRSA (methicillin-resistant *Staphylococcus aureus*), vancomycinresistant *Enterococcus spp* (VRE) and multiple-resistant Gram-negative rods such as *Pseudomonas aeruginosa, Acinetobacter spp*. and members of the family *Enterobacteriaceae,* such as resistance bacteria in severe thermal burns and injuries and nosocomial infections. It is also used in skin grafts and their infections [168]. In some of the hospital-treated burn patients, the recovery rates of 13 patients treated with honey resulted in a similar result to those treated with silver sulfadiazine. In the retrospective study of burned patients treated in the hospital, the recovery rates of 13 patients treated with honey resulted in a similar result to those treated with silver sulfadiazine. In some clinical studies conducted with prospective randomized control, it was observed that burn wounds healed much faster than treatment

with silver sulfadiazine, polyurethane film, amniotic membrane and potato peeling. Thermal injuries are oxidative injuries and free radicals increase in the wound area, which activates lipid peroxidation, which causes wounds and contractures. Honey supports wound healing by cleansing free radicals and due to this feature, decreased depigmentation effect may be seen [178]. Studies comparing honey-impregnated gauze with a polyurethane and comparing honey-impregnated gauze with the amniotic membrane have been performed, and patients who have been treated with honey have seen faster healing, less wound infection, and less injury [179-180].

1.5.3. Uses of Honey in Cosmetics Industry

Honey is also widely used in cosmetic fields as a skin and hair care products, due to the natural proteins, minerals and vitamins in honey. Through its deodorizing and moisturizing effect, honey are frequently found in shampoos, face, body and hand creams and lotions, lipstick or lip balms bath products, hair creams and cleaning products. In addition, it has been found to be used in combination with other moisturizers and wound-healing agents to increase the moisture capacity and healing properties. The amount of honey used in products containing honey generally ranges from 1 to 10 percent, but in combination with other products used, their concentration can be reached up to 70 percent. According to the International Cosmetic Ingredients (INCI) Classification, the name is “Honey” or “Mel” and (CAS no. 8028-66-8) and is in the moisturizing product class [187].

1.5.3.1. Antioxidant Effect

Honey have many natural flavonoids (such as apigenin,pinocembrin, kaempferol, quercetin, galangin, chrysin and hesperetin), phenolic acids (such as ellagic, caffeic, p-coumaric and ferulic acids), ascorbic acid, tocopherols, catalase, superoxide dismutase, reduced glutathione and working together to a high degree of antioxidant activity shows. For superoxide and hydroxyl radical groups, their effects as substrate and meddling on propagation reactions, their role in enzymatic inhibition reactions, free radical sequestration, hydrogen donation, metallic ion chelation, reactions that occur while creating antioxidant activity of honey. The presence of free radicals and reactive oxygen

species (ROS) creates cellular dysfunctions, causing rapid destruction and degradation for cells. The presence of antioxidants in honey acts by reducing these destructive and pathogenic activities [148]. A relationship was found between honey color and antioxidant effect. Due to the antioxidant activities of the phenolic compound, dark honey has been found to have more antioxidant effects because dark honey contains more phenolic compounds [181]. In a study with cerumen ethanol extract, it was found that it protects human erythrocytes from lipid peroxidation and reduces the number of ROS. Phenolic compounds in honey are thought to provide this effect [189]. A wide variety of methods have been used to measure the antioxidant activity of honey. As an example to these; DPPH (named after the reagent 2,2-diphenyl-1- picryhydrazyl), FRAP (Ferric Reducing Antioxidant Power), 3. ORAC (Oxygen Radical Absorbance Capacity), RSA (Radical Scavenging Activity), TEAC (Trolox Equivalent Antioxidant Capacity). It has been proven that honey shows a good antioxidant activity in the measurements made with these different methods. Polyphenols in honey contain hydroxyl groups, which cause antioxidant effects. The antioxidant activity in honey causes both wound healing and moisturizing properties [148]. This antioxidant activity of honey also allows it to be used as anti-aging. Because of aging due to external factors, photo-oxidative reactions occur and these weaken the antioxidant defense system and increase the reactive oxygen species (ROS) at the cellular level. These suppress the skin's defense mechanism and make it more susceptible to external factors, especially the harmful effects of UV. The antioxidant effects of honey both support the photoprotection mechanism, stimulate the production of elastin and collagen and delay the deterioration of structural components. It has also been shown to reduce the loss of moisture and elasticity in the skin and wrinkle formation caused by aging [190].

1.5.3.2. Moisturizing Effect

Another feature of honey is its moisturizing feature. Substances such as sugar, amino acid and lactic acid in the honey composition provide skin-moisturizing effect. In terminology, the terms humectant and hydrating are often used incorrectly. To describe well, humectant is the formation of a feature that gives moisture and retains moisture in this area with the absorption of the substance contacted with the stratum corneum base of the skin and hydrating (moisturizer). On the other hand, it creates a function that provides moisture to

the skin or protects it by absorbing water with the passage of water to the superficial and deep layers of the skin. Cosmetics used in the market generally have humectant efficacy, but it can be said that top quality and multifunctional products act on the deep layers of the skin and hydrating the skin. Honey is a natural product that can be hydrated by giving water compound to the skin. This feature of honey is especially related to the mechanism of action of sugar. The sugar in its composition acts by using its own osmotic power to soften the skin and increase blood pressure. Hydroxyl groups in the formulation provide moisturizing and antioxidant properties. Polyphenols found in honey are substances with a high hydroxyl group. The main ones are glycerin, propylene glycol and sorbitol, which are used as solvents or surfactant in other cosmetic products in generally [148].

The sugar composition of honey can reduce the water molecules in honey by diffusion method. In this way, a protective film base is formed to moisturize the skin, and this film layer provides a structure and fixing water molecules that protect and maintains moisture. It nourishes the internal epithelial tissues, improves blood circulation, and provides a moisturizing and revitalizing effect on the skin, preventing wrinkles [182]. Research has been carried out on exactly which type of compound the honey contains in its antioxidant capacity, and although its exact mechanism of action is unknown, it has been revealed that the phenolic compounds and flavanoids they contain have almost identical effects and are similar in antioxidant results. The fact that adding honey to fruit teas causes a decrease in phenol content has given a new perspective to the investigations while investigating the moisturizing feature of honey. In a subsequent study, a nanoemulsion system comparison of real honeys and an artificial oil-water-surfactant was made to evaluate the hydration power of honey. In a study in which the moisturizing properties of different honey types were measured, a comparison was made about the moisturizing properties of six different honey types. When the moisture rate was measured after topical application in 30-60-120 minutes, the highest humidity rate in the 120th minute was found to belong to a imitated honey. The toxicity of honey and the harmful substances released in the skin when used as dermocosmetic should be investigated [148].

Honey has good moisturizing properties due to the presence of hydroxyl groups, sugar, proteins and lactic acid. It has been observed that ingredients such as vitamins B, E and K combine with minerals such as potassium, phosphorus and calcium in honey, adding moisturizing properties [188].

2. MATERIALS AND METHODS

2.1. MATERIALS

2.1.1. Precursors and Consumables

- T-Junction Microfluidic Device and Channels
- Syringe Pump, Harvard® Apparatus Pump 11 Elite
- Gas Tank, Wika®
- Magnetic Stirrer with Heating, Heidolph® MR Hei-Standard
- Electroinic Precision Balanca, Precisa® XB 320M
- Syringe, BD® Becton Dickinson
- Beaker, Iso Lab®
- Petri Plate, Iso Lab®
- *Hypericum perforatum* Oil, Konya Selçuk University Technocity Manufacturing
- Honey, Balparmak®
- Tween 80, Sigma-Aldrich®
- Alginic Acid Sodium Salt Powder, Sigma-Aldrich®
- Calcium chloride, Sigma-Aldrich®
- Distilled Water

2.1.2. Equipments

- Vacuum Oven, CLS Scientific® CLRC-17C

- Lyophilizer, Christ® Alpha 1-4 LSC
- Freezer, New Brunswick® ultra low temperature
- Pycnometer Density Bottle Meter, Iso Lab®
- Viscosity meter, AND® Vibro Viscometer SV-10
- Surface Tension and Contact Angle Meter, KSV CAM® 200 Contact Angle Meter, Hamilton Technology® Needle
- Optical Microscope, Nicon Eclipse® LV 150
- Scaning Electron Microscope (SEM), FEI (Philips)® XL30 SFEG
- X-Ray Diffraction Spectroscopy (XRD), Rigaku Smart Lab.®
- Thermogravimetric Analysis (TGA), TGA 851 Mettler Toledo®
- Differential Scanning Calorimetry (DSC), Thermal Analysis MDSC® TAQ2000
- Raman Spectroscopy, Kaiser Raman RXN1
- Fourier-transform infrared spectroscopy (FT-IR), Perkin Elmer® 100 21
- Skin Moisture and Oil Content Analyzer, OEM® Sk-8

2.2. METHODS

2.2.1. Testing Different Formulations

While deciding on the formulations, it was tried to create a suitable dispersion to use in the microfluidic system by keeping the active substance amounts constant, changing the surfactants and the heat given while preparing dispersion. The amount of active substance decided by the pre-formulation is precise, based on the studies conducted. The percentage and distribution of active ingredients are as follows; 1 wt. percent *Hypericum perforatum* oil, 1 wt. percent Honey, 1 wt. percent Sodium Alginate. *Hypericum perforatum* Oil, which is produced in Konya Selçuk University Technocity and used in Yeditepe University

Faculity of Pharmacy laboratories, prepared in raw olive oil, contains around 10 percent *Hypericum perforatum* extract and whose main component is hypericin. The oil used in the experiments contains 0.1 wt percent *Hypericum perforatum* extract. The honey used in the experiment was made of 1 percent of Balparmak extracted honeydew honey and alginate was added to the mixture at a rate of 1 percent. In the microfluidic technique, the liquid passing through the continuous phase must be a mixture that is homogeneous and suitable for making a stable microbubble. Surfactant was used to dissolve *Hypericum perforatum* oil and honey in dispersion and to create homogeneity. By keeping the amount of active substance constant, in this study, different types of surfactants and different concentrations were tested. While the amount of active substance is kept constant, in this study, different types of surfactants and different concentrations were tested. Tween 80, hyaluronic acid and glycolipid and their combinations were tested as surfactants. Trials were carried out at 0.25 wt. percent and 0.50 wt. percent concentrations. Deciding on the ratio of tween 80 used as a surfactant has been tried by making more than one trial until a homogeneous dispersion is prepared.

After determining the surfactant to be used in the dispersion preparation procedure, experiments were carried out in the applied heat. Temperatures of 40 °C, 60 °C and 80 °C degrees were tried at certain stages of the mixture. The physicochemical properties of the dispersion prepared at this stage were observed and a stable liquid phase was tried to be produced. The physical effect of temperature on formulations has been observed.

2.2.2. General Procedure of Dispersion

The dispersion was prepared in a certain order. First, the distilled water was heated at a temperature of 60° degrees in a specific size beaker. In another vessel, *Hypericum perforatum* oil and surfactant tween 80 were mixed in certain proportions. Oil and surfactant mixture was slowly add with syringe to the beaker on the magnetic stirrer. After adding oil and surfactant mixture, the heater was turned off and only mixing was done. The water mixed with the oil stirred for half an hour will decrease to a temperature close to room temperature. Then the oil-surfactant mixture was homogeneously mixed in the water with the effect of its temperature. Then honey was added to the dispersion in a certain percentage and mixed half an hour in a magnetic stirrer with heat at 750 rpm speed. Oil

and honey were stirred for one hour at 700 rpm speed without heating to make a homogeneous dispersion. Then, a certain amount of alginate was added slowly into the vial when the dispersion was on the mixer and stirred for one more hour. At the end of this process, a homogeneous dispersion was formed without oil and film layer. The percentage and distribution of active ingredients and ingredients when preparing the dispersion are as follows; 1 wt. percent *Hypericum perforatum* oil, 1 wt. percent Honey, 1 wt. percent Sodium Alginate, 0.5 wt. percent Tween 80.

2.2.3. Characterization Studies for the Dispersions Prepared

A homogeneous and viscous dispersion had to prepare to create monodispers and durable for bursting microbubbles with microfluidic device. In this dispersion, oil and honey were mixed in a homogeneous way, and the dispersion were going to use should not have formed any oil film layer and blisters. The same mixture was prepared with values of 40° degrees, 60° degrees and 80° degrees and the viscosity, surface tension and density of the dispersions produced at these three temperatures were measured. Characterization studies have been carried out to find out at which temperature the dispersion will be prepared for microfluidic system. Viscosity measurement, density measurement, surface tension and contact angle measurements were made to make choice. Pycnometer was used for density measurement. In the measurement performed with a 25 ml density bottle three times, the average value was taken and the value of the density was found. The viscometer of the dispersions was measured with a vibro viscometer device. Viscosity measurements were made with the tuning fork method by immersing the plates in the device into a 50 ml dispersion measuring with the vibration. For these measurements, the value in the device was expected to become stable and the result was determined. Temperature values during measurement were also recorded. The dispersion taken with the Hamilton® brand needle used to measure surface tension and contact angle is found by photographing in the computerized system. As the drop falling from the needle tip breaks, a cross-sectional area is formed and the surface tension is measured by calculating the gap at that break. The contact angle is found by calculating angle between the contact surface and the liquid drop with the same device.

2.2.4. T-Junction Microfluidic Device System Set-Up and Bubble Generation

The microfluidic device used in this experimental work is made of polymethylmethacrylate (PMMA) polymer. It is a microfluidic device with three nozzles and microchannels with fluoro ethylene polypropylene (FEP) at their ends. One end is connected to the syringe pump and the other is connected to the gas tank. While a mixture of *Hypericum perforatum* oil and honey was inserted in as a continuous phase, Nitrogen gas is sent as the dispersed phase. Microbubbles were derived from these gas-dispersion mixtures. These microbubbles were collected in a petri dish. In order to obtain a stable structure while producing bubbles, production was made by combining at different flow rates and gas pressures.

2.2.5. Characterization Studies for The Microbubbles Generated

300, 250, 200, 150, 100, 50 µl / min flow rates and 0.5, 0.6, 0.75, 1.0, 1.5 bar gas pressures were studied in this thesis work by changing the gas pressure and flow rate in order to find the most suitable microbubbles for hydrogel production. The distribution, sizes and shapes of microbubbles produced with different flow rates and gas pressures with an optical microscope were observed. The micro bubbles collected in a small glass container and examined under a digital camera was shown in Figure 2.1. The optical microscope image taken was at 100µm scale and as shown in the Figure 3.2.

Figure 2.1. Micro bubbles with 200 µl / min flow rates and 0.6, bar gas pressure collected in a small glass container produced.

2.2.6. Hydrogel Production

The previously prepared calcium chloride solution was slowly added to the bubbles prepared in petri dishes using a syringe. Calcium chloride solution prepared to form hydrogel by gelling by crosslinking contains 1wt. percent calcium chloride and distilled water. Hydrogel formation was then observed by the combination of bubbles and calcium chloride solution. The hydrogel structure formed was covered and a small hole was placed on the container in order to provide moisture output and placed in a vacuum oven. It was kept in a vacuum oven for one hour. It was observed that the bubbles formed after waiting for one hour in the vacuum oven, the bubbles formed seemed to burst and a porous hydrogel structure formed in place of the bursting bubbles (Figure 2.2). At the end of these processes, a porous hydrogel structure containing *Hypericum perforatum* and honey active ingredients was obtained.

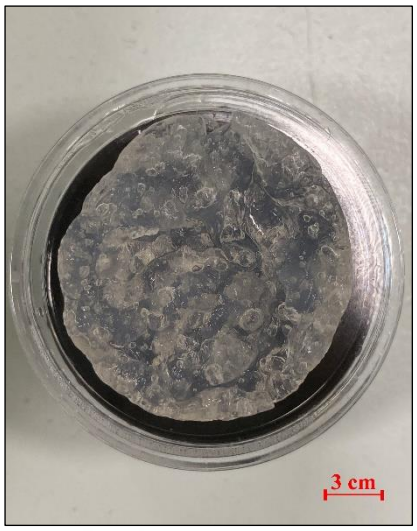

Figure 2.2. Porous hydrogel structure containing *Hypericum perforatum* and honey active ingredients produced in the experimental work.

2.2.7. Microstructure Analysis of Formed Hydrogel

The hydrogel formed placed in a vacuum oven was dried in under a pressure of 70 mbar for an hour at 30 °C degrees. In this process, air inside the hydrogel was removed and the microbubbles were evacuated. The hydrogel structure removed from the vacuum oven was then put in the freezer and kept at -80 °C for 24 hours. The hydrogel that was kept in the freezer is frozen, and then it was put into the lyophilizer and kept there for 24 hours. The dried and freeze hydrogel was prepared for analysis. Then, the pieces of dried hydrogel were taken from the dense and less dense regions, which were visible according to the concentration of the dispersion, and analyzed in a scanning electron microscope. The porous structure on the surface of the product was examined with the image taken from the scanning electron microscope. Image formation in a scanning electron microscope (SEM) is electron and photon signals are created by the interaction of high-energy electrons sent with the surface of the sample examined in the scanning electron microscope. These interactions, elastic and inelastic collisions and others result from electron beams collected with the condenser electromagnetic lens and focused with the objective lens, scaning on the sample with electromagnetic deflecting coils. The signals collected by the detector are processed with microscope software [192].

2.2.8. Analysis of the Chemical Structures of the Hydrogels Obtained

The chemical structures of the hydrogel sample were measured with Fourier Transform Infrared Spectroscopy and Raman Spectroscopy devices. The purpose of performing Fouirer Transform Infrared Spectrophotometer (FTIR) analysis is done to analyze the functional groups in the structures of the compounds, chemical binding sites and whether the two compounds are the same. It is used in the analysis of the structures of organic compounds in the form of solid, liquid and solution and in the biochemical structure analysis of carbohydrates, phospholipids, amino acids and proteins. Raman spectroscopy is a method used to understand substance content, such as FTIR method, and to interpret chemical compounds and bonds. In this method, the interaction of light with matter and the process of light scattering are analyzed. Both Raman and FTIR are used to describe the substance by interpreting the spectrum of the modes of the unique vibrations of each molecule [193].

2.2.9. Analysis of Thermal Properties of the Hydrogels Obtained

Thermal properties were investigated by using Thermogravimetric Analysis and Differential Scanning Calorimeter Device. The TGA device that is thermogravimetry was used to determine the mass change of the dried hydrogel, under the influence of temperature and time. It was analyzed at intervals of 10° degrees between 0° and 900° degrees. Phase changes and temperatures were analyzed with DSC device. It was analyzed in the range of -80° and +250°. Thermogravimetric Analysis (TGA) is the measurement of the change in the mass of the sample over time when the sample is heated. The sample was heated depending on time. The first derivative of the values of the TGA graph is calculated by time or temperature, which gives the mass change. These curves are called differential thermal gravimetry (DTG), and the purpose of this measurement is to find the weight loss at the highest temperature. Graphically, TGA curves are created in step form and DTG curves are created in peak form. The mass change is explained by the loss of material or the reaction of the sample exposed to the temperature. In the analysis made with the Differential Scanning Calorimeter Device (DSC), energy changes in the sample are observed by heating, cooling and keeping it at a constant temperature. It is used for

determining the state changes that are observed in the sample quantitatively with the energy differences and at what temperatures these state changes, and the stages such as melting, glass transition and crystallization [194].

2.2.10. Analysis of Crystal Structures of the Hydrogels Obtained

Hydrogels that were frozen and film-shaped were analyzed by X-Ray Diffraction method. The X-Ray Diffraction (XRD) method is a technique used to define the crystal structure properties of the sample to be examined with a small grain size or brought to that size. The atoms of the sample examined scatter through electrons under the influence of X-ray waves. It breaks X-rays depending on the unique atomic sequences of the crystal phases and is defined and analyzed according to these crystal structure properties [195].

2.2.11. Application of Hydrogel Masks Achieved on Volunteers

The prepared hydrogels were tested on six volunteered patients. While a mask was applied to the pimple area in their face of the three volunteer patients and a mask was applied to the injured area in their hands of the other three people. The mask applied to pimply areas on the face and injured areas on the hand was kept for 3 hours after it was put on. For moisture measurement, the healthy tissue was applied except for the damaged and scarred areas and the measurement was made after putting on a mask and waiting for about 15 minutes. At the same time, moisture measurements were made with a manual moisture-measuring device. This manually used measuring device operates with the latest bioelectrical impedance analysis technology. In this analysis method, it provides information about tissues by looking at the resistance that electric currents encounter while passing through the body tissues. This manual device makes the measurement by means of a probe. The probe is brought into contact with the skin surface and is withdrawn after a short wait. Then, the oil and water content in the skin appears as a percentage on the LCD screen of the device. Moisture values of volunteers were determined numerically by measuring device. Then these values were recorded before and after the application and the comparison between values was made statistically. Statistical analysis was made with the moisture measurement result data and the results obtained were evaluated.

3. RESULTS AND DISCUSSION

In this study, microbubbles were obtained using a t-junction microfluidic device. By gelling bubbles, it was desired to create a hydrogel mask containing *Hypericum perforatum* and honey active ingredients. Characterization studies of dispersions, microbubbles, hydrogel product and chemical, physical and microstructure analyzes were performed to determine how successful the desired hydrogel polymer structure was. The hydrogel masks produced afterwards were applied to six volunteered patients. Changes in wound and acne occurrences were observed and the moisture in the skin was quantitatively measured with a moisture meter.

3.1. EVALUATION OF DIFFERENT FORMULATION

The dissolution of the oil was important for the dispersion used in the microfluidic technique to be homogeneous and to produce stable bubbles. In particular, different surfactants have been tried to homogeneously distribute the oil in the content. Tween 80 was much more effective in mixing dispersion than other surfactants. Only Tween 80 at a concentration of 0.5 wt percent was effective from the formulations. Other formulations formed a dispersion with low transparency, containing residue and oil remaining on the surface. In trials at different temperatures, it has been observed that the dispersion prepared at 60°C degrees is the most stable and homogeneous. Although the effects of temperatures affect the physical appearance, the main effect was measured by characterization studies.

3.2. CHARACTERIZATION STUDIES FOR THE DISPERSION PREPARED

Characterization studies were carried out using the most stable and homogeneous dispersion among the formulations tested. Characterization studies were carried out using the formulation called F1 in Table 3.1. The content ratios of this formulation called F1, F2 and F3 are 1 wt. percent honey, 1 wt. percent *Hypericum perforatum* oil, 1 wt. percent alginate, 0.5 wt. percent tween 80 and distilled water. The contents of the codes are exactly the same, but their preparation temperatures are different. While preparing this formulation, the physicochemical properties of the dispersion were observed by changing

the applied temperature values. It was tried to choose the most suitable liquid phase to be used by conducting characterization studies. The characterizations of the dispersions at different temperatures were prepared and the values obtained because of the measurement are shown in Table 3.1 and contact angle pictures are in the Figure 3.1.

Small-sized bubbles had to be produced to create regular and stable microbubbles. In the studies conducted, if the viscosity, density and surface tension are high, the transition flow rate decreases and the droplet size is small. If the contact angle is small, the droplet size is small and a more stable structure is observed [36, 196]. It is a dispersion prepared at 60° degrees with low contact angle and highest viscosity, density and surface tension in dispersions prepared with these three different temperatures. Therefore, it was decided that the most suitable dispersion to be used for the system was prepared at 60° degrees.

Table 3.1. Characterization of dispersions prepared at three different temperatures.

Dispersion Formulation Code	Temperature (°C)	Density (g/ml)	Viscosity (mPas)	Surface Tension (mN/m)	Contact Angle (°)
F1	40	1,016	22.1	44,464 ± 0,385	33,98 ± 0,21
F2	60	1,018	24.5	45,819 ± 0,504	23,03 ± 0,11
F3	80	1,014	17.6	43,896 ± 0,299	40,57 ± 0,44

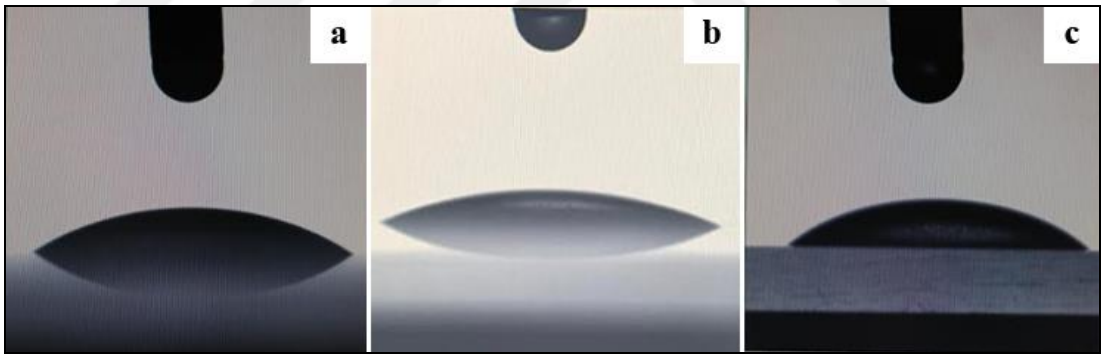

Figure 3.1. Contact angle pictures of dispersions prepared at three different temperatures (a) Contact angle of dispersion prepared at 40°C degrees (b) Contact angle of dispersion prepared at 60°C degrees (c) Contact angle of dispersion prepared at 80°C degrees.

3.3. CHARACTERIZATION STUDIES FOR THE CREATED MICROBUBBLE

300, 250, 200, 150, 100, 50 µl / min flow rates and 0.5, 0.6, 0.75, 1.0, 1.5 bar gas pressures were tired in our experiments by changing the gas pressure and flow rate in order to find the most suitable microbubbles for hydrogel production. Among these values, the most

favorable conditions were observed at 200 µl / min flow rate and 0.6 bar pressure. To achieve this, observations were made on bubble size and distribution by taking a optical microscope image with different parameters and optical microscope images of each combination were taken.

The image of the microbubbles obtained in the microfluidic device established with 200 µl / min flow rate and 0.6 bar pressure values with the dispersion prepared at 60° degrees, monodispers and stable visuals in optical microscope is as shown in the Figure 3.2. The size of the microbubbles is proportional to each other at a certain value of gas pressure and flow rate, and they are close to each other although their sizes are variable. After optical microscope images was taken, the manually measured microbubble diameters were determined. Then microbubble size distribution was calculated. When analyzed from these measured values, microbubble size distribution value was found to be 141 µm.

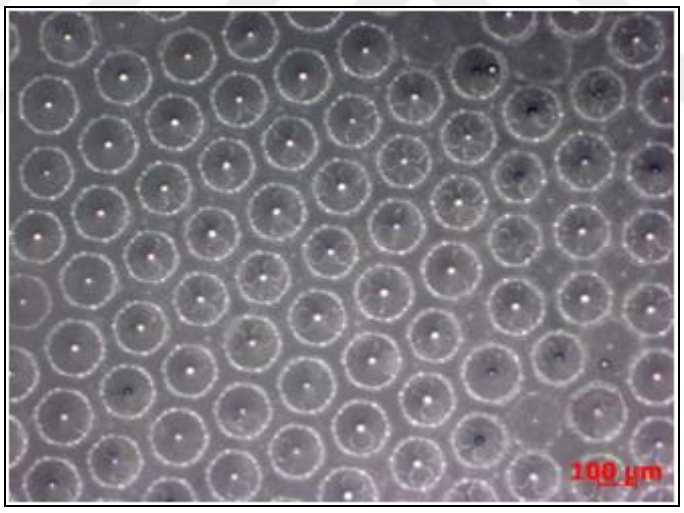

Figure 3.2. The image of the microbubbles obtained in the microfluidic device established with 200 µl / min flow rate and 0.6 bar pressure values with the dispersion prepared at 60° degrees in optical microscope (10x).

3.4. MICROSTRUCTURE ANALYSIS OF FORMED HYDROGEL WITH SCANNING ELECTRON MICROSCOPE

The effect of *Hypericum perforatum* and honey dispersion concentrations on the porous structure and microstructure of the hydrogel that dried and filmed were investigated. The hydrogel films achieved were structurally characterized using SEM technique to determine pore size and size distribution seen in Figure 3.3. Optimum production processing parameters of the hydrogel examined in SEM were dispersion prepared at 60°C degrees containing 1 wt. percent honey and 1 wt. percent *Hypericum perforatum* was converted into hydrogel by producing microbubbles with 200 µl / min flow rate and 0.6 bar pressure values.

The reason for the porous structure on the hydrogel film is that the bubbles burst in the gel during vacuuming and drying processes and leave them to a porous structure. The formation and collection of bubbles during production with the microfluidic system plays an important role in the formation of porous structure. Although all parameters are the same during production, it may be the way bubbles are collected and contacting with 1 wt. percent $CaCI_2$ solution during gelling. In the analysis taken from dense and less dense regions, there is a difference between the pore sizes. While Figure 3.3.a and b are pictures of dense region, Figure 3.3.c and d are characteristic of the less dense region. Gel film structure is thicker in dense environment and pore sizes are more irregular than less dense environment. The surface appearance in the denser environment in Figures 3.3. a and b has a more rough structure. Although this is because of the homogeneous emulsion of the oil content of our dispersion, it can be thought that it is caused by stratification during bubble formation due to its oil content. In a very dense environment, overlapping pore shapes, which can be thought to result from overlapping bubbles in the production phase, have been observed. Comparing Figures 3.3. b and d, it can be assumed that the small pores are much more in the 1000x blown-up image in dense region and are in a more advantageous state for controlled release of the active substance.

There is a non-porous structure in the microbubble-free hydrogel SEM image shown in the Figure 3.4. Images of the sample in the Figure 3.4.a and Figure 3.4.b, it is in the form of an uneven layer. Small ridges with no holes were displayed. It can be thought that this is due to the processes in the gelation stage. It was gelling by mixing manually. Therefore,

stratification and crinkle can be seen. In the higher magnified image in the Figure 3.4.c and Figure.3.4.d, the presence and excess of bumps are observed as they approach. It can be thought that these bumps are not in the form of bubbles and only create a roughness on the surface and have not role in the release of the active substance.

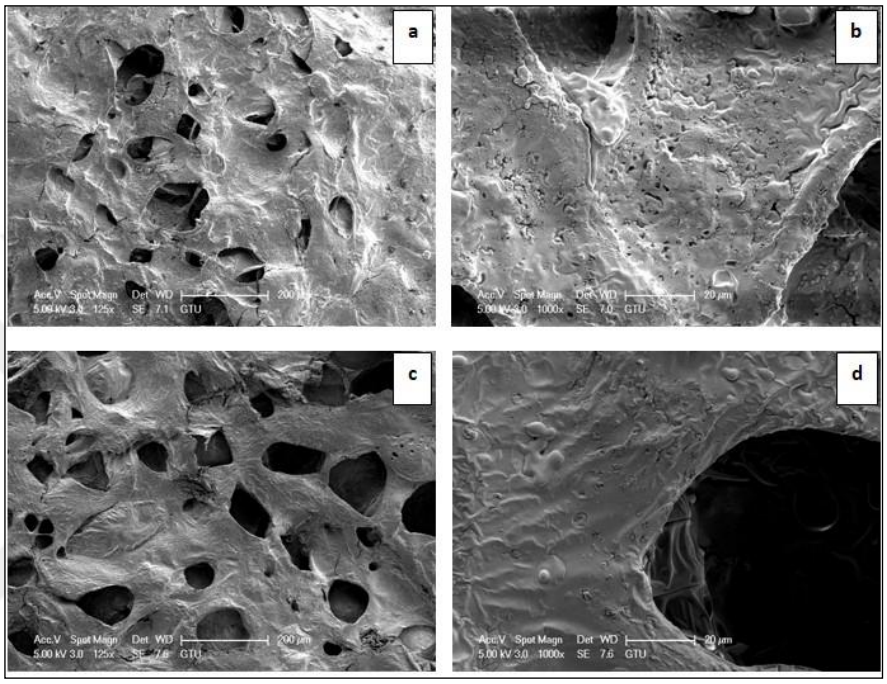

Figure 3.3. SEM images of the dried hydrogel films converted from the polymeric dispersion containing 1 wt. percent honey and 1 wt. percent *Hypericum perforatum* oil microbubbles using the processing parameters 200 µl / min flow rate and 0.6 bar pressure values (a) one location of the sample (b) higher magnified image of the sample in Figure 3.3.a, (c) another area of the same sample (d) higher magnified image of the sample in Figure 3.3.c.

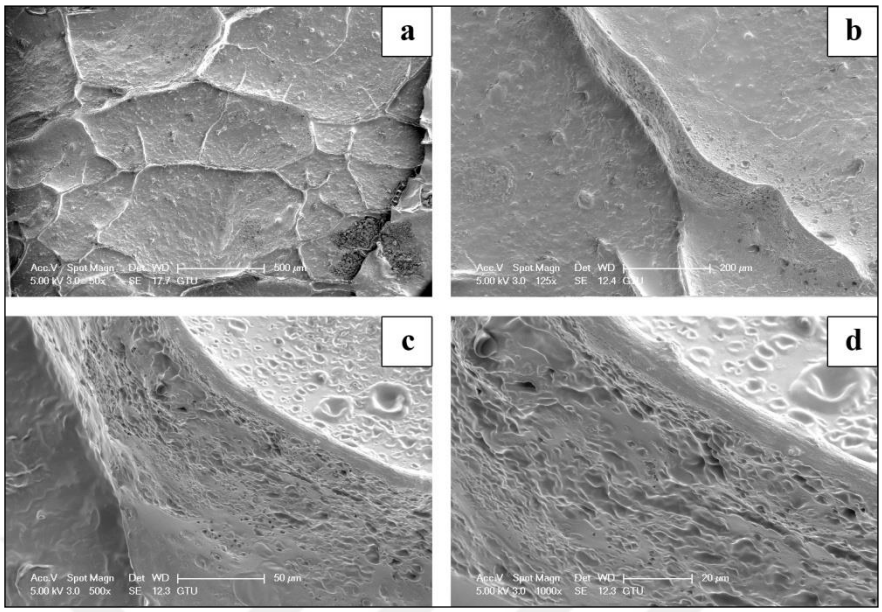

Figure 3.4. SEM images of dried hydrogel films converted from the polymeric dispersion containing 1 wt. percent honey and 1wt. percent Hypericum perforatum oil without microbubbles (a) one location of the sample 50x blown-up image (b) another location of the sample 100x blown-up image (c) 125x blown-up image of the sample (d) 500x blown-up higher magnified image of the sample

3.5. ANALYSIS OF THE CHEMICAL STRUCTURES OF FORMED HYDROGEL

Whether there is any change in the chemical structure of the active substances in the hydrogels obtained was analyzed by FTIR and Raman methods.

3.5.1. Results of Chemical Structure Analysis of Hydrogel Film Using FTIR Characterization

In the FTIR analysis, IR spectra of finished samples and active substances were compared. FTIR analysis graphics are as shown in the Figure 3.5. Finished product spectra are shown in Figure 3.5.b, honey content in Figure 3.5.a and *Hypericum perforatum* Figure 3.5.c. The primary components in the honey formulation are fructose ($C_6H_{12}O_6$), glucose ($C_6H_{12}O_6$), water (H_20), maltose ($C_{12}H_{22}O_{11}$) and sucrose ($C_{12}H_{22}O_{11}$). Other ingredients found in

small amounts in honey such as organic acids, amino acids, enzymes, vitamins, minerals flavonoids and acetylcholine etc. From the FTIR spectra for honey in Figure 3.5.a, there are 2930 cm^{-1} Methylene C-H asymetric / symetric stretching vibration, 1339 cm^{-1} Methyne C-H bending vibration is observed and 1252 cm^{-1} skeletal C-C vibration can be considered. The vibration in 1411 cm^{-1} indicates that it is the carboxylic acid salt with the formula - C (= O) OH. There is a wide twist between 3500 cm^{-1} - 3250 cm^{-1}, which can be said to be alkyne C-H, streching. Vibration modes 1020, 914, 861, 816, 772 cm^{-1} indicate cyclohexane ring vibrations and emphasize that there are multiple fused ring structures. While 1020 cm^{-1} has an aromatic C-H in plane bend at the same time, an aromatic C-H out of plane is observed in the vibration at 861 cm^{-1}. The vibration in 772 cm^{-1} indicate carbon and cloro strechs, while the vibration mode in 1020 cm^{-1} shows the presence of phosphate ion and carbon fluoro compound. It is assumed that the presence of compounds other than C, O, H atoms originates from vitamins in formulation of honey. The vibration at 1252 cm^{-1} is Aromatic ethers, aryl-O stretch. In the vibration in 1339 cm^{-1}, Primary or secondary indicates the presence of OH in-plane bend. The presence of peroxide C-O-O-C strech in honey manifests itself in vibration strech at 816 cm^{-1} [197, 198].

In the honey spectrum graph of Figure 3.5.a compared to other studies [199-202], the O-H stretching vibration band is wide and is approximately in the range of 1800 cm^{-1} and 2900 cm^{-1}. This section is the same as the C-H stress vibration region for carbon aromatic groups. Normally, the range of O-H stretching for the C-H band for carboxylic acids in the range of 2500 cm^{-1}-3000 cm^{-1} is characterized by an irregular absorption. The fluctuation seen in this graph is a sign of absorption likely to be irregular. The tension band in this range and the expansion of the band tension vibration of the OH group is not excessive may mean that hydrogen bonds may be weak. According to the study in which different types of honey were analyzed, the expected O-H stretching band between 3300 cm^{-1}-2500 cm^{-1} was left behind, slipping was detected. A downward descent and stretch were observed between 3500 $cm^{-1}$and 3300 cm^{-1}. Fluctuation was observed in the C = O streching band between 1760 cm^{-1} and 1690 cm^{-1}. Between 1320 cm^{-1} and 1210 cm^{-1}, the C-O streching band was observed more severely than expected. A band corresponding to the C-H tensile band of carboxylic acids and the NH_3 tensile band of free amino acids was observed in 2930 cm^{-1}. Corresponds to the most sensitive absorption site of the main components of 1500 cm^{-1} to 750 cm^{-1} honey, the benchmarked area to measure honey

sugar and organic acids, between 1500 cm^{-1} and 900 cm^{-1} sucrose and glucose and a saccharide configuration between 900 cm^{-1} and 750 cm^{-1} should be observed. Contrary to the study, a downward tension band was observed in the graphic in figure a. OH stretch between 3500 cm^{-1} - 3250 cm^{-1} and around 1600 cm^{-1} OH deformation bends are similar in manuka honey spectrum. Around 1600 cm^{-1} vibration bands can also be caused by N-H bending of amino acid sand vitamins in honey [199-202].

Since the *Hypericum perforatum* was used in conjunction with tween 80 during dissolution, its associated effects were investigated. Looking at the spectrum graph of the mixture of *Hypericum perforatum* and Tween 80 in Figure 3.5.c, the C-O streching band observed in 1075 cm^{-1}, the C-H band between 1609 cm^{-1} and 1443 cm^{-1}, the C = O streching band observed in 1743 cm^{-1}, and the C-H streching band observed in 2853 are observed and parallel to the study examined. The strech in 1243 cm^{-1} is also a vibration observed in the pure tween 80 spectrum and can be said to have an effect. The breaking band in 2928 cm^{-1} indicates the presence of tween 80 and can be connected to the CH_2 streching mode of the methyl and methylene groups. The stretching vibration of the carbonyl group is found at 1608 cm^{-1} as a sign of hypericin molecule from Hypericin extract. The C-O-C stretching mode, which should be in 950 cm^{-1} of pure tween 80, was seen in graphic c at 1075 cm^{-1}. *Hypericum perforatum* combined with the C-O streching band and slipped. The Tween 80 terminal hydroxyl group had the O-H streching band at 3455 cm^{-1}, and in graph c this value shifted to 3353 cm^{-1}, indicating the presence of *Hypericum perforatum* and intermolecular binding. In 2928 cm^{-1}, 2853 cm^{-1} and 3353 cm^{-1} there are bends and vibrations that are in pure tween 80 but progress with a shift of about 10 cm^{-1} . The narrowing of the spectrum band and the decrease in density are a sign of this. A large number of vibration peaks before the vibration of 1075 cm^{-1} indicate aromatic rings, the vibration caused by fluctuations between 1443 cm^{-1} and 1609 cm^{-1} appears to occur due to the streching of C = C and combination with the C-O phenolic groups in 1243 cm^{-1} vibration mode. In *Hypericum perforatum* extracts in the literature, the peaks associated with phenolic compounds have shifted towards the high wavenumber and are the only strong peaks, while they have been distributed as small peaks in this study. The vibration resulting from the stretching vibration of the hydroxyl group around 3353 cm^{-1} is similar but has a much deeper density and *Hypericum perforatum* peak points are in line with the literature [204-206, 215].

If each vibration is analyzed one by one in FTIR spectrum analysis, for Figure 3.5.c; the strech at 3353 cm^{-1} is the normal polymeric OH strech stress, but the other breakage in that area can be thought to be aliphatic secondary amine NH strech. Vibrations 2928 cm^{-1} and 2853 cm^{-1} are evaluated as methylene C-H asymetric / symetric strech. 1743 cm^{-1} can be interpreted as aromatic combination bands and ester vibration. There are around 1609 cm^{-1} aromatic ring strech, primary amine NH bend presence and open chain nitrogen (-N = N-) vibration. In the tension in 1443 cm^{-1}, methyl C-H asymetric / symetric bend is observed. Vibrations in 1243 cm^{-1} and 1075 cm^{-1} include scleeletal C-C vibration. When examined 1243 cm^{-1} alone, aromatic ether aryl - O strech is observed, while 1075 cm^{-1} is observed as alkyl substituted ether or cyclic ethers large ring C-O strech. In the vibration band extending to 1075 cm^{-1}, four different vibrations appear: aromatic C-H out of plane bend, aliphatic fluoro compound, primary amine CN strech and organic siloxane or silicone (Si-O-Si) strech [197].

Optimum production processing parameters of the hydrogel, whose graph is shown in Figure 3.5.b and analyzed in FTIR were dispersion prepared at 60°C degrees containing 1 wt. percent honey and 1 wt. percent *Hypericum perforatum* was converted into hydrogel by producing microbubbles with 200 µl / min flow rate and 0.6 bar pressure values. Methylene C-H asymetric / symetric strech is observed at 2924 cm^{-1} and 2851 cm^{-1} vibration on hydrogel FTIR spectrum graph with alginate based honey and *Hypericum perforatum* oil in Figure 3.5.b. These strechs were also observed in *Hypericum perforatum* and honey. In the vibration in 1740 cm^{-1}, aromatic combination band, ester and alkyl carbonate bends are observed. Contains methylene C-H bend in vibration in 1458 cm^{-1}. It contains OH bend and phenol or tertiary alcohol, carboxylic acid salt and C-N strech aromatic tertiary amine in the vibration in 1353 cm^{-1}. C arboxylic acid is caused by pure honey. In 1239 cm^{-1}, there are C-C strech skeletal vibration, aromatic ethers and aryl-O strech. In the vibration of 1101 cm^{-1}, the bands of aromatic C-H in plane bend and secondary alcohol C-O strech, C-O-C alkyl substituted ether and aliphatic fluoro compound compounds are observed. Vibrations in 1001 cm^{-1} indicate C-F streching and C-Cl streching. These vibrations indicate bonding with aliphatic fluoro and chloro compounds. It is caused by the presence of honey and hydrogen. The polymeric OH strech vibration between 3500 cm^{-1} and 3250 cm^{-1} is not as strong as in the *Hypericum perforatum* oil; it appears as a less severe vibration band [197].

These graph in Figure 3.5.b compared to other studies in the literature –OH. - CH2 = CH, - NH_2, -COOH and -NO_2 showed the presence of functional groups. The streching vibrations of the O-H bonds of the alginate appeared in the range of 3500 cm^{-1} - 3250 cm^{-1}. The bands at 1101 cm^{-1} were connected to the C-O stretching vibration of the pyranosyl ring and the C-O stretching with the contribution of the C-C-H and C-O-H deformation. The presence of R = H or C and R-NO bonds that occur in the presence of alginate and hydrogel can be seen in vibrations 1458 cm^{-1} , 1353 cm^{-1} and 1239 cm^{-1}. The C-H streching in 2924 cm^{-1} and 2851 cm^{-1} are observed at almost the same wavelengths as the *Hypericum perforatum* oil spectrum. The C-H bendings between 1458 cm^{-1} and 1239 cm^{-1} are vibrations spreading in the same areas as *Hypericum perforatum*, but fluctuations in the presence of honey may have caused the waves to shift. The C-O streching in 1101 cm^{-1} may have shifted partially from the presence of sugar and amino acids in the honey content or the effects of the R = H or C bonds of the alginate [202, 205, 207].

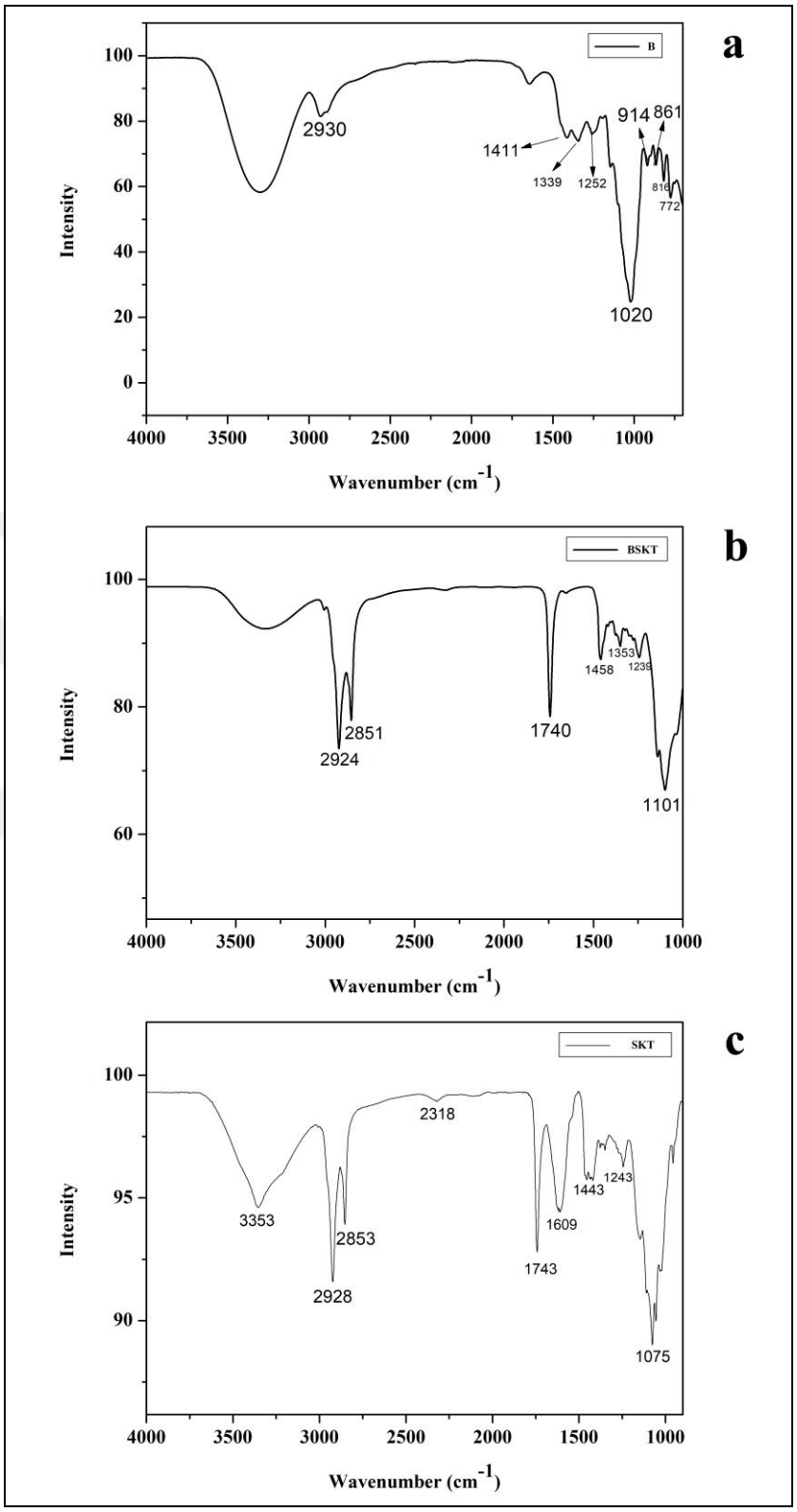

Figure 3.5. FTIR spectra of samples (a) honey (b) hydrogel film in which contain honey and *Hypericum perforatum* oil (c) *Hypericum perforatum*.

3.5.2. Chemical Structure Analysis of Hydrogel Film with FT-Raman Spectroscopy

Raman analysis was performed on an alginate-based hydrogel dried sample containing *Hypericum perforatum* and honey. Optimum production processing parameters of the hydrogel, whose graph is shown in Figure 3.6 and analyzed in Raman were dispersion prepared at 60°C degrees containing 1 wt. percent honey and 1 wt. percent *Hypericum perforatum* was converted into hydrogel by producing microbubbles with 200 µl / min flow rate and 0.6 bar pressure values. While Figure 3.6.a is the general graphic of our sample, it is a zoomed-in view of the wavenumbers between 900 cm^{-1} and 1500 cm^{-1} in Figure 3.6.b. In the FT-Raman spectra of honey, polysaccharides and *Hypericum perforatum* oil mix, it is usual to assign the bands precisely and not to see strong vibrations because most of the vibrations are due to highly bound C - O, C - OH and C - C groups. Looking at the general Raman graph, we can connect the fluctuation in Figure 3.6.a between 500 cm^{-1}-550 cm^{-1} to the vibrations of the disulfide bridge with the > S-S <bond. It is obtained by combining with R - S - S - R functional group structure or usually by combining two thiol groups. The most important region in Raman analysis for honey is the spectrum between 700 cm^{-1} and 1700 cm^{-1}. In this region, fructose and glucose do not show characteristic peaks and do not give information about their concentrations in honey. Between 200 cm^{-1} and 1600 cm^{-1} values, the vibration modes of different bonds taken from carbohydrates, proteins and organic acids in honey may cause the peaks to shrink and narrow. It is possible to see the contributions of fructose, glucose and sucrose in honey between 200 and 1.500 cm^{-1} wavelengths. The spectreal region between 200 and 1600 cm^{-1} has been found to be interesting because it represents the vibration modes of bonds different from carbohydrates, proteins and organic acids. At the same time, sharp peaks are observed due to the unknown bond vibrations of *Hypericum perforatum* and alginate in the product. The presence of a strong peak between 200 cm^{-1} and 600 cm^{-1} indicates skeletal vibration movements with great contributions from the deformation modes of the C-C-C, C-C-O, C-C and C-O saccharide groups. α-D-glucose and β-D-glucose marks can be assigned to a C2 - C1 - O1 bending vibration that performs the Raman band at 540 cm^{-1}. This band is not found in crystalline structures; it is seen in structures with water content and shows the presence of *Hypericum perforatum* oil, alginate and distilled water content. The small peak near 910 cm^{-1} may be the bending vibration of C (1) -H and COH, and between 1025 cm^{-1} and 1100 cm^{-1} there are the same bonds, as well as C-N bonds from

other components, protein and amino acids. Due to its alginate content, the peak in 1025 cm^{-1} indicates the presence of Guluronic acid and the peak in 1100 cm^{-1} indicates the presence of Mannuronic acid. The deformation band of CH_2 groups at 1400 cm^{-1} observed in the FTIR and FT-Raman spectra of commercial alginate is seen as a strong streching vibration band around 1350 cm^{-1}. The strong peak around 1350 cm^{-1} indicates the CH_2 wagging vibration. The region between 1350 cm^{-1} and 1400 cm^{-1} is associated with CH and OH bending. The peak between 1250 cm^{-1} and 1290 cm^{-1} and can provide evidence of C-OH vibration. Very fluctuating vibrations occur between 1100 cm^{-1} and 1250 cm^{-1}, which are considered as C-O streching vibration. Fluctuations between 1450 cm^{-1} - 1460 cm^{-1} are considered as CH_2 vibration. Very small fluctuations are observed in the vibration zone between 2850 cm^{-1} and 3100 cm^{-1}, and this can be considered to be due to symmetrical and asymmetrical C - H streching mode. It was determined that the type of vibration between 3200 cm^{-1} and 3300 cm^{-1} could be Stretching of O-H. For the bonds to be formed due to the presence of *Hypericum perforatum* as edible oil in the finished product, the small peak around 968 cm^{-1} may represent the C = C bond, and around 1008 cm^{-1} may indicate the CH3 bond and the high ripple =C-H bond around 1265 cm^{-1}. The flickering between 800 cm^{-1} and 860 cm^{-1} is thought to be the cause of the C-C stretching vibration mode. While C = O streching mode is the factor of breaking around 1750 cm^{-1}, C-H asymetrc streching affects the decrease after 2900 cm^{-1} while C-H symetric streching is between 1750 cm^{-1} and 2900 cm^{-1} values [208-214].

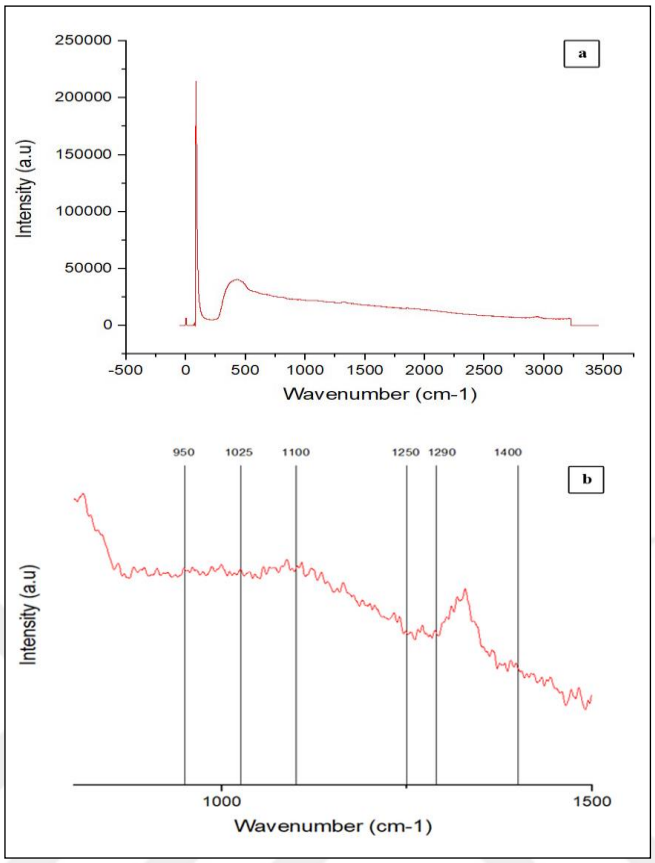

Figure 3.6. FT-Raman spectra of hydrogel film sample converted from microbubble parameters 200 µl / min flow rate and 0.6 bar pressure values with dispersion containing 1 wt. percent honey and 1 wt. percent *Hypericum perforatum* oil, (a) is the general graphic of our sample, (b) it is a zoomed-in view of the wavenumbers between 900 cm^{-1} and 1500 cm^{-1}.

3.6. ANALYSIS OF THERMAL PROPERTIES OF FORMED HYDROGEL

3.6.1. Thermal Analysis of Formed Hydrogel with DSC

As shown in the graphic in the Figure 3.7, an endothermic peak is between 90°C and 100°C degrees were observed. A single large endothermic peak was observed for the product containing all of the active ingredients, indicating that it has a fast crystallizing polymer structure. The only endothermic peak is that only dehydration occurs between the measured temperatures, biopolymer decomposition or carbonization was not observed in

this temperature range. Since honey has a high rate of glucose and fructose, the melting temperature of the glucose in the honey observed in previous studies is between 146 °C, the melting temperature of fructose is between 103 °C, and the endothermic peak value has been observed in the region where the temperature is in the range of 110-150 ° C. While the endothermic change is expected between these values, the reason for being between 90° and 100° in our result may be due to the *Hypericum perforatum* and alginate effects in the hydrogel content. In the thermograms, the melting peak of water was not observed because it is known that the water in honey is connected in the sugar molecular network. In the DSC curve of the *Hypericum perforatum* extract, it is seen that it has a very large peak and is centered at approximate 57.42 °C. While pure alginate endothermic value is 100°C, sodium alginate endothermic value is around between 90°C and 100°C.

Crystallization structure is seen in the graph in the Figure 3.7. Three stages are observed in the DSC thermoanalytical curve in the Figure 3.7. The glass transition temperature at the beginning of the thermal effect is characterized by a change in the heat capacity, although it is very weak. An endothermic phenomenon around 0° degrees can be called the transition 2 zone, a wide and excessive endothermic peak between area of 10° and 40° degrees to 160° and 220° degrees is called transition 3 [215-221].

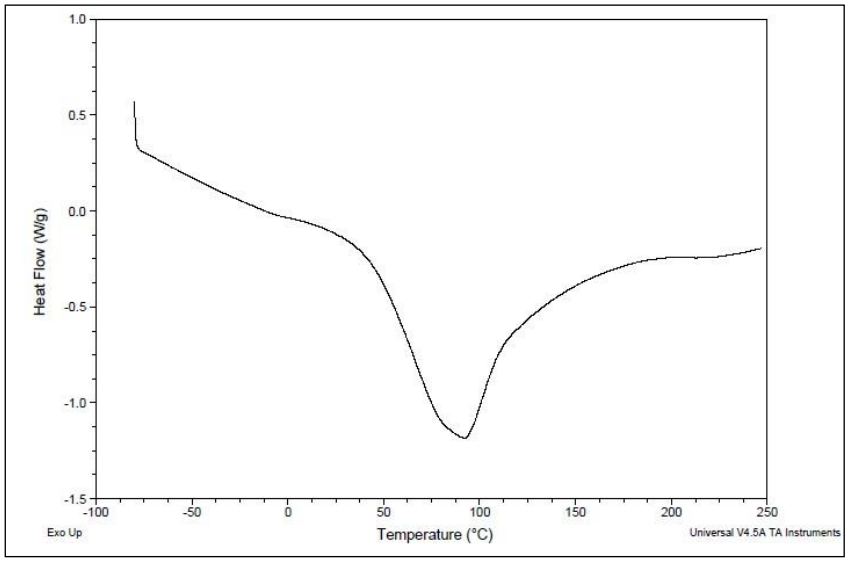

Figure 3.7. Differential scanning calorimetry thermograms of hydrogel film structure converted from microbubble parameters 200 µl / min flow rate and 0.6 bar pressure values with dispersion containing 1 wt. percent honey and 1 wt. percent *Hypericum perforatum* oil.

3.6.2. Thermal Analysis of Formed Hydrogel with TGA

Honey is the most stable product in the product content as thermal stability. Sample weight has been decreased stepless and proportional to temperature. *Hypericum perforatum* oil, on the other hand, is a product that has loses mass in more stages as the temperature increases as it is a volatile oil and consists of evaporative molecules as compounds. The amount of *Hypericum perforatum* residual material in the decomposition temperature is the highest in the formed hydrogel product.

In our analysis for DTG graphic values, the weight loss rate for Honey is important at 200° degrees. For *Hypericum perforatum*, when the decomposition temperature is around 300° degrees, this value increases in the finished formed hydrogel sample and reaches around 400° degrees. The addition of honey increased the strength and thermal stability of *Hypericum perforatum*, which makes a lot of peaks [217, 222- 223].

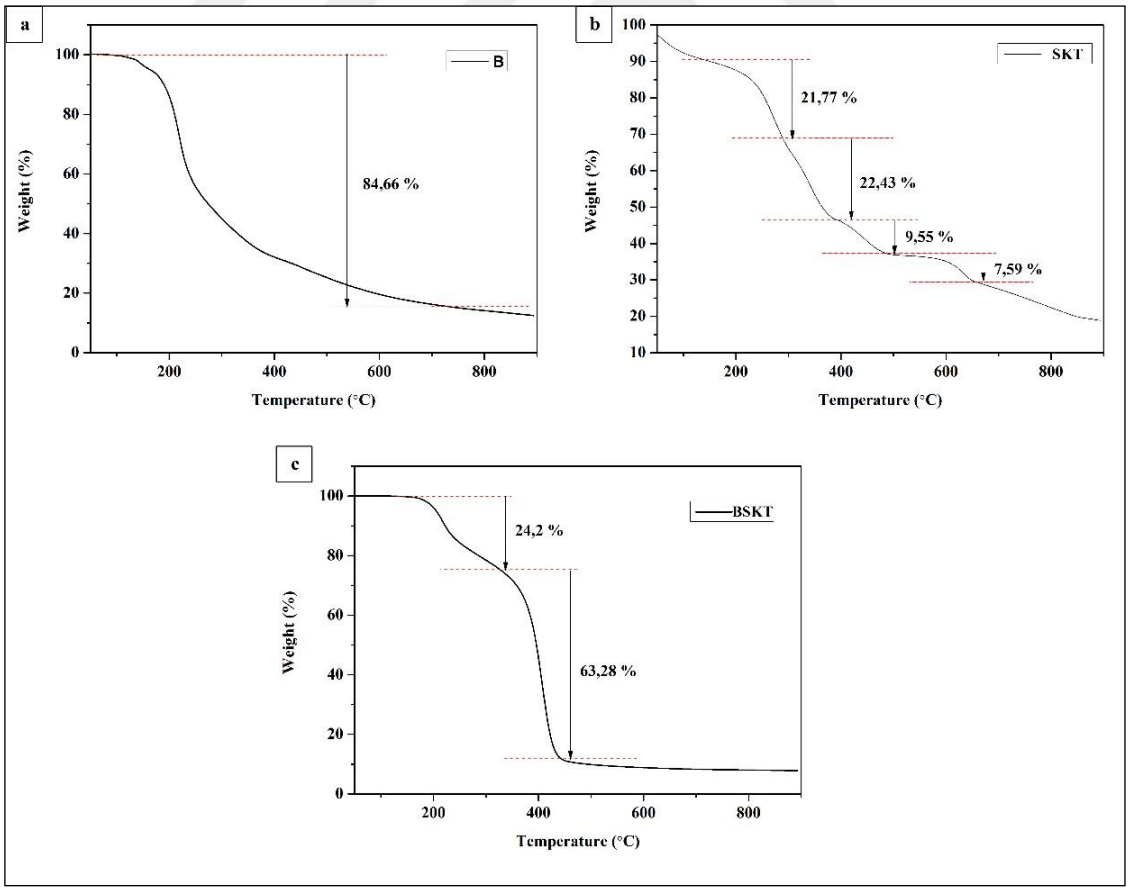

Figure 3.8. TGA analysis of (a) honey (b) *Hypericum perforatum* (c) hydrogel film contain *Hypericum perforatum* and honey.

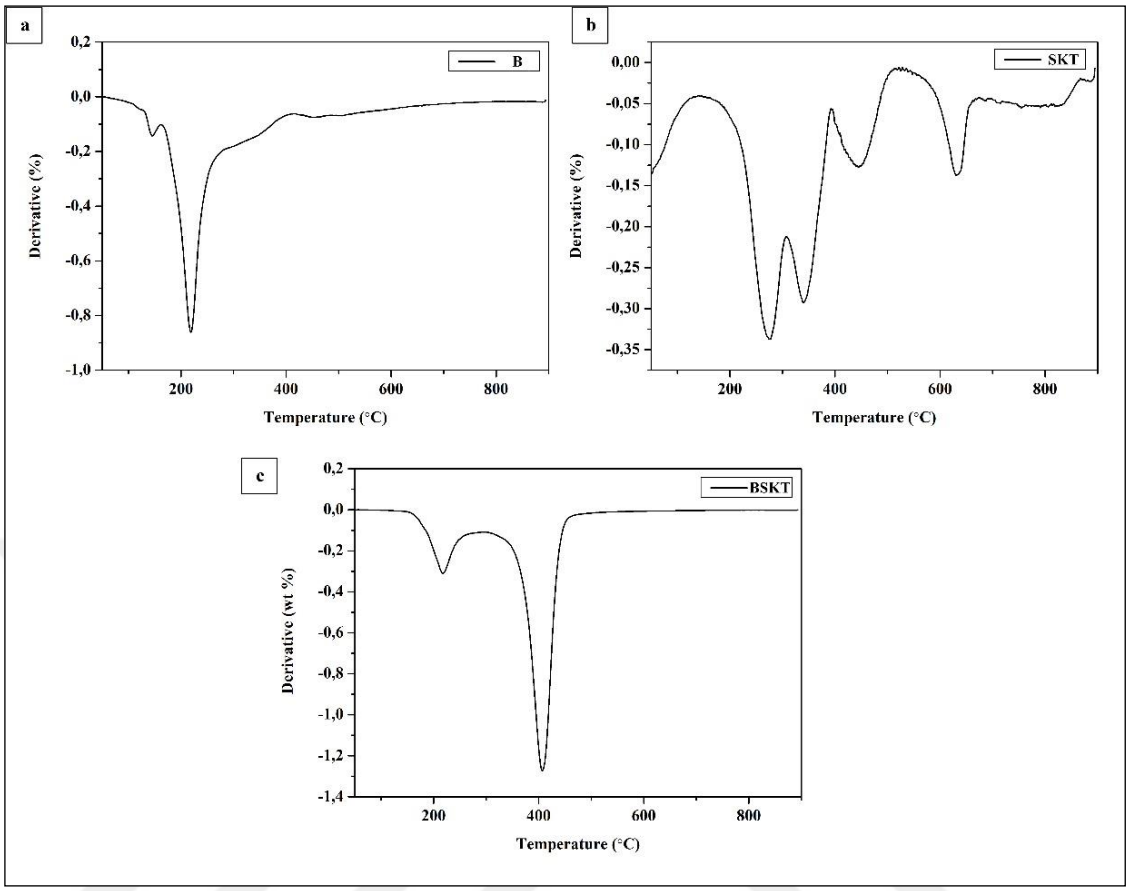

Figure 3.9. DTG graphs of (a) honey (b) *Hypericum perforatum* (c) hydrogel film converted from microbubble parameters 200 µl / min flow rate and 0.6 bar pressure values with dispersion containing 1 wt. percent honey and 1 wt. percent *Hypericum perforatum* oil.

3.7. ANALYSIS OF CRYSTAL STRUCTURES OF HYDROGEL OBTAINED WITH XRD

In Figure 3.10, it was graphically analyzed of alginate-based hydrogel containing *Hypericum perforatum* and honey by performed X-ray diffraction method. When the graph is examined, two peaks are seen; one large peak rise around 2θ=20° and a small peak around 2θ=5° were observed. In studies in the literature, a similar graphic structure was found in general in XRD analysis with honey and antibacterial mixed plant extract nanofibers, the most optimal nanofibers with amorphous structure and 2θ = 19° were

remarkably similar to XRD graphics in our study. Further, a single-peak graphic between 2θ=10° and 2θ=20° was observed in the alginate and these are similar to our result. Compared to the XRD graph of *Hypericum perforatum* extract, a main peak at around 2θ = 45° and around 2θ = 15°-20° other peaks at close level are observed, generally peak intensity is frequently and closely [222, 224]. Crystallinity index values are called CI and express the degree of crystallinity. A value can be found from the analysis of the peaks of the XRD chart. According to the equation 3.1. used in the literature, an approximate value can be found from the XRD chart.

$$CI\ (\%) = \frac{Acrystal}{Atotal} \cdot 100 \tag{3.1}$$

Where, $A_{Crystal}$ is the sum of the areas under the crystalline diffraction peaks and A_{Total} represents the total area under the diffraction curve between 2θ = 0 ° − 70 °. Our Crystallinity index (CI) takes a value between 11 percent and 15 percent approximately. CI and porosity are inversely proportional. The decrease in CI shows an effect that increases porosity and permeability. A decrease in crystallinity can affect the mechanical properties of the product, making it more flexible and amorphous [225].

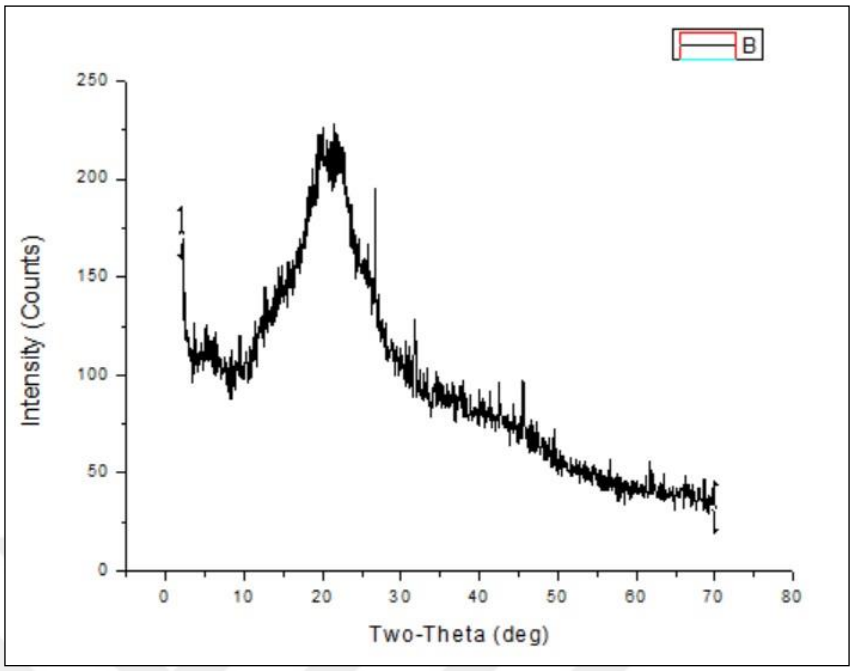

Figure 3.10. The X-ray diffraction spectrum (XRD pattern) of hydrogel film converted from microbubble parameters 200 µl / min flow rate and 0.6 bar pressure values with dispersion containing 1 wt. percent honey and 1 wt. percent *Hypericum perforatum* oil.

3.8. APPLICATION OF HYDROGEL MASK ON VOLUNTEERS

Optimum production processing parameters of the hydrogel applied on volunteered patients, were dispersion prepared at 60°C degrees containing 1 wt. percent honey and 1 wt. percent *Hypericum perforatum* was converted into hydrogel by producing microbubbles with 200 µl / min flow rate and 0.6 bar pressure values. Application was made to six volunteered patients. It was applied for a long time, about 3 hours. Once applied to the blemish area in the face area of three volunteer patients and the injured area formed in the hands of three volunteer patients. Later on, mask was applied for 15 minutes to another area that undamaged and moisture was measured when before and after application with a user manual digital moisture oil content analyzer device. The visuals of the volunteer patients that were applied before and after the application were shown in the picture and the measured moisture values are given in the Table 3.2. The moisture meter

used shows two data. After waiting for a certain time by contacting with the skin, the percentage of oil and water measured from the skin surface is given on the digital screen.

Table 3.2. Measured moisture values of the volunteers (a) before application and (b) after application of hydrogel converted from microbubble parameters 200 µl / min flow rate and 0.6 bar pressure values with dispersion containing 1 wt. percent honey and 1 wt. percent *Hypericum perforatum* oil.

MEASURED MOISTURE VALUES				
	Before Application		**After Application**	
#Number of volunteers	**Water content of the skin (%)**	**Oil content of the skin (%)**	**Water content of the skin (%)**	**Oil content of the skin (%)**
1	36,4	16,3	38,4	17,2
2	32,9	14,8	40,8	18,3
3	31,7	14,2	37,1	16,6
4	30,7	4,8	38,5	17,3
5	32,2	14,4	39,3	17,6
6	36,9	16,6	41	18,5

Table 3.3. Measured moisture values of the volunteers (a) before application and (b) after application of hydrogel with dispersion containing 1 wt. percent honey and 1 wt. percent *Hypericum perforatum* oil without microfluidic technique.

MEASURED MOISTURE VALUES				
	Before Application		**After Application**	
#Number of volunteers	**Water content of the skin (%)**	**Oil content of the skin (%)**	**Water content of the skin (%)**	**Oil content of the skin (%)**
1	30,1	13,5	47,1	21,1
2	35,6	16,0	37,5	16,8
3	38,2	17,1	46,9	21,1
4	40,3	18,1	56,2	25,2
5	35,8	16,1	48,0	21,6
6	33,2	14,9	36,6	16,4

Considering the results of the measurements made with the moisture meter shown with microbubble hydrogel in the Table 3.2, it was observed that there was an increase in both the amount of moisture and the amount of oil on the skin. The change of water and oil content values in the skin is examined in detail in the graphic in the Figure 3.11. When looking at the measurement results with the moisture meter shown with hydrogel without microbubbles in Table 3.3, it was seen that there was an increase in both the amount of moisture and the amount of oil in the skin but the increase in oil was more. After the application of microbubble-free hydrogel, the change of water and oil content values in the skin was examined in detail in the graph in Figure 3.12. There was a greater increase in the results of the application with microbubble hydrogel, but but this is not a significant difference. When the graphs of Figure 3.11 and Figure 3.12 are compared, the change in

the water and oil content values in the skin increased in both samples, but a slightly greater increase was observed after the application with microbubble hydrogel. It was found that there is a significant difference between before and after application results of amount of skin moisture as seen in Figure 3.11 and Figure 3.12. The rate of oil in the skin increased more than the water rate.

Statistical analysis was made with the values in the Table 3.2. Statistical analysis was performed by one-way analysis of variance (ANOVA) followed by Kruskal wallis test with the software package Prism 5.04 (Graph Pad Software Inc., la Jolla, CA). A value $p < 0.05$ was taken as the level of significance.

The pictures in Figure 3.13.b and Figure 3.14.b are the photograph taken 72 hours after the application while the volunteer pictures in Figure 3.13.a and Figure 3.14.a are before the application. After the application, a successful result was obtained especially in injuries in the hand region due to eczema. In acne and blemishes on the face, it can be evaluated as a factor that speeds up heals at a certain rate.

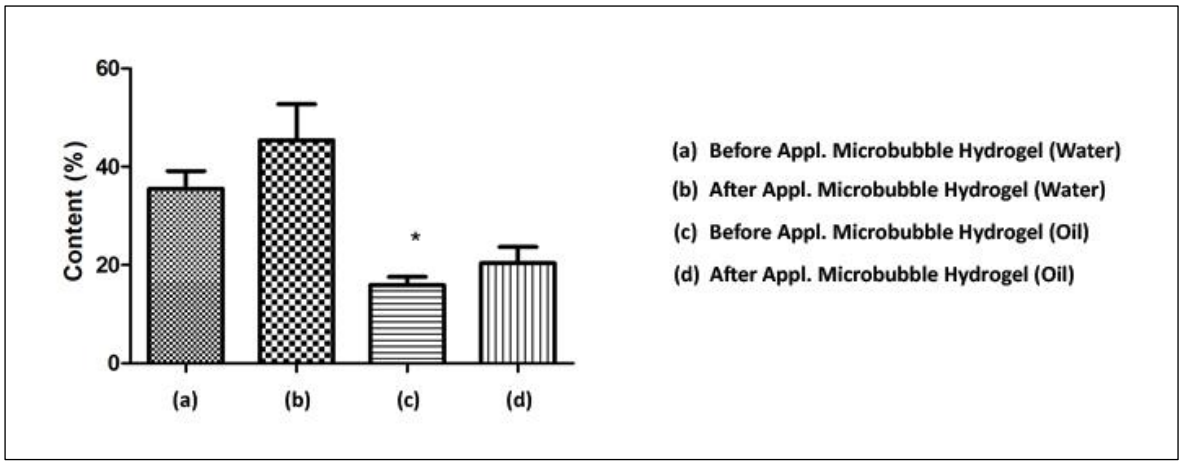

Figure 3.11. The graph of change of water content of the skin measured values of the volunteers before application and after application with hydrogel converted from microbubble parameters 200 µl / min flow rate and 0.6 bar pressure values with dispersion containing 1 wt. percent honey and 1 wt. percent *Hypericum perforatum* oil.

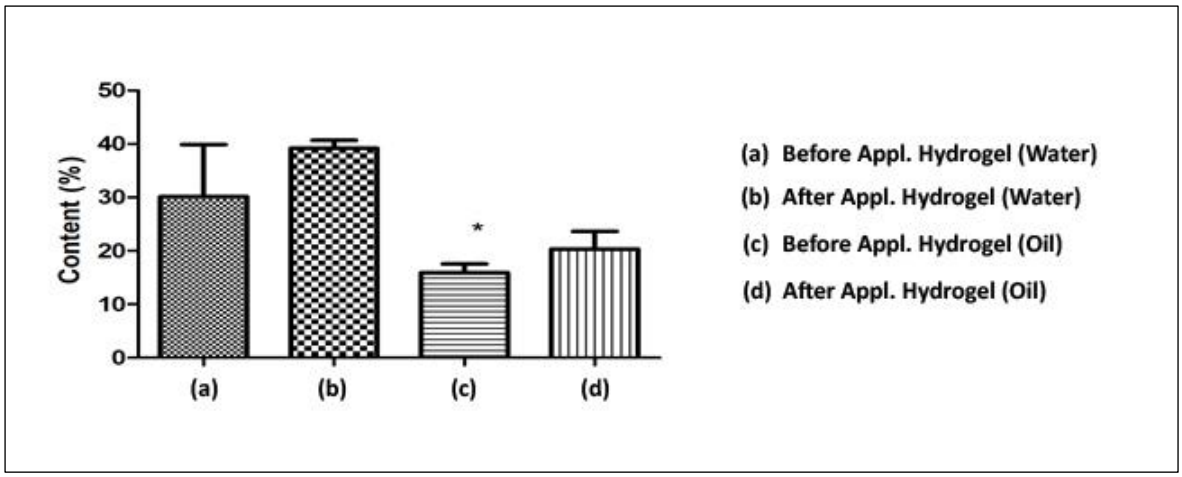

Figure 3.12. The graph of change of oil and water content of the skin measured values of the volunteers before application and after application with hydrogel with dispersion containing 1 wt. percent honey and 1 wt. percent *Hypericum perforatum* oil without microfluidic technique.

Figure 3.13. Pictures of the change of patients with wounds (a) before application and (b) after application of hydrogel converted from microbubble parameters 200 µl / min flow rate and 0.6 bar pressure values with dispersion containing 1 wt. percent honey and 1 wt. percent *Hypericum perforatum* oil.

Figure 3.14. Pictures of the change of patients with acne (a) before application and (b) after application of hydrogel converted from microbubble parameters 200 µl / min flow rate and 0.6 bar pressure values with dispersion containing 1 wt. percent honey and 1 wt. percent *Hypericum perforatum* oil.

4. CONCLUSION

In this thesis, a skin mask was produced via a T-junction microfluidic device method to be therapeutic, soothing and care supportive for skin problems. Natural and herbal raw materials have been used as an effective alternative in the cosmetic and medical industry due to their active natural compounds and fewer side effects than the synthetic materials. The mask active ingredients prepared for this are honey and *Hypericum perforatum* oil, and it is aimed to benefit from wound healing, antibacterial and moisturizing properties. It was a desired result that the mask was hydrogely and porous, to achieve this, a microfluidic technique with t-junction was used. Then characterization studies of this mask were made. The porous structure is desired to have a long-term effect on the release of active substances. In order to obtain this porous structure, microbubble was obtained with the microfluidic device and a hidogel was formed by the gelation of the microbubbles. The porous hydrogel mask shown in the characterization studies and physical analysis provided better mechanical properties for the active substances to release more efficiently. Moreover, a more efficient use was created in this way rather than the use of hydrogel without microbubbles with the same active substances. The effect on the skin was tested only in a dose-adjusted manner, and the effectiveness was wanted to be determined, without testing pure active ingredient. The dosage is adjustable and easy to use, and since it is trapped in the hydrogel, it is more compatible with the skin and bioavailability is higher. *Hypericum perforatum* and honey are frequently used among colloquially, and it is aimed to benefit from its healing properties by applying it to the skin in pure form. The purpose of this study is to use it in a dose-adjusted and controllable way. The active ingredient contents amount can also be used by altering, but this study aimed to produce controlled-release hydrogels by focusing on a different method and technique.

This study can be considered as a preliminary in vivo study. The hydrogel-structured mask that has the appropriate structure was then tested on volunteered patients, and before and after application, skin moisture was measured with skin moisture and oil content analyzer quantitatively before and after application. When these values were compared, it was observed that there was an increase in the moisture content of the skin after application. When the oil ratio and water ratio were measured, a greater increase was observed in the water and oil ratio of the skin and the skin was moistened. In the comparison between the

results of the two hydrogel products with and without microbubbles, it was seen that there was a slightly greater increase after application with microbubble hydrogel. The high moisturizing properties of the produced mask result from the moisture content of the active substance as well as the high-water content property arising from the hydrogel polymer structure and porous structure. An application was made on eczema related injuries and acne and blemishes. These were visually and qualitatively inspected. Wound healing has done much better than acne healing. In the present case, it can be considered that the active substances activate the wound healing properties with their moisturizing properties as well as the disinfection and wound healing properties. In acnes, in some areas, both healing and healing speeds were increased. It can show that the active substances are effective. These show that the active substances have the same effects as in the literature and are effective. In addition, it is observed that there is no problem in passing the substances contained in the hydrogel structure produced to the skin and in the absorption of the substances to the skin. The results of the study can be evaluated as promising and successful. It is thought that more meaningful changes will occur when the number of volunteers and uses, usage frequency and duration are increased. In future studies, it is aimed to increase the efficiency by increasing these parameters. This article explains and experiences an easy-to-apply and fast production process that contributes to the development of a lab-scale but sustainable technology in the cosmetics and medical industry.

REFERENCES

1. Chirani N, Yahia L, Gritsch L, Motta F, Chirani S, Faré S. History and applications of hydrogels. *Journal of Biomedical Sciences.* 2015;4(2):13-36.

2. Anamica M, Pande PP. Polymer hydrogels and their applications. *International Journal of Materials Science*. 2017;12(1):11-14.

3. Mohite PB, Adhav S. A hydrogels: Methods of preparation and applications. *International Journal of Advances in Pharmaceutics*. 2017;6(3):79-85.

4. Bahram M, Mohseni N, Moghtader M. An introduction to hydrogels and some recent applications. *Emerging Concepts in Analysis and Applications of Hydrogels*. 2016:9-32.

5. Enas AM. Hydrogel: Preparation, characterization, and applications: A review. *Journal of Advanced Research*. 2015;6(2):105-121.

6. Hennink WE, Nostrum CF. Novel crosslinking methods to design hydrogels. *Advanced Drug Delivery Reviews*. 2002;54(1):13-36.

7. Barbucci R, Leone G, Vecchiullo A. Novel carboxymethylcellulose-based microporous hydrogels suitable for drug delivery. *J. Biomater. Sci. Polymer*. 2004;15(5):607-619.

8. Said HM, Alla SGA, El-Naggar AWM. Synthesis and characterization of novel gels based on carboxymethyl cellulose/acrylic acid prepared by electron beam irradiation. *Reactive & Functional Polymers*. 2004;61(3):397-404.

9. Fei B, Wach RA, Mitomo H, Yoshii F, Kume T. Hydrogel of biodegradable cellulose derivatives. I. Radiation-induced crosslinking of CMC. *Journal of Applied Polymer Science*. 2000;78(2):278-283.

10. Liu P, Maolin Z, Li J, Peng J. Radiation preparation and swelling behavior ofsodium carboxymethyl cellulose hydrogels. *Radiation Physics and Chemistry*. 2002;63(3):525-528.

11. Lugao AB, Malmonge SM. Use of radiation in the production of hydrogels. Nuclear *Instruments and Methods in Physics Research B*. 2001;185(1):37-42.

12. Al-Assaf S, Phillips GO, Williams PA. Controlling the molecular structure of food hydrocolloids. *Food Hydrocolloids*. 2006;20(2-3):369-377.

13. Al-Assaf S, Phillips GO, Williams PA, Plessis TA. Application of ionizing radiations to produce new polysaccharides and proteins with enhanced functionality. Nuclear *Instruments and Methods in Physics Research B*. 2007;265(1):37-43.

14. Chai Q, Jiao Y, and Yu X. Hydrogels for biomedical applications: Their characteristics and the mechanisms behind them. *Gels*. 2017;3(1):6-33.

15. Shin SJ, Park JY, Lee JY, Park H, Park YD, Lee KB, et al. "On the Fly" Continuous generation of alginate fibers using a microfluidic device. *Langmuir*. 2007;23(17):9104-9108.

16. Chung BG, Lee KH, Khademhosseinicdef A, Lee SH. Microfluidic fabrication of microengineered hydrogels and their application in tissue engineering. *Lab on a Chip*. 2012;12(1):45-59.

17. Aketagawa K, Hirama H, Torii T. Hyper-miniaturisation of monodisperse janus hydrogel beads with magnetic anisotropy based on coagulation of fe3o4 nanoparticles. *Journal of Materials Science and Chemical Engineering*. 2013;1(2):1-5.

18. Dendukuri D, Pregibon DC, Collins J, Hatton AT, Doyle PS. Continuous-flow lithography for high-throughput microparticle synthesis. *Nature Materials*. 2006;5(5):365-699.

19. Panda P, Ali S, Lo E, Chung BG, Hatton TA, Khademhosseini A, et al. stop-flow lithography to generate cell-laden microgel particles. *Lab Chip*. 2008;8(7):1056-1061.

20. Hwang DK, Dendukuria D, Doyle PS. Microfluidic-based synthesis of non-spherical magnetic hydrogel microparticles. *Lab Chip*. 2008;8(10):1640-1647.

21. Franze GT, Ni B, Ling Y, Khademhosseini A. A controlled-release strategy for the generation of cross-linked hydrogel microstructures. *J. Am. Chem. Soc.* 2006;128(47):15064-15065.

22. Wang K, Lu Y, Xu JH, Tan J. Generation of micromonodispersed droplets and bubbles in the capillary embedded t-junction microfluidic devices. *AIChE Journal*. February 2011;57(2):299-306.

23. Herrada M, Ga˜n´an-Calvo MA, Montanero JM. Theoretical investigation of a technique to produce microbubbles by a microfluidic T junction. *Physical Review E*. 2013;88(3):1-10.

24. Thorsen T, Roberts RW, Arnold FH, Quake SR. Dynamic pattern formation in a vesicle-generating microfluidic device. *Physical Review Letters*. 2001;86(18):4163-4166.

25. Elsayed M, Kothandaraman A, Edirisinghe M, Huang J. Porous Polymeric Films from Microbubbles Generated Using a T-junction Microfluidic Device. *Langmuir*. 2016;32(50):13377-13385.

26. Yeh CH, Zhao Q, Leea SJ, Lin YC. Using a T-junction microfluidic chip for monodisperse calcium alginate microparticles and encapsulation of nanoparticles. *Sensors and Actuators A*. 2009;151(2):231-236.

27. Jiang X, Zhang Y, Edirisinghe M, Parhizkar M. Combining microfluidic devices with coarse capillaries to reduce the size of monodisperse microbubbles. *RSC Advances*. 2016;6(8):63568-63577.

28. Zhang Y, Wang L. Experimental Investigation of Bubble Formation in a Microfluidic T-Shaped Junction. *Nanoscale and Microscale Thermophysical Engineering*. 2009;13(4):228-242.

29. Chanmanwar RM, Balasubramaniam R, Wankhade LN. Application and manufacturing of microfluidic devices: Review. *International Journal of Modern Engineering Research (IJMER)*. 2013;3(2):849-856.

30. Huerre A, Miralles V, Jullien MC. Bubbles and foams in microfluidics. *Soft Matter*. 2014;12(36):1-15.

31. Wang L, Zhang Y, Cheng L. Magic microfluidic T-junctions: Valving and bubbling. *Solitons and Fractals*. 2009;39(4):1530-1537.

32. Parhizkar M, Edirisinghe M, Stride E. Effect of operating conditions and liquid physical properties on the size of monodisperse microbubbles produced in a capillary embedded T-junction device. *Microfluidics and Nanofluidics*. 2013;14(5):797-808.

33. Garstecki P, Fuerstman MJ, Stonec HA, Whitesides GM. Formation of droplets and bubbles in a microfluidic T-junction-Scaling and mechanism of break-up. *Lab on a Chip*. 2006;6(1):437-446.

34. Hallow DM, Seeger RA, Kamaev PP, Prado GR, LaPlaca MC, Prausnitz MR. Shear-Induced Intracellular loading of cells with molecules by controlled microfluidics. *Biotechnology & Bioengineering*. 2008;99(4):846-854.

35. Parhizkar M, Edirisinghe M, Stride E. The effect of surfactant type and concentration on the size and stability of microbubbles produced in a capillary embedded t-junction device. *RSC Advances*. 2015;5(14):10751-10762.

36. Yaghoub M, Jamalabadi A, DaqiqShirazi M, Kosar A, Shadloo MS. Effect of injection angle, density ratio, and viscosity on droplet formation in a microfluidic T-junction. *Theoretical & Applied Mechanics Letters.* 2017;7(4):243-251.

37. Nekouei M, Vanapalli SA. Volume-of-fluid simulations in microfluidic t-junction devices: Influence of viscosity ratio on droplet size. *Physics of Fluids*. 2007;29(3):3-22.

38. Van der Graaf S, Schroën CGPH, Van der Sman RGM, Boom RM. Influence of dynamic interfacial tension on droplet formation during membrane emulsification. *Journal of Colloid and Interface Science*. 2004;277(2):456-463.

39. Aprilliza HM. Characterization and properties of sodium alginate from brown algae used as an ecofriendly superabsorbent. *IOP Conference Series: Materials Science and Engineering.* 2017;188(1):1-5.

40. Hecht H, Srebnik S. Structural Characterization of sodium alginate and calcium alginate. *Biomacromolecules.* 2016;17(6):2160-2167.

41. Fertah M, Belfkira A, Dahmane EM, Taourirte M, Brouillette F. Extraction and characterization of sodium alginate from Moroccan Laminaria digitata brown seaweed. *Arabian Journal of Chemistry*. 2017;10(5):3707-3714.

42. Eiselt P, Lee KY, Mooney DJ. Rigidity of two-component hydrogels prepared from alginate and poly (ethylene glycol)-diamines. *Macromolecules.* 1999;32(7):5561-5566.

43. Lee KY, Mooney DJ. Alginate: properties and biomedical applications. *Prog Polym Sci*. 2012;37(1):106–126.

44. Kolarsick PAJ, BS, Kolarsick MA, Goodwin C. Anatomy and Physiology of the Skin. *Journal of the Dermatology Nurses' Association.* 2011;3(4):203-213.

45. Brodell L, Rosenthal K. Skin Structure and Function the Body's Primary Defense Against Infection. *Infectious Diseases in Clinical Practice*. 2008;16(2):113-117

46. James W, Berger T, Elston D. *Andrews' Diseases of the skin: Clinical dermatology*. Philadelphia: Elsevier Saunders 10th ed; 2006.

47. Elder D. Histology of the skin. *Lever's histopathology of the skin*. 1997:5-45.

48. D'Orazio J, Jarrett S, Amaro-Ortiz A, Scott TL. UV Radiation and the Skin. *International Journal of Molecular Sciences*. 2013;14(6):12222-12248.

49. Cichorek M, Wachulska M, Stasiewicz A, Tymińska A. Skin melanocytes: biology and development. *Postep Derm Alergol*. 2013;30(1):30-41.

50. Chu DH. Overview of biology, development, and structure of skin. *Fitzpatrick's dermatology in general medicine*. 2008:57–73.

51. Udey MC. Cadherins and Langerhans cell immunobiology. *Clinical and Experimental Immunology*. 1997;107(1):6–8.

52. Goldsmith L, Katz S, Gilchrest BA, Paller AS, Leffell DJ, Wolff K. *Fitzpatrick'sdermatology in general medicine*. 2008:713–720.

53. Flament F, Francois G, Qiu H, Ye C, Hanaya T, Batisse D, et al. Facial skin pores: a multiethnic study. *Dove Press Journal*. 2015;8(2):85-93.

54. Lawton S. Skin 1: the structure and functions of the skin. *Nursing Times.* 2019; 115(12):30–33.

55. Gayraud B, Hopfner B, Jassim A, Aumailley M, Bruckner-Tuderman L. Characterization of a 50-kDa component of epithelial basement membranes using GDA-J/F3 monoclonal antibody. *Journal of Biological Chemistry*. 1997;272(14): 9531–9538.

56. Cork MJ. The importance of skin barrier function. *Journal of Dermatological Treatment.* 1997;8(7):7-13.

57. Grubauer G, Feingold KR, Harris RM, Elias PM. Lipid content and lipid type as determinants of the epidermal permeability barrier. *Journal of Lipid Research.* 1989;30(1):89-96.

58. Baumann L. Understanding and treating various skin types: the baumann skin type indicator. *Dermatol Clin.* 2008;26(3):359–373.

59. Zouboulis CC, Katsambas AD, Kligman AM. Sebum secretion, skin type, and pH. *Pathogenesis and Treatment of Acne and Rosacea*. 2014; 299-303.

60. Youn SW, Humbert P. Cosmetic Facial Skin Type. *Measuring the Skin.* 2015;1-6.

61. Moulin VJ. Growth factors in skin wound healing. *European Journal of Cell Biology.* 1995;68(1):1-7.

62. Gonzalez ACO, Costa TF, Andrade ZA, Ribeiro A, Medrado AP. Wound healing - A literature review. *An Bras Dermatol.* 2016;91(5):614-620.

63. Martin P. Wound healing-aiming for perfect skin regeneration. *Science.* 1997;276(5309):75-81.

64. McGraw MKS, Jones TR, Baer DG, Soft tissue wounds and principles of healing. *Emerg Med Clin N Am*. 2007;25(1):1-22.

65. Whitney JD. Overview: Acute and chronic wounds. *Nurs Clin N Am*. 2005;40(2):191-205.

66. Brook I, Frazier EH. Aerobic and anaerobic microbiology of chronic venous ulcers. *Int J Dermatol*.1998;37(6):426-428.

67. Hansson C, Hoborn J, Moller A, Swanbeck G. The microbial flora in venous leg ulcers without clinical signs of infection using a validated standardized microbiological technique. *Acta Derm Venereo*. 1995;75(1):24-30.

68. McLigeyo OS, Oumah S, Otieno SL. Diabetic ulcers - a clinical and bacteriological study. *West Afr J Med*. 1990;9(2):135-138.

69. Stephens P, Wall IB, Wilson MJ, Hill KE, Davies CE, Hil CM, et al. Anaerobic cocci populating the deep tissues of chronic wounds impair cellular wound healing responses in vitro. *British Journal of Dermatology*. 2003;148(9):456–66.

70. Zouboulıs CC. Acne and sebaceous gland function. *Clinics in Dermatology Y*. 2004;22(3):360–366.

71. Gollnick H, Cunliffe W, Berson D, Dreno B, Finlay A, Leyden JJ, et al. Management of acne: a report from a global alliance to improve outcomes in acne. *J Am Acad Dermatol*. 2003;49(1):1-8.

72. Jeremy AHT, Holland DB, Roberts SG, Thomson KF, Cunliffe WJ. Inflammatory events are involved in acne lesion initiation. *J Invest Dermatol*. 2003;121(1):20-27.

73. Tanghettı EA. The role of inflammation in the pathology of acne. *J Clinical Aesthetic Dermatology*. 2013;6(9):27-35.

74. Fujimura T, Hotta M. The preliminary study of the relationship between facial movements and wrinkle formation. *Skin Research and Technology*. 2012;18(2):219-224.

75. Langton AK, Sherratt MJ, Griffiths CEM, Watson REB. A new wrinkle on old skin: the role of elastic fibres in skin ageing. *International Journal of Cosmetic Science.* 2010;32(5):330-339.

76. Kappes UP. Skin ageing and wrinkles: clinical and photographic scoring. *Journal of Cosmetic Dermatology*. 2004;3(1):23-25.

77. Türsen Ü. Deri yaşlanmasının topikal ajanlarla önlenmesi. *Dermatose.* 2006;5(4):267-283.

78. D'Orazio J, Jarrett S, Ortiz AA, Scott T. UV radiation and the skin. *International Journal of Molecular Sciences*. 2013;14(6):12222-12248.

79. Romanhole RC, Ataide JA, Moriel P, Mazzola PG. Update on ultraviolet A and B radiation generated by the sun and artificial lamps and their effects on skin. *International Journal of Cosmetic Science*. 2015;37(2):366–370.

80. Pandel R, Poljšak B, Godic A, Dahmane R. Skin photoaging and the role of antioxidants in its prevention. *ISRN Dermatology*. 2013;2013(11):1-11.

81. Wilson PD, Kligman AM. Experimental induction of freckles by ultraviolet-B. *British Journal of Dermatology*. 1982;106(4):401-406.

82. Sévrain SV, Bonté F. Skin hydration: a review on its molecular mechanisms. *Journal of Cosmetic Dermatology*. 2006;6(2):75–82.

83. Polaskova J, Pavlackova J, Vltavska P, Mokrejs P, Janıs R. Moisturizing effect of topical cosmetic products applied to dry skin. *J. Cosmet. Sci.* 2013;64(5):329-340.

84. Laden K, Spıtzer R. identification of a natural moisturizing agent in skin. *J. Soc. Cosmetic Chemists.* 1967;18(4):351--360.

85. Lod´en M. Role of topical emollients and moisturizers in the treatment of dry skin barrier disorders. *Am J Clin Dermatol*. 2003;4(11):771-788

86. Lodén M. Effect of moisturizers on epidermal barrier function. *Clinics in Dermatology*. 2012;30(3):286–296.

87. Lodén M. The increase in skin hydration after application of emollients with different amounts of lipids. *Acta Derm Venereol*. 1992;72(5):327-30.

88. Wolf R, Parish L. Barrier-repair prescription moisturizers: Do we really need them? Facts and controversies. *Jefferson Digital Commons*. 2013;31(6):787-791.

89. Nilforoushzadeh MA, Amirkhani MA, Zarrintaj P, Moghaddam AS, Mehrabi T, Alavi A, et al. Skin care and rejuvenation by cosmeceutical facial mask. *J Cosmet Dermatol*. 2018;17(5):693-702.

90. Surını S, Aulıyya A. Formulatıon of an antı-wrınkle hydrogel face mask contaınıng ethanol extract of nonı fruıt (morında cıtrıfolıa l) for use as a nutracosmeceutıcal product. *Int J App Pharm*. 2017;9(1):74-76.

91. Velasco MVR, Vieira RP, Fernandes AR, Dario MF, Pinto CASO, Pedriali CA, et al. Short-term clinical of peel-off facial mask moisturizers. *International Journal of Cosmetic Science*. 2014;36(4):355–360.

92. Yamını K, Onesımus T. Preparatıon and evaluatıon of herbal antı-acne gel. *Int J Pharm Bio Sci*. 2013;4(2):956-960.

93. Suhery WN, Anggraini N. Formulation and evaluation of peel-off gel masks from red rice bran extract with various kind of bases. *International Journal of PharmTech Research*. 2016;9(12):574-580.

94. Perugini P, Bleve M, Cortinovis F, Colpani A. Biocellulose masks as delivery systems: A novel methodological approach to assure quality and safety. *Cosmetics*. 2018;5(4):66-86.

95. Liu BS, Lin SN, Lien CW, Lai HH. Determined the critical factors of facial mask products and size design. *2014 IEEE International Conference on Management of Innovation and Technology*;2014: IEEE.

96. Laguens M, Rendon MI, Reeves WH. The effects of a new transdermal hydrating and exfoliating cosmetic face mask in the maintenance of facial skin. *Cosmetic Dermatology*. 2010;23(8):370-383.

97. Mullaicharam AR, Halligudi N. St John's wort (*Hypericum perforatum* L.): A review of its chemistry, pharmacology and clinical properties. *Int. J. Res. Phy. & Pharm. Sci.* 2018;1(1):5-11.

98. Nahrstedt A, Butterweck V. Biologically active and other chemical constituents of the herb of Hypericum perforaturn L. *Pharmacopsychiat.* 1997;30(2):129-134.

99. Çırak C, Kurt D. Önemli tıbbi bitkiler olarak hypericum türleri ve kullanım alanları. *ANADOLU, J. of AARI*. 2014;24(1):38-52.

100. Đorđević AS. Chemical composition of *Hypericum perforatum* L. essential oil. *Advanced technologies*. 2015;4(1):64-68.

101. McGuffin M, Hobbs C, Upton R, Goldberg A. American Herbal Product Association's. *Botanical Safety Handbook.* Boca Raton: CRC Press; 1997.

102. EMEA (European Medicines Agency). HMPC Community herbal monograph on *Hypericum perforatum L*., herba (Traditional use). 2009.

103. Altan A, Damlar İ, Aras MH, Alpaslan C. Sarı kantaronun (*Hypericum perforatum*) yara iyileşmesi üzerine etkisi. *Archives Medical Review Journal*. 2015;24(4):578-591.

104. Patočka J. The chemistry, pharmacology, and toxicology of the biologically active constituents of the herb *Hypericum perforatum* L. *Journal of Applied Biomedicine.* 2003;1(7):61-70.

105. Pietta P, Gardana C, Pietta A. Comparative evaluation of St. John's wort from different Italian regions. *Farmac.* 2001;56(5-7):491-496.

106. Stavric B. Quercetin in our diet: From potent mutagen to probable anticarcinogen. *Clin. Biochem*. 1994;27(4):245-248.

107. Kim HK, Son KH, Chang HW, Kang SS, Kim HP. Amentoflavone, a plant biflavone: a new potential anti-inflammatory agent. *Arch. Pharm. Res*. 1998;21(4):406-410.

108. Cada AM, Hansen DK, LaBorde JB, Ferguson SA. Minimal effects from developmental exposure to St. John's wort (*Hypericum perforatum*) in Sprague–Dawley rats. *Nutr Neurosci.* 2001;4(2):135-141.

109. Saljic J. Ointment for the treatment of burns. *Ger. Offen.* 1975;2(8):406-452.

110. Cabbaroglu D, Kodik MS, Uyanıkgil Y, Uyanıkgil EÖÇ, Karabey F, Kıyan GS. Treatment of contact burn injury with *Hypericum perforatum*: An experimental study. *Ege Journal of Medicine*. 2019;58(2):154-160.

111. Maisenbacher P, Kovar KA. Adhyperforin: a homologue of hyperforin from *Hypericum perforatum*. *Planta Medica*. 1992;58(3):291-293.

112. Schempp CM, Windeck T, Hezel S, Simon JC. Topical treatment of atopic dermatitis with St. John's Wort cream – a randomized, placebo controlled, double blind half-side comparison. *Phytomedicine*. 2003;10(4):31-37.

113. Schempp CM, Kiss J, Kirkin V, Averbeck M, Simon-Haarhaus B, Kremer B, et al. Hyperforin acts as an angiogenesis inhibitor. *Planta Medica*. 2005;71(11):999-1004.

114. Oztürk N, Korkmaz S, Öztürk Y. Wound-healing activity of St. John's Wort (*Hypericum perforatum* L.) on chicken embryonic fibroblasts. *Journal of Ethnopharmacology*. 2007;111(1):33-39.

115. Lenard J, Rabson A, Vanderoef R. Photodynamic inactivation of infectivity of human immunodeficiency virus and other enveloped viruses using hypericin and rose Bengal: inhibition of fusion and syncytia formation. *Proc Natl Acad Sci USA.* 1993;90(1):158-162.

116. Schempp C, Pelz K, Wittmer A, Schopf E, Simon JC. Antibacterial activity of hyperforin from St John's wort, against multiresistant Staphylococcus aureus and grampositive bacteria. *Lancet.* 1999;353(9170):2129.

117. Peeva-Naumovska V, Panovski N, Grdanovska T, Kumbaradzi EF. Formulations of St. John's Wort oil ointment and evaluation of its antibacterial effect. [cited 2013 28 April]. Available from: www. www.amapseec.org/cmapseec.1/Papers/pap p067.htm.

118. Lasik M, Nowak J, Stachowiak B, Czarnecki Z. Evaluation of the antagonistic properties of natural antibacterial substances extracted from herbs: poster presentation; 2007: Eurobiotech.

119. Yow CM, Tang HM, Chu ES, Huang Z. Hypericin-mediated photodynamic antimicrobial effect on clinically isolated pathogens. *Photochem Photobiol.* 2012;88(3):626-632.

120. Borchardt JR, Wyse DL, Sheaffer CC, Kauppi KL, Fulcher RG, Ehlke NG, et al. Antimicrobial activity of native and naturalized plants of Minnesota and Wisconsin. *J Med Plants Res*. 2008;2(5):98-110.

121. Avato P, Raffo F, Guglielmi G, Vitali C, Rosato A. Extracts from St John's Wort and their antimicrobial activity. *Phytother Res*. 2004;18(3):230-232.

122. Reichling J, Weseler A, Saller R. A current reviewof the antimicrobial activity of *Hypericum perforatum* L. *Pharmacopsychiatry.* 2001;34(1):116-118.

123. Süntar I, Oyardı O, Akkol EK, Ozçelik B. Antimicrobial effect of the extracts from *Hypericum perforatum* against oral bacteria and biofilm formation. *Pharmaceutıcal Bıology*. 2016;54(6):1065–1070.

124. Mishenkova EL, Derbentseva NA, Garagulya AD, Litvin LN. Antiviral properties of St John's wort and preparations produced from it. *Transactions of the Congress of Microbiologists of the Ukraine*. 1975.

125. Vlietinck AJ, Bruyne TD, Apers S, Pieters LA. Plant derived leading compounds chemotherapy of human immunodeficiency virus (HIV-1) infection. *Planta Medica.* 1998;64(2):97-109.

126. Kirakosyan A, Sirvent TM, Gibson DM, Kaufman PB. The production of hypericins and hyperforin by in vitro cultures of St. John's wort (*Hypericum perforatum*). *Biotechnol Appl Biochem*. 2004;39(1):71–81.

127. Takahashi I, Nakanishi S, Kobayashi E, Nakano H, Suzuki K, Tamaoki T. Hypericin and pseudohypericin specifically inhibit protein kinase C: possible relation to their antiretroviral activity. *Biochem Biophys Res Commun*. 1989;165(3):1207-1212.

128. John J. Vollmer, Jon Rosenson. Chemistry of St. John's Wort: hypericin and hyperforin. *Journal of Chemical Education.* 2004;81(10):1450-1456.

129. Thomas C, MacGill RS, Miller GC, Pardini RS. Photoactivation of hypericin generates singlet oxygen in mitochondria and inhibitssuccinoxidase. *Photochem Photobiol*. 1992;55(1):47-53.

130. Hadjur C, Richard MJ, Parat MO, et al. Photodynamically induced cytotoxicity of hypericin dye on human fibroblast cell line MRC5. *J Photochem Photobiol Biol B.* 1995;27(2):139-146.

131. Franco P, Potenza I, Moretto F, Segantin M, Grosso M, Lombardo A, et al. *Hypericum perforatum* and neem oil for the management of acute skin toxicity in head and neck cancer patients undergoing radiation or chemo-radiation: A Single-arm prospective observational study. *Radiat Oncol.* 2014;9(297):2-7.

132. Thomas C, Pardini RS. Oxygen dependence of hypericin-induced phototoxicity to EMT6 mouse mammary carcinoma cells. *Photochem Photobiol*. 1992;55(6):831-837.

133. Vandenbogaerde AL, Delaey EM, Vantieghem AM, Himpens BE, Merlevede WJ, Witte PA. Cytotoxicity and antiproliferative effect of hypericin and derivatives after photosensitization. *Photochem Photobiol*. 1998;67(1):119-125.

134. Schempp CM, Wınghofer B, Lüdtke R, Haarhaus BS, Schöpf E, Sımon JC. Topical application of St John's wort (*Hypericum perforatum* L.) and of its metabolite hyperforin inhibits the allostimulatory capacity of epidermal cells. *British Journal of Dermatology*. 2000;142(5):979-984.

135. Sagratini G, Ricciutelli M, Vittori S, Oztürk N, Oztürk Y, Maggi F. Phytochemical and antioxidant analysis of eight Hypericum taxa from Central Italy. *Fitoterapia.* 2008;79(3):210–213.

136. Rainha N, Lima E, Baptista J. Comparison of the endemic Azorean Hypericum foliosum with other Hypericum species: antioxidant activity and phenolic profile. *Nat Prod Res*. 2011;25(2):123-135.

137. Orhan IE, Kartal M. LC-DAD-MS-assisted quantification of marker compounds in *Hypericum perforatum* L. (St. John's Wort) and its antioxidant activity. *Turk J Pharm Sci*. 2015;12(3):279-286.

138. Zou Y, Lu Y, Wei D. Antioxidant activity of a flavonoid-rich extract of *Hypericum perforatum* L. in Vitro. *J. Agric. Food Chem.* 2004;52(16):5032-5039.

139. Meinke MC, Schanzer S, Haag SF, Casetti F, Müller ML, Wölfle U, et al. In vivo photoprotective and anti-inflammatory effect of hyperforin is associated with high antioxidant activity in vitro and ex vivo. *Eur J Pharm Biopharm*. 2012;81(2):346-50.

140. Schempp C, Ludtke R, Winghofer B, Simon JC. Effect of topical application of *Hypericum perforatum* extract (St. John's wort) on skin sensitivity to solar simulated radiation. *Photodermatol Photoimmunol Photome*. 2000;16(3):125-128.

141. Schempp CM, Müller K, Winghofer B, Schulte-Mönting J, Simon JC. Single-dose and steady-state administration of *Hypericum perforatum* extract (St John's Wort) does not influence skin sensitivity to UV radiation, visible light, and solar-simulated radiation. *Arch Dermatol*. 2001;137(4):512-513.

142. Schmitt LA, Liua Y, Murphya PA, Petrich JW, Dixona PM, Birt DF. Reduction in hypericin-induced phototoxicity by *Hypericum perforatum* extracts and pure compounds. *J Photochem Photobiol B*. 2006;85(2):118–130.

143. Hadi H, Omar SSS, Awadh AI. Honey, a gift from nature to health and beauty: A review. *British Journal of Pharmacy*. 2016;1(11):46-54.

144. Cooper R. Honey in wound care: antibacterial properties. *GMS Krankenhaushygiene Interdisziplinär*. 2007;2(2):51-59.

145. Martinotti S, Ranzato E. Honey, wound repair and regenerative medicine. *J. Funct. Biomater*. 2018;9(4):34-41.

146. Hajar R. History of medicine. *Heart Views*. 2002;3(4):10.

147. Crane EE. *The World History of Beekeeping and Honey Hunting*. Routledge;2013.

148. Marylenlid I, Atilio C, Lorena D, Pérez-Pérez, Mariana E, Patricia V. Cosmetic properties of honey. 1. Antioxidant activity. *Stingless bees process honey and pollen in cerumen pots.* 2013:1-8.

149. Mullen EK, Thompson GJ. Understanding honeybee worker self-sacrifice: a conceptual-empirical framework. *Advances in Insect Physiology*. 2015:325-354.

150. Bogdanov S. Honey Composition. *The Honey Book.* 2016:50-55.

151. Ferreira IC, Aires E, Barreira JC, Estevinho LM. Antioxidant activity of Portuguese honey samples: Different contributions of the entire honey and phenolic extract. *Food Chem.* 2009;114(4):1438-1443.

152. Socha R, Juszczak L, Pietrzyk S, Galkowska D, Fortuna T, Witczak T. Phenolic profile and antioxidant properties of Polish honeys. *Int J Food Sci Technol.* 2011;46(3):528-534.

153. Ciulu M, Solinas S, Floris I, Panzanelli A, Pilo MI, Piu PC, et al. RP-HPLC determination of water-soluble vitamins in honey. *Talanta.* 2011;83(3):924-929.

154. Singh MP, Chourasia HR, Agarwal M, Malhotra A, Sharma M, Sharma D, et al. Honey as complementary medicine: A review. *Int J Pharma Biol Sci.* 2012;3(2):12-31.

155. Molan PC. Re-introducing honey in the management of wounds and ulcers-theory and practice. *Ostomy Wound Manag*. 2011;48(11):28-40.

156. Adams CJ, Manley-Harris M, Molan PC. The origin of methylglyoxal in New Zealand manuka (Leptospermum scoparium) honey. Carbohydr. *Res.* 2009;344(3):1050-1053.

157. Burlando B, Cornara L. Honey in dermatology and skin care: a review. *J Cosmet Dermatol.* 2011;12(4):306-13.

158. Kwakman PHS, Te Velde AA, Boer L, Vandenbroucke-Grauls CMJE, Zaat SAJ. Two major medicinal honeys have different mechanisms of bactericidal activity. *PLoS One*. 2011;6(3):1-20.

159. Saikaly SK, Khachemoune A. Honey and wound healing: An update. *Am J Clin Dermatol.* 2017;18(1):237-251.

160. Abbas M, Ugkay I, Lipsky BA. In diabetic foot infections antibiotics are to treat infection, not to heal wounds. Expert Opin. *Phamacother*. 2015;16(6):821-832.

161. Martinotti S, Ranzato E. *In cellular and molecular mechanisms of honey wound healing*. Nova Publishers Inc.: Hauppauge, NY, USA; 2014.

162. Molan PC. The antibacterial activity of honey: 1. The nature of the antibacterial activity. *Bee world*. 1992;73(1):5-28.

163. Molan PC. The role of honey in the management of wounds. *J Wound Care*. 1999;8(8):415-418.

164. Leigh SJ. Leg ulcer management with topical medical honey. *Br J Community Nurs.* 2008;13(4):22-32.

165. Mohamed H, Abu Salma M, Allenjawi B, Barakat N, Gouda Z, Abdi S, et al. Natural honey as an adjunctive alternative in the management of diabetic foot ulcers. *Wound Pract Res.* 2012;20(4):212-216.

166. Weissenstein A, Luchter E, Bittmann S. Medical honey and its role in paediatric patients. *Br J Nurs*. 2014;23(6):30-34.

167. Kaufman T, Eichenlaub EH, Angel MF. Topical acidification promotes healing of experimental deep parrial thickness skin burns: A randomized double-blind preliminary study. *Burns.* 1985;12(2):84-90.

168. Vallianou NG, Gounari P, Skourtis A, Panagos J, Kazazis C. Honey and its anti-inflammatory, anti-bacterial and antioxidant properties. *Gen Med*. 2014;2(2):1-5.

169. Prakash A, Medhi B, Avti PK, Saikia UN, Pandhi P, et al. Effect of different doses of Manuka honey in experimentally induced inflammatory bowel disease in rats. *Phytother Res*. 2008;22(11):1511-1519.

170. Aljadi AM, Kamaruddin MY. Evaluation of the phenolic contents and antioxidant capacities of two Malaysian floral honeys. *Food Chem.* 2004;85(4):513-518.

171. Kassim M, Achoui M, Mansor M, Yusoff KM. The inhibitory effects of Gelam honey and its extracts on nitric oxide and prostaglandin E (2) in inflammatory tissues. *Fitoterapia*. 2010;81(8):1196-1201.

172. Lee D, Sinno S, Khachemoune A. Use of sugar in infected wounds. *Gop Doct.* 1993;23(4):185.

173. Molan PC. Potential of honey in the treatment of wounds and burns. *Am J Clin Dermatol*. 2001;2(1):13-19.

174. Allen KL, Molan PC, Reid GM. A survey of the antibacterial activity of some New-Zealand honeys. *J. Pharm. Pharmacol*. 1991;43(12):817-822.

175. Cooper RA, Molan PC, Harding KG. Antibacterial activity of honey against strains of Staphylococcus aureus from infected wounds. *J Roy Soc Med*. 1999;92(6):283-285.

176. Mohapatra DP, Thakur V, Brar SK. Antibacterial efficacy of raw and processed honey. *Biotechnology Research Internationa*. 2011;2011(917505):1-6.

177. Chauhan A, Pandey V, Chacko KM, Khandal RK. Antibacterial activity of raw and processed honey. *Electronic Journal of Biology*. 2010;5(3):58-66.

178. Subrahmanyam M. Topıcal applıcatıon of honey for burn wound treatment - an overvıew. *Annals of Burns and Fire Disaster*. 2007;20(3):137-139.

179. Subrahmanyam M. Honey impregnated gauze versus polyurethane film (OpSite®) in the treatment of burns – a prospective randomised study. *Br J Plast Surg.* 1993;46(4): 322-323.

180. Subrahmanyam M. Honey-impregnated gauze versus amniotic membrane in the treatment of burns. *Burns*. 1994;20(4):331-333.

181. Alvarez-Suarez, Jagdish T, Joseph I. Quantification of saccharides in multiple floral honeys using fourier transform infrared microattenuated total reflectance spectroscopy. *J Agri Food Chem*. 2004;52(11):3237-3243.

182. Ahshawat MS, Saraf S, Saraf S. Preparation and characterization of herbal creams for improvement of skin viscoelastic properties. *International Journal of Cosmetic Science*. 2008;30(3):183-193.

183. Weyden EA. Treatment of a venous leg ulcer with a honey alginate dressing. *Wound Care*. 2005;10(2):21-27.

184. El-Kased RF, Amer RI, Attia D, Elmazar MM. Honey-based hydrogel: In vitro and comparative in vivo evaluation for burn wound healing. *Scientific Reports*. 2017;7(1):1-33.

185. Mirzaei B, Etemadian S, Goli HR, Bahonar S, Gholami SA, Karami P, et al. Construction and analysis of alginate-based honey hydrogel as an ointment to heal of rat burn wound related infections. *Int J Burn Trauma*. 2018;8(4):88-97.

186. Bogdanov S. External applications of honey. Book of Honey. *Bee Product Science*. 2009;1-8.

187. Burlando B, Cornara L. Honey in dermatology and skin care: a review. *Journal of Cosmetic Dermatology*. 2013;12(4):306-313.

188. Jalil MAA, Kasmuri AR, Hadi H. Stingless bee honey, the natural wound healer: A review. *Skin Pharmacol Physiol*. 2017;30(8):66-75.

189. Campos JF, dos Santos UP, Macorini LFB, de Melo AMMF, Balestieri JBP, Paredes-Gamero EJ, et al: Antimicrobial, antioxidant and cytotoxic activities of propolis from Melipona orbignyi (Hymenoptera, Apidae). *Food Chem Toxicol*. 2014;65(3):374-380.

190. Altuntaş E, Yener G. Anti-aging potential of a cream containing herbal oils and honey: Formulation and in vivo evaluation of effectiveness using non- invasive biophysical techniques. *IOSR Journal of Pharmacy and Biological Sciences (IOSR-JPBS)*. 2015;10(6):51-60.

191. Moleıu L, Jıanu C, Bujanca G, Doros G, Mısca C, Ilıe OC, et al. Essential oil of *Hypericum perforatum*. The chemical composition and antimicrobial activity. *REV. CHIM (Bucharest)*. 2017;68(4):687-692.

192. Zhou W, Apkarian RP, Wang ZL, Joy D. Fundamentals of scanning electron microscopy. *Scanning Microscopy for Nanotechnology*. 2006; 1-40.

193. Naumann D. FT-Infrared and FT-Raman spectroscopy in bıomedıcal research. *Applıed Spectroscopy Revıews*. 2001;36(2-3):239-298.

194. Wielagea B, Lampkea Th, Marxb G, Nestlerb K, Starke D. Thermogravimetric and differential scanning calorimetric analysis of natural fibres and polypropylene. *Thermochimica Acta*. 1999;337(1-2):169-177.

195. Murthy NS, Minor H. General procedure for evaluating amorphous scattering and crystallinity from X-ray diffraction scans of semicrystalline polymers. *Polymer*. 1990;31(6):996-1002.

196. Wehking JD, Gabany M, Chew L, Kumar R. Effects of viscosity, interfacial tension, and flow geometry on droplet formation in a microfluidic T-junction. *Microfluid Nanofluid*. 2014;16(3):441-453.

197. Coates J. *Interpretation of infrared spectra, a practical approach, encyclopedia of analytical chemistry*. R.A. Meyers (Ed.), John Wiley & Sons Ltd, Chichester; 2000.

198. Tewarı J, Irudayaraj J. Quantification of saccharides in multiple floral honeys using fourier transform infrared microattenuated total reflectance spectroscopy. *J. Agric. Food Chem*. 2004;52(11):3237-3243.

199. Irudayaraj J, Sivakesava S. Detectıon of adulteratıon in honey by dıscrımınant analysıs usıng FTIR spectroscopy. *American Society of Agricultural Engineers*. 2001;44(3):643-650.

200. Sivakesava S, Irudayaraj J. Detection of inverted beet sugar adulteration of honey by FTIR spectroscopy. *Journal of the Science of Food and Agriculture*. 2001;81(8):683-690.

201. Anjos O, Campos MG, Ruiz PC, Antunes P. Applıcatıon of FTIR-ATR spectroscopy to the quantıficatıon of sugar in honey. *Food Chemistry*. 2014;169(2):218-223.

202. Bonifacio M, Cometa S, Cochis A, Gentile P, Ferreira A, Azzimonti B, et al. Data on Manuka Honey / Gellan Gum composite hydrogels for cartilage repair. *Data inBrief.* 2018;20(8):831-839.

203. Kędzierska-Matysek M, Matwijczuk A, Florek M, Barłowska J, Wolanciuk A, Matwijczuk A, et al. Application of FTIR spectroscopy for analysis of the quality of honey. *BIO Web of Conferences*; 2018: BIO Web.

204. Gıtea D, Teodorescu A, Pantıs C, Tıt DM, Bungau AF, Bogdan M, et al. Green Synthesis of silver nanoparticles using *Hypericum perforatum* L. extract and evaluation of their antibacterial activity. *Revista de Chimie Bucharest Original Edition*. 2020;71(2):273-279.

205. Eğri Ö, Erdemir N. Production of *Hypericum perforatum* oil-loaded membranes for wound dressing material and in vitro tests. *Artıfıcıal Cells, Nanomedıcıne, And Bıotechnology*. 2019;47(1):1404-1415.

206. Huanga YG, Zhenga FH, Zhanga XH, Lib QY, Wanga HQ. Effect of carbon coating on cycle performance of LiFePO4/C compositecathodes using Tween80 as carbon source. *Electrochimica Acta*. 2014;130(6):740-747.

207. Mirzaei B, Etemadian S, Goli HR, Bahonar S, Gholami SA, Karami P, et al. Construction and analysis of alginate-based honey hydrogel as an ointment to heal of rat burn wound related infections. *Int J Burn Trauma*. 2018;8(4):88-97.

208. Batsoulıs AN, Sıatıs NG, Kımbarıs AC, Alıssandrakıs EK, et al. FT-Raman spectroscopic simultaneous determination of fructose and glucose in honey. *J. Agric. Food Chem*. 2005;53(2):207-210.

209. Pierna JAF, Abbas O, Dardenne P, Baeten V. Discrimination of Corsican honey by FT-Raman spectroscopy and chemometrics. *Biotechnol. Agron. Soc. Environ.* 2011;15(1):75-84.

210. Paradkar MM, Irudayaraj J. Discrimination and classification of beet and cane inverts in honey by FT-Raman spectroscopy. *Food Chemistry*. 2001;76(2):231–239.

211. Olıveıra LFCD, Colombara R, Edwards HGM. Fourier transform raman spectroscopy of honey. *Applıed Spectroscopy*. 2002;56(3):306-311.

212. Pereira L, Sousa A, Coelho H, Amado AM, Ribeiro-Claro PJA. Use of FTIR, FT-Raman and 13C-NMR spectroscopy for identification of some seaweed phycocolloids. *Biomolecular Engineering*. 2003;20(4-6):223-228.

213. El-Abassy RM, Donfack P, Materny A. Visible Raman spectroscopy for the discrimination of olive oils from different vegetable oils and the detection of adulteration. *J. Raman Spectrosc*. 2009;40(9):1284-1289.

214. Adar F. Introduction to interpretation of raman spectra using database searching and functional group detection and identification. *Spectroscop.* 2016;31(7):16-23.

215. Pourhojat F, Sohrabi M, Shariati S, Mahdavi H, Asadpour L. Evaluation of poly e-caprolactone electrospun nanofibers loaded with *Hypericum perforatum* extract as a wound dressing. *Res Chem Intermed*. 2017;43(1):297-320.

216. Cordella C, Faucon JP, Cabrol-Bass D, Sbirrazzuoli N. Application of DSC as a tool for honey floral specıes characterızatıon and adulteratıon detection. *Journal of Thermal Analysis and Calorimetry.* 2003;71(10):275-286.

217. Soares JP, Santos JE, Chierice GO, Cavalheiro ETG. Thermal behavior of alginic acid and its sodium salt. *Ecl. Quím., São Paulo*. 2004;29(2):53-56.

218. Venir E, Spaziani M, Maltini E. Crystallization in ‘‘Tarassaco” Italian honey studied by DSC. *Food Chemistry*. 2010;122(2):410-415.

219. Rahman S. *Food Properties handbook*. CRC Press, Bocaraten;1995.

220. Lupano CE. DSC study of honey granulation stored at various temperatures. *Food Research International*. 1997;30(9):683-688.

221. Huda MN, Dragaun H, Bauer S, Muschik H, Skalicky P. A study of the crystallinity index of polypropylene fibres. *Colloid & Polymer Sci*. 1985;263(9):730-737.

222. Smitha B, Sridhar S, Khan AA. Chitosan–sodium alginate polyion complexes as fuel cell membranes. *European Polymer Journal*. 2005;41(8):1859-1866.

223. Chao CY, Mani MP, Jaganathan SK. Engineering electrospun multicomponent polyurethane scaffolding platform comprising grapeseed oil and honey/propolis for bone tissue regeneration. *Plos One*. 2018;13(10):1-17.

224. Shahbazi E, Bahrami K. Production and properties analysis of honey nanofibers enriched with antibacterial herbal extracts for repair and regeneration of skin and bone tissues. *Journal of Pharmacy and Pharmacology*. 2019;7(2):37-50.

225. Kaco H, Zakarıa S, Razalı NF, Chıa CH, Zhang L, Janı SM. Properties of cellulose hydrogel from kenaf core prepared via pre-cooled dissolving method. *Sains Malaysiana.* 2014;43(8):1221–1229.

226. Wölfle U, Seelinger G, Schempp CM. Topical application of St. John's Wort (*Hypericum perforatum*). *Planta Med*. 2014;80(2-3):109-120.